

To-do list

| | |
|-----------------------------|----|
| 1. Which section? | 40 |
| 2. Chapter X | 49 |

Contents

| | |
|--|----------|
| 5 I-priors for categorical responses | 2 |
| 5.1 A naïve model | 4 |
| 5.2 A latent variable motivation: the I-probit model | 7 |
| 5.3 Identifiability and IIA | 9 |
| 5.4 Estimation | 12 |
| 5.4.1 Laplace approximation | 13 |
| 5.4.2 Variational inference | 14 |
| 5.4.3 Markov chain Monte Carlo methods | 15 |
| 5.4.4 Comparison of estimation methods | 16 |
| 5.5 A variational algorithm | 18 |
| 5.5.1 Latent propensities \mathbf{y}^* | 21 |
| 5.5.2 I-prior random effects \mathbf{w} | 22 |
| 5.5.3 Kernel parameters η | 23 |
| 5.5.4 Intercepts $\boldsymbol{\alpha}$ | 24 |
| 5.5.5 The CAVI algorithm | 24 |
| 5.6 Post-estimation | 25 |
| 5.7 Computational consideration | 28 |
| 5.7.1 Efficient computation of class probabilities | 28 |
| 5.7.2 Computational complexity of the CAVI algorithm | 31 |
| 5.7.3 Difficulties faced with estimating $\boldsymbol{\Psi}$ | 32 |
| 5.8 Examples | 33 |
| 5.8.1 Predicting cardiac arrhythmia | 33 |

| | | |
|---------------------|---|-----------|
| 5.8.2 | Meta-analysis of smoking cessation | 37 |
| 5.8.3 | Multiclass classification: Vowel recognition data set | 42 |
| 5.8.4 | Spatio-temporal modelling of bovine tuberculosis in Cornwall . . . | 45 |
| 5.9 | Conclusion | 52 |
| 5.10 | Miscellanea | 54 |
| 5.10.1 | A brief introduction to variational inference | 54 |
| 5.10.2 | Variational methods and the EM algorithm | 58 |
| 5.10.3 | The EM algorithm for I-probit models is intractable—variational Bayes EM? | 61 |
| 5.11 | Some distributions and their properties | 62 |
| 5.11.1 | Multivariate normal distribution | 63 |
| 5.11.2 | Matrix normal distribution | 64 |
| 5.11.3 | Truncated univariate normal distribution | 67 |
| 5.11.4 | Truncated multivariate normal distribution | 68 |
| 5.12 | Proofs related to conically truncated multivariate normal distribution . . | 71 |
| 5.12.1 | Proof of Lemma 5.4: Pdf | 71 |
| 5.12.2 | Proof of Lemma 5.4: Moments | 71 |
| 5.12.3 | Proof of Lemma 5.4: Entropy | 76 |
| 5.13 | Derivation of the CAVI algorithm | 76 |
| 5.13.1 | Derivation of $\tilde{q}(\mathbf{y}^*)$ | 79 |
| 5.13.2 | Derivation of $\tilde{q}(\mathbf{w})$ | 79 |
| 5.13.3 | Derivation of $\tilde{q}(\eta)$ | 82 |
| 5.13.4 | Derivation of $\tilde{q}(\Psi)$ | 85 |
| 5.13.5 | Derivation of $\tilde{q}(\alpha)$ | 87 |
| 5.14 | Deriving the ELBO expression | 87 |
| 5.14.1 | Terms involving distributions of \mathbf{y}^* | 88 |
| 5.14.2 | Terms involving distributions of \mathbf{w} | 89 |
| 5.14.3 | Terms involving distributions of η | 89 |
| 5.14.4 | Terms involving distribution of α | 90 |
| 5.14.5 | ELBO summarised | 90 |
| Bibliography | | 95 |

Haziq Jamil

Department of Statistics

London School of Economics and Political Science

PhD thesis: ‘Regression modelling using Fisher information covariance kernels (I-priors)’

Chapter 5

I-priors for categorical responses

In a regression setting such as (1.1), consider polytomous response variables y_1, \dots, y_n , where each y_i takes on exactly one of the values from the set of m possible choices $\mathcal{M} = \{1, \dots, m\}$. Modelling categorical response variables is of profound interest in statistics, econometrics and machine learning, with applications aplenty. In the social sciences, categorical variables often arise from survey responses, and one may be interested in studying correlations between explanatory variables and the categorical response of interest. Economists are often interested in discrete choice models to explain and predict choices between several alternatives, such as consumer choice of goods or modes of transport. In this age of big data, machine learning algorithms are used for classification of observations based on what is usually a large set of variables or features.

The normality assumption (1.2) is not entirely appropriate anymore. As an extension to the I-prior methodology, we propose a flexible modelling framework suitable for regression of categorical response variables. In the spirit of generalised linear models (McCullagh and Nelder, 1989), we relate class probabilities of the observations to a normal I-prior regression model via a link function. Perhaps though, it is more intuitive to view it as machine learners do: since the regression function is ranged on the entire real line, it is necessary to “squash” it through some sigmoid function to conform it to the interval $[0, 1]$ suitable for probability ranges.

Expanding on this idea further, assume that the y_i ’s follow a categorical distribution, denoted by

$$y_i \sim \text{Cat}(p_{i1}, \dots, p_{im}),$$

with the class probabilities satisfying $p_{ij} \geq 0, \forall j = 1, \dots, m$ and $\sum_{j=1}^m p_{ij} = 1$. The probability mass function (pmf) of y_i is given by

$$p(y_i) = p_{i1}^{[y_i=1]} \dots p_{im}^{[y_i=m]}$$

where the notation $[\cdot]$ refers to the Iverson bracket¹. The dependence of the class probabilities on the covariates is specified through the relationship

$$g(p_{i1}, \dots, p_{im}) = (\alpha_1 + f_1(x_i), \dots, \alpha_m + f_m(x_i))$$

where $g : [0, 1]^m \rightarrow \mathbb{R}^m$ is some specified link function. As we will see later, a normal regression model as in (1.1) subject to (1.2) naturally implies a *probit* link function. With an I-prior assumed on the f_j 's, we call this method of probit regression using I-priors the *I-probit* regression model.

Due to the nature of the model, unfortunately, the posterior distribution of the regression functions cannot be found in closed form. In particular, marginalising the I-prior from the joint likelihood involves a high-dimensional intractable integral. We explore a fully Bayesian approach to estimate I-probit models using *variational inference*. The main idea is to replace the difficult posterior distribution with an approximation that is tractable. Working in a Bayesian setting together with variational inference allows us to estimate the model much faster than traditional MCMC sampling methods, yet provides us with the conveniences that come with Bayesian machinery. For example, inferences around log-odds is usually cumbersome for probit models, but a credibility interval can easily be obtained by resampling methods from the relevant posteriors, which are typically made up of densities which are familiar and readily available in software.

By choosing appropriate RKHSs/RKKSs for the regression functions, we are able to fit a multitude of binary and multinomial models, including multilevel or random-effects models, linear and non-linear classification models, and even spatio-temporal models. Examples of these models applied to real-world data is shown in Section 5.8. We find that the many advantages of the normal I-prior methodology transfer over quite well to the I-probit model for binary and multinomial regression.

¹ $[A]$ returns 1 if the proposition A is true, and 0 otherwise. The Iverson bracket is a generalisation of the Kronecker delta.

sec:iprobit
naive

5.1 A naïve model

A naïve application of the normal I-prior methodology to fit categorical data is insightful for the upcoming sections. Suppose, as before, we observe data $\{(y_1, x_1), \dots, (y_n, x_n)\}$ where each $x_i \in \mathcal{X}$, for $i = 1, \dots, n$. Here, the responses are categorical $\mathbf{y}_i \in \{1, \dots, m\} =: \mathcal{M}$, and additionally, write $y_{i\cdot} = (y_{i1}, \dots, y_{im})^\top$ where the class responses y_{ij} equal one if individual i 's response category is $y_i = j$, and zero otherwise. In other words, there is exactly a single '1' at the j 'th position in the vector $\mathbf{y}_{i\cdot}$, and zeroes everywhere else. For $j = 1, \dots, m$, we model

$$\begin{aligned} y_{ij} &= \alpha + \alpha_j + f_j(x_i) + \epsilon_{ij} \\ (\epsilon_{i1}, \dots, \epsilon_{im})^\top &\stackrel{\text{iid}}{\sim} N_m(\mathbf{0}, \Psi^{-1}). \end{aligned} \tag{5.1}$$

{eq:naiveclassmod}

The idea here being that we attempt to model the class responses y_{ij} using class-specific regression functions f_j , and the class responses are assumed to be independent among individuals, but may or may not be correlated among classes for each individual. The class correlations are manifest themselves in the variance of the errors Ψ^{-1} , which is an $m \times m$ matrix.

Denote the regression function f in (5.1) on the set $\mathcal{X} \times \mathcal{M}$ as $f(x_i, j) = \alpha_j + f_j(x_i)$. This regression function can be seen as an ANOVA decomposition of the spaces $\mathcal{F}_{\mathcal{M}}$ and $\mathcal{F}_{\mathcal{X}}$ of functions over \mathcal{M} and \mathcal{X} respectively. That is, $\mathcal{F} = \mathcal{F}_{\mathcal{M}} \oplus (\mathcal{F}_{\mathcal{M}} \otimes \mathcal{F}_{\mathcal{X}})$ is a decomposition into the main effects of 'class', and an interaction effect of the covariates for each class. Let $\mathcal{F}_{\mathcal{M}}$ and $\mathcal{F}_{\mathcal{X}}$ be RKHSs respectively with kernels $a : \mathcal{M} \times \mathcal{M} \rightarrow \mathbb{R}$ and $b : \mathcal{X} \times \mathcal{X} \rightarrow \mathbb{R}$. Then, the ANOVA RKKS \mathcal{F} possesses the reproducing kernel $h : (\mathcal{X} \times \mathcal{M})^2 \rightarrow \mathbb{R}$ as defined by

$$b_\eta((x, j), (x', j')) = a(j, j') + a(j, j')h_\eta(x, x'). \tag{5.2}$$

{eq:anovaclass}

The kernel h_η may be any of the kernels described in this thesis, ranging from the linear kernel, to the fBm kernel, or even an ANOVA kernel. Choices for $a : \mathcal{M} \times \mathcal{M} \rightarrow \mathbb{R}$ include

1. **The Pearson kernel** (as defined in Definition 2.34). With $J \sim P$, a probability measure over \mathcal{M} ,

$$a(j, j') = \frac{\delta_{jj'}}{P(J = j)} - 1.$$

2. **The identity kernel.** With δ denoting the Kronecker delta function,

$$a(j, j') = \delta_{jj'}.$$

The purpose of either of these kernels is to contribute to the class intercepts α_j , and to associate a regression function in each class. We have a slight preference for the identity kernel, which lends itself as being easy to handle computationally. The only difference between the two is the inverse probability weighting per class that is applied in the Pearson kernel, but not in the identity kernel.

As a remark, the functions in $\mathcal{F}_{\mathcal{M}}$ and $\mathcal{F}_{\mathcal{X}}$ need necessarily be zero-mean functions (as per the functional ANOVA definition in [Definition 2.37](#)). What this means is that $\sum_{j=1}^m \alpha_j = 0$, $\sum_{j=1}^m f_j(x_i) = 0$, and $\sum_{i=1}^n f_j(x_i) = 0$. In particular,

$$\begin{aligned} \sum_{j=1}^m y_{ij} &= \sum_{j=1}^m (\alpha + \alpha_j + f_j(x_i)) \\ &= m\alpha + \sum_{j=1}^m \alpha_j + \sum_{j=1}^m f_j(x_i) \end{aligned}$$

and since $\sum_{j=1}^m y_{ij} = 1$, we have that $\alpha = 1/m$ and can thus be fixed to resolve identification. The Pearson RKHS will contain zero mean functions, but the RKHS of constant functions induced by the identity kernel may not. If this is the case, then it should be ensured that $\sum_{j=1}^m \alpha_j = 0$ in other ways; perhaps, as a requirement during estimation.

With $f \in \mathcal{F}$ the RKKS with kernel h_η , it is straightforward to assign an I-prior on f . It is in fact

$$\begin{aligned} f(x_i, j) &= \sum_{j'=1}^m \sum_{i'=1}^n a(j, j') (1 + h_\eta(x_i, x_{i'})) w_{i'j'} \\ (w_{i'1}, \dots, w_{i'm})^\top &\stackrel{\text{iid}}{\sim} N_m(\mathbf{0}, \Psi) \end{aligned} \tag{5.3}$$

{eq:naivecl
assiprior}

assuming a zero prior mean $f_0(x, j) = 0$. It is much more convenient to work in vector and matrix form, so let us introduce some notation. Let \mathbf{w} (c.f. \mathbf{y} , \mathbf{f} and $\boldsymbol{\epsilon}$) be an $n \times m$ matrix whose (i, j) entries contain w_{ij} (c.f. y_{ij} , $f(x_i, j)$, and ϵ_{ij}). The row-wise entries of \mathbf{w} are independent of each other (independence assumption of the n observations), while any two of their columns have covariance as specified in Ψ . This means that \mathbf{w} follows a matrix normal distribution $MN_{n,m}(\mathbf{0}, \mathbf{I}_n, \Psi)$, which implies $\text{vec } \mathbf{w} \sim N_{nm}(\mathbf{0}, \Psi \otimes \mathbf{I}_n)$.

and similarly, $\epsilon \sim N_{nm}(\mathbf{0}, \Psi^{-1} \otimes \mathbf{I}_n)$. Denote by \mathbf{H}_η the $n \times n$ kernel matrix with entries supplied by $1 + h_\eta$, and \mathbf{A} the $m \times m$ matrix with entries supplied by a . From (5.3), we have that

$$\mathbf{f} = \mathbf{H}_\eta \mathbf{w} \mathbf{A} \in \mathbb{R}^{n \times m},$$

and thus $\text{vec } \mathbf{f} \sim N_{nm}(\mathbf{0}, \mathbf{A} \Psi \mathbf{A} \otimes \mathbf{H}_\eta^2)$. As $\mathbf{y} = \mathbf{1}_n \alpha^\top + \mathbf{f} + \epsilon$, where $\alpha \in \mathbb{R}^m$ with j 'th component $\alpha + \alpha_j = 1/m + \alpha_j$, by linearity we have that

$$\text{vec } \mathbf{y} \sim N_{nm}(\text{vec } \alpha, (\mathbf{A} \Psi \mathbf{A} \otimes \mathbf{H}_\eta^2) + (\Psi^{-1} \otimes \mathbf{I}_n)) \quad (5.4)$$

and

$$\text{vec } \mathbf{y} | \text{vec } \mathbf{w} \sim N_{nm}(\text{vec}(\alpha + \mathbf{H}_\eta \mathbf{w} \mathbf{A}), (\Psi^{-1} \otimes \mathbf{I}_n)). \quad (5.5)$$

which can then be estimated using the methods described in Chapter 4.

When using the identity kernel in conjunction with an assumption of iid errors ($\Psi = \psi \mathbf{I}_n$), the above distributions simplify further. Specifically, the variance in the marginal distribution becomes

$$\begin{aligned} \text{Var}(\text{vec } \mathbf{y}) &= (\psi \mathbf{I}_m \otimes \mathbf{H}_\eta^2) + (\psi^{-1} \mathbf{I}_m \otimes \mathbf{I}_n) \\ &= (\mathbf{I}_m \otimes \psi \mathbf{H}_\eta^2) + (\mathbf{I}_m \otimes \psi^{-1} \mathbf{I}_n) \\ &= \mathbf{I}_m \otimes \underbrace{(\psi \mathbf{H}_\eta^2 + \psi^{-1} \mathbf{I}_n)}_{\mathbf{V}_y}. \end{aligned}$$

which implies independence and identical variances \mathbf{V}_y for the vectors $(y_{1j}, \dots, y_{nj})^\top$ for each class $j = 1, \dots, m$. Evidently, this stems from the implied independence structure of the prior on f too, since now $\text{Var}(\text{vec } \mathbf{f}) = \text{diag}(\psi \mathbf{H}_\eta^2, \dots, \psi \mathbf{H}_\eta^2)$, which could be interpreted as having independent and identical I-priors on the regression functions for each class $\mathbf{f}_{\cdot j} = (f(x_{1,j}), \dots, f(x_{n,j}))^\top$.

There are several downfalls to using the model described above. Unlike in the case of continuous response variables, the normal I-prior model is highly inappropriate for categorical responses. For one, it violates the normality and homoscedasticity assumptions of the errors. For another, predicted values may be out of the range $[0, m]$ and thus poorly calibrated. Furthermore, it would be more suitable if the class probabilities—the probability of an observation belonging to a particular class—were also part of the model. In the next section, we propose an improvement to this naïve I-prior classification model by considering a probit-like transformation of the regression functions.

5.2 A latent variable motivation: the I-probit model

Let $y_i, \mathbf{y}_i. = (y_{i1}, \dots, y_{im})^\top$ and $x_i \in \mathcal{X}$ be as described in [Section 5.1](#), and additionally, for $i = 1, \dots, n$, let $y_i \sim \text{Cat}(p_{i1}, \dots, p_{im})$. In this formulation, each y_{ij} is distributed as Bernoulli with probability p_{ij} . Now, assume that, for each y_{i1}, \dots, y_{im} , there exists corresponding *continuous, underlying, latent variables* $y_{i1}^*, \dots, y_{im}^*$ such that

$$y_i = \begin{cases} 1 & \text{if } y_{i1}^* \geq y_{i2}^*, y_{i3}^*, \dots, y_{im}^* \\ 2 & \text{if } y_{i2}^* \geq y_{i1}^*, y_{i3}^*, \dots, y_{im}^* \\ \vdots & \\ m & \text{if } y_{im}^* \geq y_{i2}^*, y_{i3}^*, \dots, y_{i,m-1}^*. \end{cases} \quad (5.6)$$

{eq:latentmodel}

In other words, $y_{ij} = \arg \max_{k=1}^m y_{ik}^*$. Such a formulation is common in economic choice models, and is rationalised by a utility-maximisation argument: an agent faced with a choice from a set of alternatives will choose the one which benefits them most. In this sense, the y_{ij}^* 's represent individual i 's *latent propensities* for choosing alternative j .

Instead of modelling the observed y_{ij} 's directly, we model instead the n latent variables in each class $j = 1, \dots, m$ according to the regression problem

$$\begin{aligned} y_{ij}^* &= \alpha + \alpha_j + f_j(x_i) + \epsilon_{ij} \\ (\epsilon_{i1}, \dots, \epsilon_{im})^\top &\stackrel{\text{iid}}{\sim} N_m(\mathbf{0}, \mathbf{\Psi}^{-1}). \end{aligned} \quad (5.7)$$

{eq:multinomial-latent}

We can see some semblance of this model with the one in [\(5.3\)](#), and ultimately the aim is to assign I-priors to the regression function of these latent variables, which we shall describe shortly. For now, write $\boldsymbol{\mu}(x_i) \in \mathbb{R}^m$ whose j 'th component is $\alpha + \alpha_j + f_j(x_i)$, and realise that each $\mathbf{y}_i. = (y_{i1}^*, \dots, y_{im}^*)^\top$ has the distribution $N_m(\boldsymbol{\mu}(x_i), \mathbf{\Psi}^{-1})$, conditional on the data x_i , the intercepts $\alpha, \alpha_1, \dots, \alpha_m$, the evaluations of the functions at x_i for each class $f_1(x_i), \dots, f_m(x_i)$, and the error covariance matrix $\mathbf{\Psi}^{-1}$.

The probability p_{ij} of observation i belonging to class j is calculated as

$$\begin{aligned} p_{ij} &= P(y_i = j) \\ &= P(\{y_{ij}^* > y_{ik}^* \mid \forall k \neq j\}) \\ &= \int \cdots \int_{\{y_{ij}^* > y_{ik}^* \mid \forall k \neq j\}} \phi(y_{i1}^*, \dots, y_{im}^* \mid \boldsymbol{\mu}(x_i), \mathbf{\Psi}^{-1}) dy_{i1}^* \cdots dy_{im}^*, \end{aligned} \quad (5.8)$$

{eq:pij}

where $\phi(\cdot|\mu, \Sigma)$ is the density of the multivariate normal with mean μ and variance Σ . This is the probability that the normal random variable \mathbf{y}_i^* belongs to the set $\{y_{ij}^* > y_{ik}^* | \forall k \neq j\}$, which are cones in \mathbb{R}^m . Since the union of these cones is the entire m -dimensional space of reals, the probabilities add up to one and hence they represent a proper probability mass function for the classes. While this does not have a closed-form expression and highlights one of the difficulties of working with probit models, the integral is by no means impossible to compute—see [Section 5.7.1](#) for a note regarding this matter.

Now, we'll see how to specify an I-prior on the regression problem (5.7). In the naïve I-prior model, we wrote $f(x_i, j) = \alpha_j + f_j(x_i)$, and called for f to belong to an ANOVA RKKS with kernel defined in (5.2). Instead of doing the same, we take a different approach. Treat the α_j 's in (5.7) as intercept parameters to estimate with the additional requirement that $\sum_{j=1}^m \alpha_j = 0$. Further, let \mathcal{F} be a (centred) RKHS/RKKS of functions over \mathcal{X} with reproducing kernel h_η . Now, consider putting an I-prior on the regression functions $f_j \in \mathcal{F}$, $j = 1 \dots, m$, defined by

$$f_j(x_i) = f_0(x_i) + \sum_{k=1}^n h_\eta(x_i, x_k) w_{ik}$$

with $\mathbf{w}_i. := (w_{i1}, \dots, w_{im})^\top \stackrel{\text{iid}}{\sim} \mathbf{N}(0, \Psi)$. This is similar to the naïve I-prior specification (5.3), except that the intercept have been treated as parameters rather than accounting for them using an RKHS of constant functions. Importantly, the overall regression relationship still satisfies the ANOVA functional decomposition. We find that this approach bodes well down the line computationally.

We call the multinomial probit regression model of (5.6) subject to (5.7) and I-priors on $f_j \in \mathcal{F}$, the *I-probit model*. For completeness, this is stated again: for $i = 1, \dots, n$, $y_i = \arg \max_{k=1}^m y_{ik}^* \in \{1, \dots, m\}$, where, for $j = 1, \dots, m$,

$$\begin{aligned} y_{ij}^* &= \alpha + \alpha_j + \overbrace{f_0(x_i) + \sum_{k=1}^n h_\eta(x_i, x_k) w_{ik}}^{f_j(x_i)} + \epsilon_{ij} \\ \epsilon_i. &:= (\epsilon_{i1}, \dots, \epsilon_{im})^\top \stackrel{\text{iid}}{\sim} \mathbf{N}_m(\mathbf{0}, \Psi^{-1}) \\ \mathbf{w}_i. &:= (w_{i1}, \dots, w_{im})^\top \stackrel{\text{iid}}{\sim} \mathbf{N}_m(\mathbf{0}, \Psi). \end{aligned} \tag{5.9}$$

{eq:iprobit
mod}

The parameters of the I-probit model are denoted by $\theta = \{\alpha_1, \dots, \alpha_m, \eta, \Psi\}$. To establish notation, let

- $\epsilon \in \mathbb{R}^{n \times m}$ denote the matrix containing (i, j) entries ϵ_{ij} , whose rows are ϵ_i . and columns are $\epsilon_{.j}$. Its distribution is $\epsilon \sim \text{MN}_{n,m}(\mathbf{0}, \mathbf{I}_n, \Psi^{-1})$;
- $\mathbf{w} \in \mathbb{R}^{n \times m}$ denote the matrix containing (i, j) entries w_{ij} , whose rows are \mathbf{w}_i . and columns are $\mathbf{w}_{.j}$. Its distribution is $\mathbf{w} \sim \text{MN}_{n,m}(\mathbf{0}, \mathbf{I}_n, \Psi)$;
- $\mathbf{f} \in \mathbb{R}^{n \times m}$ denote the matrix containing (i, j) entries $f_j(x_i)$, and \mathbf{f}_0 a vector equal to $(f_0(x_1), \dots, f_0(x_n))^\top$. We then have $\mathbf{f} = \mathbf{1}_n \mathbf{f}_0^\top + \mathbf{H}_\eta \mathbf{w} \sim \text{MN}_{n,m}(\mathbf{1}_n \mathbf{f}_0^\top, \mathbf{H}_\eta^2, \Psi)$;
- $\alpha = (\alpha + \alpha_1, \dots, \alpha + \alpha_m)^\top \in \mathbb{R}^m$ be the vector of intercepts;
- $\mu = \mathbf{1}_n \alpha^\top + \mathbf{f}$, whose (i, j) entries are $\mu_j(x_i) = \alpha + \alpha_j + f_j(x_i)$; and
- $\mathbf{y}^* \in \mathbb{R}^{n \times m}$ denote the matrix containing (i, j) entries y_{ij}^* . That is, $\mathbf{y}^* = \mu + \epsilon$, so $\mathbf{y}^* | \mathbf{w} \sim \text{MN}_{n,m}(\mu = \mathbf{1}_n \alpha^\top + \mathbf{H}_\eta \mathbf{w}, \mathbf{I}_n, \Psi^{-1})$ and $\text{vec } \mathbf{y}^* \sim \text{N}_{nm}(\text{vec}(\mathbf{1}_n \alpha^\top), \Psi \otimes \mathbf{H}_\eta^2 + \Psi^{-1} \otimes \mathbf{I}_n)$. The marginal distribution of \mathbf{y}^* cannot be written as a matrix normal, except when $\Psi = \mathbf{I}_m$.

Before proceeding with estimating the I-probit model (5.9), we lay out several standing assumptions:

A4 Centred responses. Set $\alpha = 0$.

A5 Zero prior mean. Assume a zero prior mean $f_0(x) = 0$ for all $x \in \mathcal{X}$.

A6 Fixed error precision. Assume Ψ is fixed.

Assumption A4 is a requirement for identifiability. Assumption A5 is motivated by a similar argument to assumption A2 in the normal I-prior model. As for assumption A6, we do not consider estimation of the error precision in this thesis mainly due to time limitations. More on this in Section 5.7.3.

5.3 Identifiability and IIA

The parameters in a linear multinomial probit model is well known to be unidentified (Michael P. Keane, 1992; Train, 2009), and the reason for this is two-fold. Firstly, an addition of a constant to the latent variables y_{ij}^* 's in (5.6) will not change which latent variable is maximal, and therefore leaves the model unchanged. Secondly, all

latent variables can be scaled by some positive constant without changing which latent variable is largest. Therefore, a *linear parameterisation* for the multinomial probit model is not identified as there can be more than one set of parameters for which the class probabilities are the same. To fix this issue, constraints are imposed on location and scale of the latent variables.

However, for the I-probit model, this is not the case, because the model is not related to the parameters $\theta = \{\alpha_1, \dots, \alpha_m, \eta, \Psi\}$ linearly. One cannot simply add to or multiply θ by a constant and expect the model to be left unchanged. Thus, the I-probit model is identified in the parameter set θ without having to impose any restrictions, particularly on the precision matrix Ψ (if this is to be estimated).

To see how the I-probit model is location identified, suppose assumptions A4 and A5 hold, and consider a constant a added to the latent propensities. This would then imply the relationship

$$a + y_{ij}^* = \overbrace{a + \alpha_j}^{\alpha_j^*} + f_j(x_i) + \epsilon_{ij},$$

which is similar to adding the constant a to all of the intercept parameters α_j —denote these new intercepts by α_j^* . As a requirement of the functional ANOVA decomposition, the α_j^* ’s need to sum to zero, but we already have that $\sum_{j=1}^m \alpha_j = 0$, so it must be that $a = 0$. This also highlights the reason behind assumption A4 and A5 for fixing the grand intercept α to zero.

As for identification in scale, consider multiplying the latent variables by $c > 0$. Denote by $\mathbf{V}_y^*(\omega) \in \mathbb{R}^{nm \times nm}$ the marginal covariance matrix of the latent propensities, which depends on the scale parameters $\omega = \{\eta, \Psi\}$. The scaled latent variables $\{c^{1/2}y_{ij}^* \mid \forall i, j = 1, \dots\}$, which collectively has (marginal) variance and covariances given by the matrix $c\mathbf{V}_y^*(\omega)$, is expected to have been generated from the model with parameters $c\omega$. However, we have that

$$\begin{aligned} c\mathbf{V}_y^*(\omega) &= c(\Psi \otimes \mathbf{H}_\eta^2) + c(\Psi^{-1} \otimes \mathbf{I}_n) \\ &= (c\Psi \otimes \mathbf{H}_\eta^2) + (c\Psi^{-1} \otimes \mathbf{I}_n) \\ &\neq \mathbf{V}_y^*(c\omega). \end{aligned}$$

Now, we turn to a discussion of the role of Ψ in the model. In decision theory, the independence axiom states that an agent’s choice between a set of alternatives should not be affected by the introduction or elimination of a choice option. The probit model

is suitable for modelling multinomial data where the independence axiom, which is also known as the *independence of irrelevant alternatives* (IIA) assumption, is not desired. Such cases arise frequently in economics and social science, and the famous Red-Bus-Blue-Bus example is often used to illustrate IIA: suppose commuters face the decision between taking cars and red busses. The addition of blue busses to commuters' choices should, in theory, be more likely chosen by those who prefer taking the bus over cars. That is, assuming commuters are indifferent about the colour of the bus, commuters who are predisposed to taking the red bus would see the blue bus as an identical alternative. Yet, if IIA is imposed, then the three choices are distinct, and the fact that red and blue busses are substitutable is ignored.

To put it simply, the model is IIA if choice probabilities depend only on the choice in consideration, and not on any other alternatives. In the I-probit model, or rather, in probit models in general, choice dependency is controlled by the error precision matrix Ψ . Specifically, the off-diagonal elements Ψ_{jk} capture the correlation between alternatives j and k . Allowing all $m(m+1)/2$ covariance elements of Ψ to be non-zero leads to the *full I-probit model*, and would not assume an IIA position.

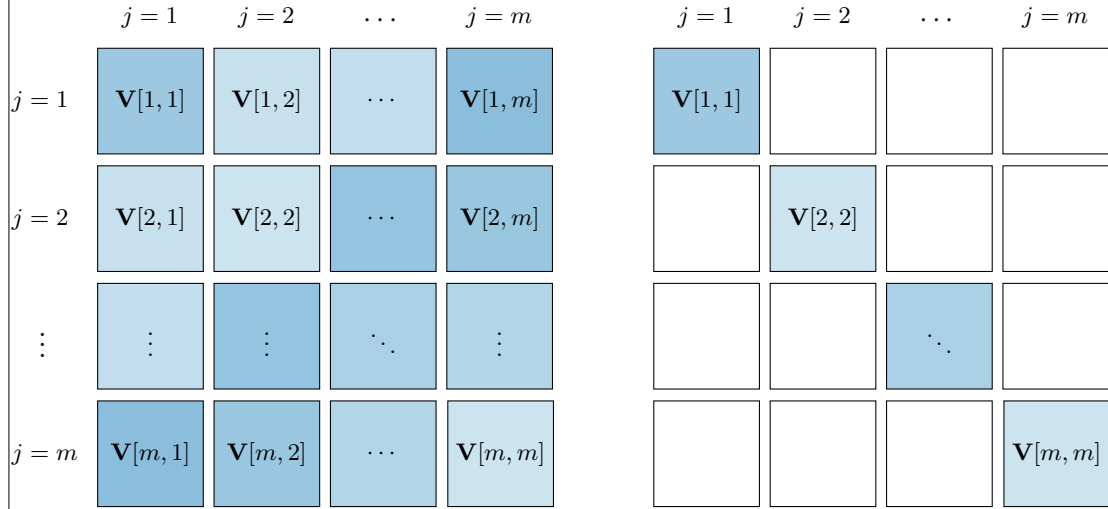


Figure 5.1: Illustration of the covariance structure of the full I-probit model (left) and the independent I-probit model (right). The full model has m^2 blocks of $n \times n$ symmetric matrices, and the blocks themselves are arranged symmetrically about the diagonal. The independent model, on the other hand, has a block diagonal structure, and its sparsity induces simpler computational methods for estimation.

fig:iprobco
vstr

While it is an advantage to be able to model the correlations across choices (unlike in logistic models), there are applications where the IIA assumption would not adversely affect the analysis, such as classification tasks. Some analyses might also be indifferent as to whether or not choice dependency exists. In these situations, it would be beneficial, algorithmically speaking, to reduce the I-probit model to a simpler version by assuming $\Psi = \text{diag}(\psi_1, \dots, \psi_m)$, which would trigger the IIA assumption in the I-probit model. We refer to this model as the *independent I-probit model*.

The independence assumption causes the distribution of the latent variables to be $y_{ij}^* \sim N(\mu_k(x_i), \sigma_j^2)$ for $j = 1, \dots, m$, where $\sigma_j^2 = \psi_j^{-1}$. As a continuation of line (5.8), we can show the class probability p_{ij} to be

$$\begin{aligned}
 p_{ij} &= \int \cdots \int \prod_{\substack{k=1 \\ \{y_{ik}^* > y_{ij}^* | \forall k \neq j\}}}^m \left\{ \phi(y_{ik}^* | \mu_k(x_i), \sigma_k^2) dy_{ik}^* \right\} \\
 &= \int \prod_{\substack{k=1 \\ k \neq j}}^m \Phi\left(\frac{y_{ij}^* - \mu_k(x_i)}{\sigma_k}\right) \cdot \phi(y_{ij}^* | \mu_j(x_i), \sigma_j^2) dy_{ij}^* \\
 &= E_Z \left[\prod_{\substack{k=1 \\ k \neq j}}^m \Phi\left(\frac{\sigma_j}{\sigma_k} Z + \frac{\mu_j(x_i) - \mu_k(x_i)}{\sigma_k}\right) \right] \tag{5.10}
 \end{aligned}$$

{eq:pij2}

where $Z \sim N(0, 1)$, $\Phi(\cdot)$ its cdf, and $\phi(\cdot | \mu, \sigma^2)$ is the pdf of $X \sim N(\mu, \sigma^2)$. The equation (5.8) is thus simplified to a unidimensional integral involving the Gaussian pdf and cdf, which can be computed fairly efficiently using quadrature methods. The probit link function is evidently seen in the above equation.

5.4 Estimation

As with the normal I-prior model, an estimate of the posterior regression function with optimised hyperparameters is sought. The log likelihood function $L(\cdot)$ for θ using all n observations $\{(y_1, x_1), \dots, (y_n, x_n)\}$ is obtained by integrating out the I-prior from the

categorical likelihood, as follows:

$$\begin{aligned} L(\theta) &= \log \int p(\mathbf{y}|\mathbf{w}, \theta) p(\mathbf{w}|\theta) d\mathbf{w} \\ &= \log \int \prod_{i=1}^n \prod_{j=1}^m \left(g_j^{-1} \left(\alpha_k + \overbrace{f_k(x_i)}^{\sum_{i'=1}^n h_\eta(x_i, x_{i'}) w_{i'k}} \right)_{k=1}^m \right)^{[y_i=j]} \cdot \text{MN}_{n,m}(\mathbf{w}|\mathbf{0}, \mathbf{I}_n, \Psi) d\mathbf{w} \end{aligned} \quad (5.11)$$

{eq:intractablelikelihood}

where we have denoted the probit relationship from (5.8) using the function $g_j^{-1} : \mathbb{R}^m \rightarrow [0, 1]$. Unlike in the continuous response models, the integral does not present itself in closed form due to the conditional categorical PMF of the y_i 's, which they themselves involve integrals of multivariate normal densities. For binary response models, g^{-1} is simply the probit function, but for multinomial responses, this can be quite challenging to evaluate—more on this in Section 5.7.1.

Furthermore, the posterior distribution of the regression function, which requires the density of $\mathbf{w}|\mathbf{y}$, depends on the marginalisation provided by (5.11). The challenge of estimation is then to first overcome this intractability by means of a suitable approximation of the integral. We present three possible avenues to achieve this aim, namely the Laplace approximation, variational Bayes, and Markov chain Monte Carlo (MCMC) methods.

5.4.1 Laplace approximation

To compute the posterior density $p(\mathbf{w}|\mathbf{y}) \propto p(\mathbf{y}|\mathbf{w})p(\mathbf{w}) =: e^{Q(\mathbf{w})}$ with normalising constant equal to the marginal density of \mathbf{y} , $p(\mathbf{y}) = \int e^{Q(\mathbf{w})} d\mathbf{w}$, we have established that this is intractable. Laplace's method (Kass and Raftery, 1995, §4.1.1, pp. 777–778) entails expanding a Taylor series for Q about its posterior mode $\hat{\mathbf{w}} = \arg \max_{\mathbf{w}} p(\mathbf{y}|\mathbf{w})p(\mathbf{w})$, which gives the relationship

$$\begin{aligned} Q(\mathbf{w}) &= Q(\hat{\mathbf{w}}) + \underbrace{(\mathbf{w} - \hat{\mathbf{w}})^\top \nabla Q(\hat{\mathbf{w}})}_{\rightarrow 0} - \frac{1}{2}(\mathbf{w} - \hat{\mathbf{w}})^\top \mathbf{\Omega}(\mathbf{w} - \hat{\mathbf{w}}) + \dots \\ &\approx Q(\hat{\mathbf{w}}) + -\frac{1}{2}(\mathbf{w} - \hat{\mathbf{w}})^\top \mathbf{\Omega}(\mathbf{w} - \hat{\mathbf{w}}), \end{aligned}$$

because, assuming that Q has a unique maxima, ∇Q evaluated at its mode is zero. This is recognised as the logarithm of an unnormalised Gaussian density, implying $\mathbf{w}|\mathbf{y} \sim N_n(\hat{\mathbf{w}}, \mathbf{\Omega}^{-1})$. Here, $\mathbf{\Omega} = -\nabla^2 Q(\mathbf{w})|_{\mathbf{w}=\hat{\mathbf{w}}}$ is the negative Hessian of Q evaluated at the

posterior mode, and is typically obtained as a byproduct of the maximisation routine of Q using gradient or quasi-gradient based methods.

The marginal distribution is then approximated by

$$\begin{aligned}
 p(\mathbf{y}) &\approx \int \exp \overbrace{Q(\mathbf{w})}^{Q(\hat{\mathbf{w}}) - \frac{1}{2}(\mathbf{w} - \hat{\mathbf{w}})^\top \boldsymbol{\Omega}(\mathbf{w} - \hat{\mathbf{w}})} d\mathbf{w} \\
 &= (2\pi)^{n/2} |\boldsymbol{\Omega}|^{-1/2} e^{Q(\hat{\mathbf{w}})} \int (2\pi)^{-n/2} |\boldsymbol{\Omega}|^{1/2} \exp \left(-\frac{1}{2}(\mathbf{w} - \hat{\mathbf{w}})^\top \boldsymbol{\Omega}(\mathbf{w} - \hat{\mathbf{w}}) \right) d\mathbf{w} \\
 &= (2\pi)^{n/2} |\boldsymbol{\Omega}|^{-1/2} p(\mathbf{y}|\hat{\mathbf{w}}) p(\hat{\mathbf{w}}).
 \end{aligned}$$

The log marginal density of course depends on the parameters θ , which becomes the objective function to maximise in a likelihood maximising approach. Note that, should a fully Bayesian approach be undertaken, i.e. priors prescribed on the model parameters using $\theta \sim p(\theta)$, then this approach is viewed as a maximum a posteriori approach.

In any case, each evaluation of the objective function $L(\theta) = \log p(\mathbf{y}|\theta)$ involves finding the posterior modes $\hat{\mathbf{w}}$. This is a slow and difficult undertaking, especially for large sample sizes n —even assuming computation of the class probabilities g^{-1} is efficient—because the dimension of this integral is exactly the sample size. Furthermore, obtaining standard errors for the parameters are cumbersome, and it is likely that a computationally burdensome bootstrapping approach is needed. Lastly, as a comment, Laplace’s method only approximates the true marginal likelihood well if the true function is small far away from the mode.

5.4.2 Variational inference

We turn to variational inference as a method of estimation. Variational methods are widely discussed in the machine learning literature, but there have been efforts to popularise it in statistics (Blei et al., 2017). In a fully Bayesian setting, one obtains an approximation to the intractable posterior distribution of interest, which is then used for inferential purposes in lieu of the actual posterior distribution.

In addition to the I-probit model, suppose that prior distributions are assigned on the hyperparameters of the model, $\theta \sim p(\theta)$. By appending the latent variables $\{\mathbf{y}^*, \mathbf{w}\}$ to the hyperparameters θ , we seek an approximation

$$p(\mathbf{y}^*, \mathbf{w}, \theta | \mathbf{y}) \approx \tilde{q}(\mathbf{y}^*, \mathbf{w}, \theta),$$

where \tilde{q} satisfies $\tilde{q} = \arg \min_q \text{KL}(q||p)$, subject to certain constraints. The constraint considered by us in this thesis is that q satisfies a *mean-field* factorisation

$$q(\mathbf{y}^*, \mathbf{w}, \theta) = q(\mathbf{y}^*)q(\mathbf{w})q(\theta).$$

Under this scheme, the posterior for \mathbf{y}^* is found to be a *conically truncated multivariate normal* distribution, and for \mathbf{w} , a multivariate normal distribution. The posterior density $q(\theta)$ is often of a recognisable form, and usually one of the exponential family densities (normal, Wishart or gamma). This is useful, because point estimates of the hyperparameters can be taken to be either the mean or mode of these well-known distributions. In cases where $q(\theta)$ does not conform to an exponential family type density, then inference can still be done by sampling methods.

It can be shown that, for some variational density q , the marginal log-likelihood is an upper-bound for the quantity \mathcal{L}

$$\log p(\mathbf{y}) \geq \mathbb{E}_q \log p(\mathbf{y}, \mathbf{y}^*, \mathbf{w}, \theta) - \mathbb{E}_q \log \tilde{q}(\mathbf{y}^*, \mathbf{w}, \theta) =: \mathcal{L},$$

a quantity often referred to as the *evidence lower bound* (ELBO). It turns out that minimising $\text{KL}(q||p)$ is equivalent to maximising the ELBO, a quantity that is more practical to work with than the KL divergence. That is, if \tilde{q} approximates the true posterior well, then the ELBO is a suitable proxy for the maximised marginal log-likelihood.

The algorithm to obtain \tilde{q} which maximises the ELBO is known as the *coordinate ascent variational inference* (CAVI) algorithm. The algorithm itself typically condenses to that of a simple, sequential updating scheme, akin to the expectation-maximisation (EM) algorithm for exponential families we saw in Chapter 4, which is very fast to implement compared to the other methods described in the previous subsections. A full derivation of the variational algorithm used by us will be described in [Section 5.5](#).

5.4.3 Markov chain Monte Carlo methods

As an alternative to the deterministic Bayesian approach of variational inference, it is possible to use Markov chain Monte Carlo sampling methods as an approach to stochastically approximate the intractable posterior distribution.

Albert and Chib (1993) showed that the latent variable approach to probit models can be analysed using exact Bayesian methods, due to the underlying normality structure. Paired with corresponding conjugate prior choices, sampling from the posterior is very simple using a Gibbs sampling approach. On the other hand, this data augmentation scheme enlarges the variable space to $n + q$ dimensions, where q is the number of parameters to estimate, which is inefficient and computationally challenging especially when n is large. It is no longer possible to marginalise the normal latent variables from the model, as this is intractable, as discussed previously.

Hamiltonian Monte Carlo is another possibility, since it does not require conjugacy. For binary models, this is a feasible approach because the class probabilities are a function of the normal CDF, which means that it is doable using off-the-shelf software such as Stan. However, with multinomial responses, the arduous task of computing class probabilities, which involve integration of an at most m -dimensional normal density, must be addressed separately.

5.4.4 Comparison of estimation methods

In this subsection, we utilise a toy binary classification data set which has been simulated according to a spiral pattern, as in Figure 5.2. The predictor variables are X_1 and X_2 , each of which are scaled similarly.

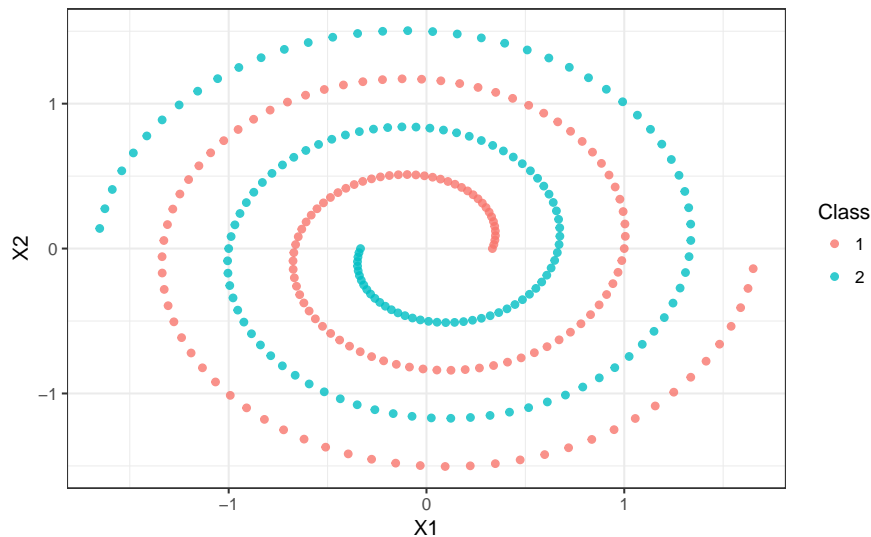


Figure 5.2: A plot of simulated spiral data set.

fig:example
iprobit

The I-probit model that is fitted is

$$y_i \sim \text{Bern}(p_i)$$

$$\Phi^{-1}(p_i) = \alpha + \sum_{k=1}^n h_{\lambda}(x_i, x_k) w_k$$

$$w_1, \dots, w_n \stackrel{\text{iid}}{\sim} \text{N}(0, 1).$$

This binary model follows from the more general multinomial I-probit model by fixing all latent propensities in one of the classes to zero, and setting $\Psi = \mathbf{I}_m$. This is possible because only differences in latent propensities are of interest, and not the actual values themselves, and thus only $m - 1$ sets of posterior regression functions need to be estimated—see [Section 5.7.1](#) for further details.

The three estimation methods described aim to overcome the intractable integral by means of either a deterministic approximation (Laplace and variational inference) or a stochastic approximation (Hamiltonian MC). For the Bayesian methods, i.e. variational inference and Hamiltonian MC, vague priors were used on α and λ , namely $\text{N}(0, 100)$ and $\text{N}_+(0, 100)$ respectively. Restriction of λ to the positive orthant is required for identifiability. The Laplace and variational methods were performed in the **iprobit** package, while **Stan** was used to code the Hamiltonian MC sampler. The results are presented in [Table 5.1](#).

Table 5.1: Table comparing the estimated parameter values, (marginal) log-likelihood values, and also time taken for the three estimation methods.

| | Laplace approximation | Variational inference | Hamiltonian MC |
|------------------------|-----------------------|-----------------------|----------------|
| Intercept (α) | -0.02 (0.03) | 0.00 (0.06) | 0.00 (0.58) |
| Scale (λ) | 0.85 (0.01) | 5.67 (0.23) | 29.3 (5.21) |
| Log density | -202.7 | -140.7 | -163.8 |
| Error rate (%) | 44.7 | 0.00 | 2.24 |
| Brier score | 0.20 | 0.02 | 0.01 |
| Iterations | 20 | 56 | 2000 |
| Time taken (s) | >3600 | 5.32 | >3600 |

The three methods pretty much concur on the estimation of the intercept, but not on the RKHS scale parameter. As a result, the log-density value at the optima is also different in all three methods. Notice the high posterior standard deviation for the scale

tab:comprei
probit

parameter in the HMC method. The posterior density for λ was very positively skewed, and this contributed to the large posterior mean.

A plot of the log-likelihood surface for three methods in [Figure 5.3](#) reveals some insight. The variational likelihood reveals two ridges, with the maxima occurring around the intersection of these two ridges. The Laplace likelihood seems to indicate a similar shape—in both the Laplace and variational method, the posterior distribution of \mathbf{w} is approximated by a Gaussian distribution, with different means and variances. However, parts of the Laplace likelihood are poorly approximated resulting in a loss of fidelity around the supposed maxima, which might have contributed to the set of values that were estimated. Laplace’s method is known to yield poor approximations to probit-type likelihoods, as studied by [Kuss and Rasmussen \(2005\)](#). On the other hand, the log-likelihood using the posterior distribution of the Hamiltonian MC sampler (treating parameters as fixed values) yields a completely different shape compared to the other two methods.

In terms of predictive abilities, both the variational and Hamiltonian MC methods, even though the posteriors are differently estimated, has good predictive performance as indicated by their error rates and Brier scores. [Figure 5.3](#) shows that HMC is more confident of new data predictions compared to variational inference, as indicated by the intensity of the shaded regions (HMC is stronger than VI). Laplace’s method gave poor predictive performance.

Finally, on the computational side, variational inference was by far the fastest method to fit the model. Sampling using Hamiltonian MC was very slow, because the parameter space is in effect $O(n + 2)$ (parameters are $\{w_1, \dots, w_n, \alpha, \lambda\}$), and unlike in the normal model, we are not able to easily marginalise out the I-prior. As for Laplace, each Newton step involves obtaining posterior modes of the w ’s, and this contributed to the slowness of this method. The reality is that variational inference takes seconds to complete what either the Laplace or full MCMC methods would take hours to. The predictive performance, while not as good as HMC, is certainly an acceptable compromise in favour of speed.

5.5 A variational algorithm

We present a variational inference algorithm to estimate the I-probit latent variables \mathbf{y}^* and \mathbf{w} , together with the parameters $\theta = \{\boldsymbol{\alpha} = (\alpha_1, \dots, \alpha_m)^\top, \eta\}$ with *fixed error*

sec:iprobit
var

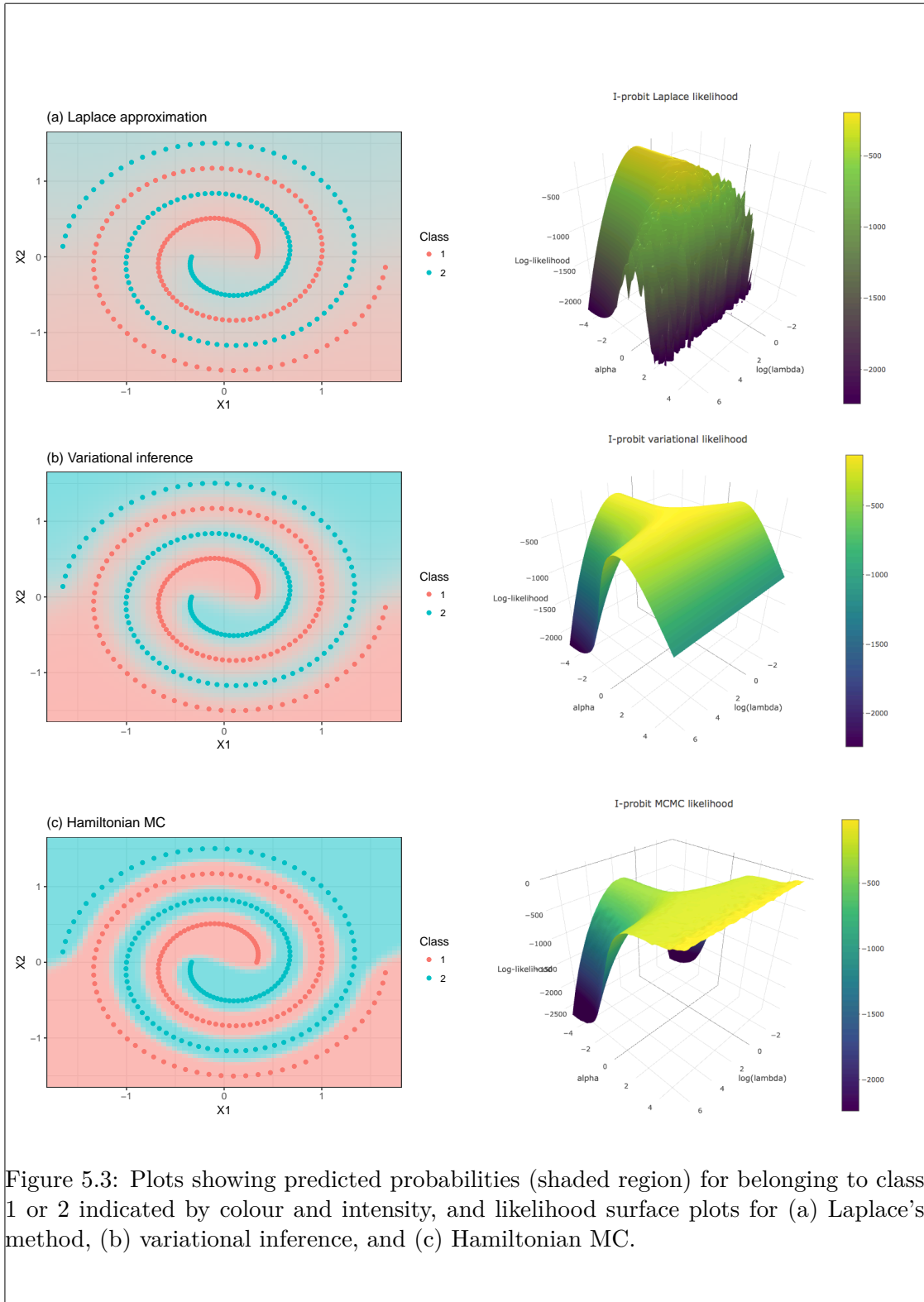


fig:example
iprobitfit

precision Ψ^2 . Begin by choosing prior distributions on the parameters, $p(\theta) = p(\boldsymbol{\alpha})p(\eta)$. The following flat, uninformative priors are suggested:

- **Kernel parameters** η . This may include parameters such as the Hurst index, lengthscale and offset parameters, in addition to the RKHS scale parameters $\lambda_1, \dots, \lambda_p$, and each with their own support. For the scale parameters, assign each λ_k the vague prior

$$\lambda_k \stackrel{\text{iid}}{\sim} \text{N}(0, v_\lambda = 0.001^{-1}), \quad k = 1, \dots, p.$$

As $v_k^{-1} \rightarrow 0$, the prior becomes $p(\lambda_k) \propto \text{const.}$, an improper prior. The default choice for the rest of the kernel parameters is an improper prior $p(\eta) \propto \text{const.}$

- **Intercepts** $\alpha_1, \dots, \alpha_m$. Assign independent, vague normal priors for each intercept

$$\alpha_j \stackrel{\text{iid}}{\sim} \text{N}(0, v_\alpha = 0.001^{-1}).$$

Although one may devote more attention to the prior specification of these parameters, for our purposes it suffices that they are independent component-wise, and that they are conjugate priors for the complete conditional density $p(\theta|\mathbf{y}, \mathbf{y}^*, \mathbf{w})$.

The posterior density of $\mathcal{Z} = \{\mathbf{y}^*, \mathbf{w}, \theta\}$ is approximated by a mean-field variational density q , i.e.

$$p(\mathbf{y}^*, \mathbf{w}, \theta|\mathbf{y}) = q(\mathbf{y}^*)q(\mathbf{w})q(\theta).$$

Additionally, we assume independence among the components of θ so that $q(\theta) = \prod_k q(\theta_k)$. We now present the mean-field variational distributions for each of unknowns in \mathcal{Z} . On notation: we will typically refer to posterior means of the parameters \mathbf{y}^* , \mathbf{w} , θ and so on by the use of a tilde. For instance, we write $\tilde{\mathbf{w}}$ to mean $\text{E}_{\mathbf{w} \sim q}[\mathbf{w}]$, the expected value of \mathbf{w} under the pdf $q(\mathbf{w})$. The distributions are simply stated, but a full derivation is given in the appendix.

²It turns out that the variational algorithm as presented is not suited to estimate Ψ . This issue is discussed further in Section X.

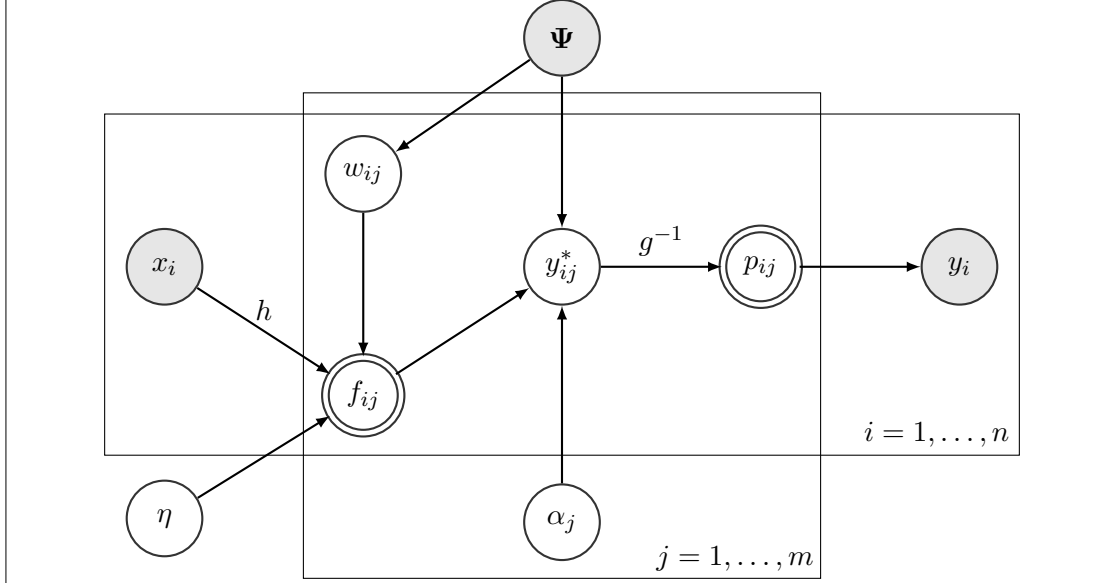


Figure 5.4: A DAG of the I-probit model. Observed/fixed nodes are shaded, while double-lined nodes represents calculable quantities.

5.5.1 Latent propensities \mathbf{y}^*

The fact that the rows $\mathbf{y}_i^* \in \mathbb{R}^m$, $i = 1, \dots, n$ of $\mathbf{y}^* \in \mathbb{R}^{n \times m}$ are independent can be exploited, which yields an induced factorisation $q(\mathbf{y}^*) = \prod_{i=1}^n q(\mathbf{y}_i^*)$. Define the set $\mathcal{C}_j = \{y_{ij}^* > y_{ik}^* \mid \forall k \neq j\}$. Then $q(\mathbf{y}_i^*)$ is the density of a multivariate normal distribution with mean $\tilde{\boldsymbol{\mu}}_{i.} = \tilde{\boldsymbol{\alpha}} + \tilde{\mathbf{w}}^\top \tilde{\mathbf{h}}_\eta(x_i)$, and variance $\boldsymbol{\Psi}^{-1}$ subject to the truncation of its components to the set \mathcal{C}_{y_i} . That is, for each $i = 1, \dots, n$ and noting the observed value $y_i \in \{1, \dots, m\}$, the \mathbf{y}_i^* 's are distributed according to

$$\mathbf{y}_i^* \stackrel{\text{iid}}{\sim} \begin{cases} N_m(\tilde{\boldsymbol{\mu}}_{i.}, \boldsymbol{\Psi}^{-1}) & \text{if } y_{iy_i}^* > y_{ik}^*, \forall k \neq y_i \\ 0 & \text{otherwise.} \end{cases} \quad (5.12)$$

{eq:ystandardi
st}

We denote this by $\mathbf{y}_i^* \stackrel{\text{iid}}{\sim} \text{tN}(\tilde{\boldsymbol{\mu}}_{i.}, \boldsymbol{\Psi}^{-1}, \mathcal{C}_{y_i})$, and the important properties of this distribution are explored in the appendix.

The required expectations $E\mathbf{y}_i^* = E(y_{i1}^*, \dots, y_{im}^*)^\top$ are tricky to compute. One strategy might be Monte Carlo integration: using samples from $N_m(\tilde{\boldsymbol{\mu}}_{i.}, \boldsymbol{\Psi}^{-1})$, disregard those that do not satisfy the condition $y_{iy_i}^* > y_{ik}^*, \forall k \neq y_i$, and then take the sample average. This works reasonably well so long as the truncation region does not fall into the extreme tails of the multivariate normal. Alternatively, a fast, Gibbs based approach

to estimating the mean or any other quantity $\mathbb{E}[r(\mathbf{y}_{i.}^*)]$ can be implemented, and this is detailed in the appendix.

If the independent I-probit model is considered, where the covariance matrix has the independent structure $\Psi = \text{diag}(\sigma_1^{-2}, \dots, \sigma_m^{-2})$, then the expected value can be considered component-wise, and each component of this expectation is given by

$$\tilde{y}_{ik}^* = \begin{cases} \tilde{\mu}_{ik} - \sigma_k C_i^{-1} \int \phi_{ik}(z) \prod_{l \neq k, j} \Phi_{il}(z) \phi(z) dz & \text{if } k \neq y_i \\ \tilde{\mu}_{iy_i} - \sigma_{y_i} \sum_{k \neq y_i} (\tilde{y}_{ik}^* - \tilde{\mu}_{ik}) & \text{if } k = y_i \end{cases} \quad (5.13)$$

with

$$\begin{aligned} \phi_{ik}(Z) &= \phi\left(\frac{\sigma_{y_i}}{\sigma_k} Z + \frac{\tilde{\mu}_{iy_i} - \tilde{\mu}_{ik}}{\sigma_k}\right) \\ \Phi_{ik}(Z) &= \Phi\left(\frac{\sigma_{y_i}}{\sigma_k} Z + \frac{\tilde{\mu}_{iy_i} - \tilde{\mu}_{ik}}{\sigma_k}\right) \\ C_i &= \int \prod_{l \neq j} \Phi_{il}(z) \phi(z) dz \end{aligned}$$

and $Z \sim \mathcal{N}(0, 1)$ with pdf and cdf $\phi(\cdot)$ and $\Phi(\cdot)$ respectively. The integrals that appear above are functions of a unidimensional Gaussian pdf, and these can be computed rather efficiently using quadrature methods.

5.5.2 I-prior random effects w

Given that both $\text{vec } \mathbf{y}^* | \text{vec } \mathbf{w}$ and $\text{vec } \mathbf{w}$ are normally distributed, we find that the conditional posterior distribution $p(\mathbf{w} | \mathcal{Z}_{-\mathbf{w}}, \mathbf{y})$ is also normal, and therefore the approximate posterior density q for $\text{vec } \mathbf{w} \in \mathbb{R}^{nm}$ is also normal with mean and precision given by

$$\text{vec } \tilde{\mathbf{w}} = \tilde{\mathbf{V}}_w (\Psi \otimes \tilde{\mathbf{H}}_\eta) \text{vec}(\tilde{\mathbf{y}}^* - \mathbf{1}_n \tilde{\boldsymbol{\alpha}}^\top) \quad \text{and} \quad \tilde{\mathbf{V}}_w^{-1} = (\Psi \otimes \tilde{\mathbf{H}}_\eta^2) + (\Psi^{-1} \otimes \mathbf{I}_n). \quad (5.14)$$

We note the similarity between (5.14) above and the posterior distribution for the I-prior random effects in a normal model (4.7) seen in the previous chapter. Naïvely computing the inverse $\tilde{\mathbf{V}}_w^{-1}$ presents a computational challenge, as this takes $O(n^3 m^3)$ time. By exploiting the Kronecker product structure in $\tilde{\mathbf{V}}_w$, we are able to efficiently compute the required inverse in roughly $O(n^3 m)$ time—see the appendix for details.

If the independent I-probit model is assumed, i.e. $\tilde{\Psi} = \text{diag}(\tilde{\psi}_1, \dots, \tilde{\psi}_m)$, then the posterior covariance matrix $\tilde{\mathbf{V}}_w$ has a simpler structure: random matrix \mathbf{w} will have columns which are independent of each other. By writing $\mathbf{w}_{\cdot j} = (w_{1j}, \dots, w_{nj})^\top \in \mathbb{R}^n$, $j = 1, \dots, m$, to denote the column vectors of \mathbf{w} and with a slight abuse of notation, we have that

$$N_{nm}(\text{vec } \mathbf{w} | \text{vec } \tilde{\mathbf{w}}, \tilde{\mathbf{V}}_w) = \prod_{j=1}^m N_n(\mathbf{w}_{\cdot j} | \tilde{\mathbf{w}}_{\cdot j}, \tilde{\mathbf{V}}_{w_j}),$$

where

$$\tilde{\mathbf{w}}_{\cdot j} = \psi_j \tilde{\mathbf{V}}_{w_j} \tilde{\mathbf{H}}_\eta (\tilde{\mathbf{y}}_j^* - \tilde{\alpha}_j \mathbf{1}_n) \quad \text{and} \quad \tilde{\mathbf{V}}_{w_j} = (\psi_j \tilde{\mathbf{H}}_\eta^2 + \psi_j^{-1} \mathbf{I}_n)^{-1}.$$

The consequence of this is that the posterior regression functions are class independent, the exact intended effect by specifying a diagonal precision matrix $\tilde{\Psi}$.

5.5.3 Kernel parameters η

The posterior density q involving the kernel parameters is of the form

$$\begin{aligned} \log q(\eta) = & -\frac{1}{2} \text{tr} \mathbb{E}_{\mathcal{Z} \setminus \{\eta\} \sim q} \left[(\mathbf{y}^* - \mathbf{1}_n \boldsymbol{\alpha}^\top - \mathbf{H}_\eta \mathbf{w}) \Psi (\mathbf{y}^* - \mathbf{1}_n \boldsymbol{\alpha}^\top - \mathbf{H}_\eta \mathbf{w})^\top \right] + \log p(\eta) \\ & + \text{const.} \end{aligned}$$

where $p(\eta)$ is an appropriate prior density for η . Generally, samples $\eta^{(1)}, \dots, \eta^{(T)}$ from $\tilde{q}(\eta)$ may be obtained using a Metropolis algorithm, so that quantities such as $\tilde{\mathbf{H}}_\eta = \mathbb{E}_{\eta \sim q} \mathbf{H}_\eta$ and the like may be approximated using $\frac{1}{T} \sum_{t=1}^T \mathbf{H}_{\eta^{(t)}}$. Details of the Metropolis sampler is available in the appendix.

When only RKHS scale parameters are involved, then the distribution q can be found in closed-form, much like in the exponential family EM algorithm described in [Section 4.3.3](#). Under the same setting as in that subsection, assume that only $\eta = \{\lambda_1, \dots, \lambda_p\}$ need be estimated, and for each $k = 1, \dots, p$, we can decompose the kernel matrix as $\mathbf{H}_\eta = \lambda_k \mathbf{R}_k + \mathbf{S}_k$ and its square as $\mathbf{H}_\eta^2 = \lambda_k^2 \mathbf{R}_k^2 + \lambda_k \mathbf{U}_k + \mathbf{S}_k^2$. Additionally, we impose a further mean-field restriction on $q(\eta)$, i.e., $q(\eta) = \prod_{k=1}^p p(\lambda_k)$. Then, by using independent and identical normal priors on the λ_k 's, such as the one listed at the beginning of this section, we find that $q(\lambda_k)$ is the density of a normal distribution with

mean $d_k c_k^{-1}$ and variance c_k^{-1} , where

$$c_k = \text{tr} \left(\Psi \mathbf{E}[\mathbf{w}^\top \mathbf{R}_k^2 \mathbf{w}] \right) + v_\lambda^{-2}$$

and

$$d_k = \text{tr} \left(\Psi (\tilde{\mathbf{y}}^* - \mathbf{1}_n \tilde{\boldsymbol{\alpha}}^\top)^\top \mathbf{R}_k \tilde{\mathbf{w}} - \frac{1}{2} \Psi \mathbf{E}[\mathbf{w}^\top \mathbf{U}_k \mathbf{w}] \right).$$

For a method of evaluating quantities such as $\text{tr}(\mathbf{C} \mathbf{E}[\mathbf{w}^\top \mathbf{D} \mathbf{w}])$ for suitably sized matrices \mathbf{C} and \mathbf{D} , refer to the appendix.

5.5.4 Intercepts $\boldsymbol{\alpha}$

Finally, the posterior distribution for the intercepts follow a normal distribution with the normal priors specified earlier. The posterior mean and variance for the intercepts are given by $\tilde{\boldsymbol{\alpha}} = \tilde{\mathbf{A}}^{-1} \tilde{\mathbf{a}}$ and $\tilde{\mathbf{A}}^{-1}$ respectively, where

$$\tilde{\mathbf{a}} = \sum_{i=1}^n \Psi (\tilde{\mathbf{y}}_{i\cdot}^* - \tilde{\mathbf{w}}^\top \tilde{\mathbf{h}}_\eta(x_i)) \quad \text{and} \quad \tilde{\mathbf{A}} = n\Psi + v_\alpha \mathbf{I}_m.$$

If Ψ is diagonal, the components of $\boldsymbol{\alpha}$ would be independent, and each would be distributed according to

$$\text{N} \left(\frac{\psi_j \sum_{i=1}^n (\tilde{y}_{ij}^* - \tilde{f}_{ij})^2}{n\psi_j + v_\alpha^{-1}}, \frac{1}{n\psi_j + v_\alpha^{-1}} \right).$$

Here, we used the notation \tilde{f}_{ij} to mean the (i, j) 'th element of $\mathbf{E}[\mathbf{H}_\eta \mathbf{w}] = \tilde{\mathbf{H}}_\eta \tilde{\mathbf{w}} \in \mathbb{R}^{n \times m}$. Note that it is necessary, as discussed earlier, that $\sum_{j=1}^m \alpha_j = 0$ for identifiability.

5.5.5 The CAVI algorithm

One will have noticed that the evaluation of each component of the posterior depends on knowing the posterior distribution of the rest of the components. This circular dependence is dealt with by way of an iterative updating scheme of the components. Using an arbitrary starting value, each component is updated in turn according to the above derivations, until a maximum number of iterations is reached, or ideally, until a convergence criterion is met. In variational inference, the ELBO is used to assess convergence.

The expression for the ELBO for the I-probit model is derived in the appendix. The CAVI algorithm for the I-probit model is summarised in [Algorithm 1](#).

Similar to the EM algorithm, each iteration of the algorithm increases the ELBO to a stationary point ([Blei et al., 2017](#))—hence the name coordinate ascent variational inference (CAVI). Unlike the EM algorithm though, the CAVI algorithm does *not* guarantee an increase in the marginal log-likelihood at each step, nor does it guarantee convergence to the global maxima of the log-likelihood.

Further, the ELBO expression to be maximised is often not convex, which means the CAVI algorithm may terminate at local modes, for which they may be many. Note that the variational distribution with the higher ELBO value is the distribution that is closer, in terms of the KL divergence, to the true posterior distribution. In our experience, multiple random starts alleviates this issue for the I-probit model.

5.6 Post-estimation

Working within a variational Bayesian framework means that we are able to perform inferences on any quantity of interest using the (approximate) posterior distributions obtained. Any of the post estimation procedures explained in the previous chapter when dealing with normal I-prior models can be extended here.

Prediction of a new data point x_{new} is described. Step one is to determine the distribution of the posterior regression functions in each class, $\mathbf{f}(x_{\text{new}}) = \mathbf{w}^\top \mathbf{h}_\eta(x_{\text{new}})$, given values for the parameters θ of the I-probit model. To this end, we use the posterior mean estimate for θ , and denote them with tildes, as we have done so far in this chapter. As we know, $\text{vec } \mathbf{w}$ is normally distributed with mean and variance according to [\(5.14\)](#). By writing $\text{vec } \tilde{\mathbf{w}} = (\tilde{\mathbf{w}}_{\cdot 1}, \dots, \tilde{\mathbf{w}}_{\cdot m})^\top$ to separate out the I-prior random effects per class, we have that $\mathbf{w}_{\cdot j} | \tilde{\theta} \sim N_n(\tilde{\mathbf{w}}_{\cdot 1}, \tilde{\mathbf{V}}_w[j, j])$, and $\text{Cov}(\mathbf{w}_{\cdot j}, \mathbf{w}_{\cdot k}) = \tilde{\mathbf{V}}_w[j, k]$, where the ‘ $[\cdot, \cdot]$ ’ indexes the $n \times n$ sub-block of the block matrix structured matrix \mathbf{V}_w . Thus, for each class $j = 1, \dots, m$ and any $x \in \mathcal{X}$,

$$f_j(x) | \mathbf{y}, \tilde{\theta} \sim N(\tilde{\mathbf{h}}_\eta(x)^\top \mathbf{w}_{\cdot j}, \tilde{\mathbf{h}}_\eta(x)^\top \tilde{\mathbf{V}}_w[j, j] \tilde{\mathbf{h}}_\eta(x)),$$

and the covariance between the regression functions in two different classes is

$$\text{Cov}[f_j(x), f_k(x) | \mathbf{y}, \tilde{\theta}] = \tilde{\mathbf{h}}_\eta(x)^\top \tilde{\mathbf{V}}_w[j, k] \tilde{\mathbf{h}}_\eta(x).$$

alg:caviipr
obit

Algorithm 1 CAVI for the I-probit model

```

1: procedure INITIALISATION
2:   Initialise  $\tilde{\mathbf{y}}^{*(0)}, \tilde{\mathbf{w}}^{(0)}, \tilde{\boldsymbol{\alpha}}^{(0)}, \tilde{\mathbf{H}}_{\eta^{(0)}}, \boldsymbol{\Psi}$ 
3:    $t \leftarrow 0$ 
4: end procedure

5: while not converged do
6:   for  $i = 1, \dots, n$  do ▷ Update  $\mathbf{y}^*$ 
7:      $q^{(t+1)}(\mathbf{y}_{i.}^*) \leftarrow {}^t\text{N}_m(\tilde{\boldsymbol{\alpha}}^{(t)} + \tilde{\mathbf{w}}^{(t)\top} \tilde{\mathbf{h}}_{\eta^{(t)}}(x_i), \boldsymbol{\Psi}, \mathcal{C}_{y_i})$ 
8:      $\tilde{\mathbf{y}}_{i.}^{*(t+1)} \leftarrow \text{E}_{q^{(t+1)}}[\mathbf{y}_{i.}^*]$ 
9:   end for

10:   $\mathbf{V}_w^{(t+1)} \leftarrow ((\boldsymbol{\Psi} \otimes \tilde{\mathbf{H}}_{\eta^{(t)}}^2) + (\boldsymbol{\Psi}^{-1} \otimes \mathbf{I}_n))^{-1}$  ▷ Update  $\mathbf{w}$ 
11:   $\tilde{\mathbf{w}}^{(t+1)} \leftarrow \tilde{\mathbf{V}}_w^{(t+1)}(\boldsymbol{\Psi} \otimes \tilde{\mathbf{H}}_{\eta^{(t)}}) \text{vec}(\tilde{\mathbf{y}}^{*(t+1)} - \mathbf{1}_n \tilde{\boldsymbol{\alpha}}^{(t)\top})$ 
12:   $q^{(t+1)}(\mathbf{w}) \leftarrow \text{N}_{nm}(\tilde{\mathbf{w}}^{(t+1)}, \mathbf{V}_w^{(t+1)})$ 

13:  Update  $q^{(t+1)}(\eta)$  as per Section 5.5.3 ▷ Update  $\eta$ 
14:  Sample  $\eta^{[1]}, \dots, \eta^{[T]} \sim q^{(t+1)}(\eta)$ 
15:   $\tilde{\mathbf{H}}_{\eta^{(t+1)}} \leftarrow \frac{1}{T} \sum_{i=1}^T \mathbf{H}_{\eta^{[i]}}$  and  $\tilde{\mathbf{H}}_{\eta^{(t+1)}}^2 \leftarrow \frac{1}{T} \sum_{i=1}^T \mathbf{H}_{\eta^{[i]}}^2$ 

16:   $\tilde{\boldsymbol{\alpha}}^{(t+1)} \leftarrow \frac{1}{n} \sum_{i=1}^n (\tilde{\mathbf{y}}_{i.}^{*(t+1)} - \tilde{\mathbf{w}}^{(t+1)\top} \tilde{\mathbf{h}}_{\eta^{(t+1)}}(x_i))$  ▷ Update  $\boldsymbol{\alpha}$ 
17:   $q^{(t+1)}(\boldsymbol{\alpha}) \leftarrow \text{N}_m(\tilde{\boldsymbol{\alpha}}^{(t+1)}, \frac{1}{n} \boldsymbol{\Psi}^{-1})$ 

18:  Calculate ELBO  $\mathcal{L}^{(t+1)}$ 
19:   $t \leftarrow t + 1$ 
20: end while

```

Then, in step two, using the results obtained in the previous chapter in [Section 4.4](#), we have that the latent propensities $y_{\text{new},j}^*$ for each class are normally distributed with mean, variance, and covariances

$$\begin{aligned}
\text{E}[y_{\text{new},j}^* | \mathbf{y}, \tilde{\boldsymbol{\theta}}] &= \tilde{\alpha}_j + \text{E}[f_j(x_{\text{new}}) | \mathbf{y}, \tilde{\boldsymbol{\theta}}] && =: \hat{\mu}_j(x_{\text{new}}) \\
\text{Var}[y_{\text{new},j}^* | \mathbf{y}, \tilde{\boldsymbol{\theta}}] &= \text{Var}[f(x_{\text{new}}) | \mathbf{y}, \tilde{\boldsymbol{\theta}}] + \boldsymbol{\Psi}_{jj}^{-1} && =: \hat{\sigma}_j^2(x_{\text{new}}) \\
\text{Cov}[y_{\text{new},j}^*, y_{\text{new},k}^* | \mathbf{y}, \tilde{\boldsymbol{\theta}}] &= \text{Cov}[f_j(x), f_k(x) | \mathbf{y}, \tilde{\boldsymbol{\theta}}] + \boldsymbol{\Psi}_{jk}^{-1} && =: \hat{\sigma}_{jk}(x_{\text{new}}).
\end{aligned}$$

From here, step three would be to extract class information of data point x_{new} , which are contained in the normal distribution $N_m(\hat{\boldsymbol{\mu}}_{\text{new}}, \hat{\mathbf{V}}_{\text{new}})$, where

$$\hat{\boldsymbol{\mu}}_{\text{new}} = (\mu_1(x_{\text{new}}), \dots, \mu_m(x_{\text{new}}))^{\top} \quad \text{and} \quad \hat{\mathbf{V}}_{\text{new},jk} = \begin{cases} \hat{\sigma}_j^2(x_{\text{new}}) & \text{if } i = j \\ \hat{\sigma}_{jk}(x_{\text{new}}) & \text{if } i \neq j. \end{cases}$$

The predicted class is inferred from the latent variables via

$$\hat{y}_{\text{new}} = \arg \max_k \hat{\mu}_k(x_{\text{new}}),$$

while the probabilities for each class are obtained via integration of a multivariate normal density, as per (5.8), and restated here for convenience:

$$\hat{p}_{\text{new},j} = \int \cdots \int_{\{y_{ij}^* > y_{ik}^* \mid \forall k \neq j\}} \phi(y_{i1}^*, \dots, y_{im}^* \mid \hat{\boldsymbol{\mu}}_{\text{new}}, \hat{\mathbf{V}}_{\text{new}}) dy_{i1}^* \cdots dy_{im}^*.$$

For the independent I-probit model, class probabilities are obtained in a more compact manner via

$$\hat{p}_{\text{new},j} = \mathbb{E}_Z \left[\prod_{\substack{k=1 \\ k \neq j}}^m \Phi \left(\frac{\hat{\sigma}_j(x_{\text{new}})}{\hat{\sigma}_k(x_{\text{new}})} Z + \frac{\hat{\mu}_j(x_{\text{new}}) - \hat{\mu}_k(x_{\text{new}})}{\hat{\sigma}_k^2(x_{\text{new}})} \right) \right],$$

as per (5.10), since the m components of $\mathbf{f}(x_{\text{new}})$, and hence the $\mathbf{y}_{\text{new},j}^*$'s, are independent of each other ($\boldsymbol{\Psi}$ and $\hat{\mathbf{V}}_{\text{new}}$ are diagonal).

In this Bayesian setting, the analogue of standard errors for the parameters are their posterior standard deviations, which explain the uncertainty surrounding parameters. For the most part, these are easy to come by, and their posterior densities are easy to sample from. This allows us to conduct inference on transformed parameters, such as log odds ratios, quite easily. The procedure would be like this: first obtain samples of $\theta^{(1)}, \dots, \theta^{(T)}$ from their respective distributions, then sample $\mathbf{w}^{(i)} \sim p(\mathbf{w} \mid \theta^{(i)})$ for $i = 1, \dots, T$, and finally obtain samples of class probabilities $\hat{p}_{xj}^{(1)}, \dots, \hat{p}_{xj}^{(T)}$, $j = 1, \dots, m$, for a given data point $x \in \mathcal{X}$. To obtain a statistic of interest, say, a 95% credibility interval of a function $r(p_{xj})$ of the probabilities, simply take the empirical lower 2.5th and upper 97.5th percentile of this transformed sample. In this manner, all aspects of uncertainty, from the parameters to the latent variables of the generative model, are accounted for.

It is possible to perform model comparison by comparing the maximised ELBO quantity of several candidate models (Beal and Ghahramani, 2003), and the justification for this is that it supposedly gives a tight lower bound to the marginal likelihood (model evidence), especially if the variational density is close in the KL divergence sense to the true posterior density. This would allow model selection using Bayes factor as a model selection criterion. Kass and Raftery (1995) suggest the following interpretation of observed Bayes factor values for comparing model M_1 against model M_0 .

Table 5.2: Guidelines for interpreting Bayes factors.

| $2 \log \text{BF}(M_1, M_0)$ | $\text{BF}(M_1, M_0)$ | Evidence against M_0 |
|------------------------------|-----------------------|------------------------------------|
| 0–2 | 1–3 | Not worth more than a bare mention |
| 2–6 | 3–20 | Positive |
| 6–10 | 20–150 | Strong |
| >10 | >150 | Very strong |

It should be noted that while this works in practice, there is no theoretical basis for model comparison using the ELBO (Blei et al., 2017).

5.7 Computational consideration

Computational challenges for the I-probit model stems from two sources: 1) calculation of the class probabilities (5.8); and 2) storage and time requirements for the CAVI. We also discuss issues faced with the estimation of the error precision Ψ , and suggest ways to overcome this for future work.

5.7.1 Efficient computation of class probabilities

As an opening remark, note that the dimension of the integral (5.8) is $m - 1$, since the j 'th coordinates is fixed relative to the others. An alternative specification of the I-probit model can be made in terms of *relative differences* of the latent propensities. Choosing the first category as the reference category, define new random variables $z_{ij} = y_{ij}^* - y_{i1}^*$, for $j = 2, \dots, m$. The model (5.6) is equivalently represented by

$$y_i = \begin{cases} 1 & \text{if } \max(z_{i2}, \dots, z_{im}) < 0 \\ j & \text{if } \max(z_{i2}, \dots, z_{im}) = z_{ij} \geq 0. \end{cases} \quad (5.15)$$

Write $\mathbf{z}_{i\cdot} = (z_{i2}, \dots, z_{im})^\top \in \mathbb{R}^{m-1}$. Then $\mathbf{z}_{i\cdot} = \mathbf{Q}\mathbf{y}_{i\cdot}^*$, where $\mathbf{Q} \in \mathbb{R}^{(m-1) \times m}$ is the $(m-1)$ identity matrix pre-augmented with a column vector of minus ones. We have that $\mathbf{z}_{i\cdot} \stackrel{\text{iid}}{\sim} \mathcal{N}_{m-1}(\boldsymbol{\nu}, \boldsymbol{\Omega})$, where $\boldsymbol{\nu}_{i\cdot} = \mathbf{Q}\boldsymbol{\mu}_i$ and $\boldsymbol{\Omega} = \mathbf{Q}\boldsymbol{\Psi}^{-1}\mathbf{Q}^\top$. Note that if $\boldsymbol{\Psi}$ is diagonal, then the transformation to $\boldsymbol{\Omega}$ will not retain diagonality—indeed, each component will undoubtedly be correlated with one another as they are all anchored on the same latent variable.

Now, the class probabilities for $j = 2, \dots, m$ are

$$p_{ij} = \int_{\{z_{ik} < 0 \mid \forall k \neq 1, j\}} \mathbb{1}[z_{ij} \geq 0] \phi(\mathbf{z}_{i\cdot} | \boldsymbol{\nu}_{i\cdot}, \boldsymbol{\Omega}) d\mathbf{z}_{i\cdot}. \quad (5.16)$$

{eq:pj3}

The class probability p_{i1} is simply $p_{i1} = 1 - \sum_{k \neq 1} p_{ik}$. From this representation of the model, with $m = 2$ (binary outcomes) we see that

$$p_{i1} = \Phi\left(\frac{z_{i2} - \nu}{\omega^{1/2}}\right) \quad \text{and} \quad p_{i2} = 1 - \Phi\left(\frac{z_{i2} - \nu}{\omega^{1/2}}\right),$$

where $\Phi(\cdot)$ is the CDF of the standard normal univariate distribution, and ν and ω are the mean and variance of the univariate random variable $\mathbf{z}_{i\cdot} = z_{i2}$. The probit link function involving the cdf of a standard normal is clearly seen here, especially if the error precision is treated as fixed such that $\omega = 1$.

The issue at hand here is that for $m > 4$, the evaluation of the class probabilities in (5.8) is computationally burdensome using classical methods such as quadrature methods [Geweke et al. \(1994\)](#).

The simplest strategy to overcome this is a frequency simulator (otherwise known as Monte Carlo integration): obtain random samples from $\mathcal{N}_{m-1}(\boldsymbol{\nu}_{i\cdot}, \boldsymbol{\Omega})$, and calculate how many of these samples fall within the required region. This method is fast and yields unbiased estimates of the class probabilities. However, accuracy of this method is questionable when the mean $\boldsymbol{\nu}_{i\cdot}$ of the multivariate normal is many standard deviations away from zero (the cutoff region as per (5.16)).

A more reliable method is the probability simulator of Geweke-Hajivassiliou-Keane (GHK) ([Geweke, 1991](#); [Hajivassiliou et al., 1996](#); [Michael P Keane, 1994](#)), which we describe now. For clarity, we drop the subscript i denoting individuals, and write $\mathbf{z} = (z_1, \dots, z_m)$, remembering that $z_1 = 0$. Suppose that an observation $y = j$ has been

made. Rewrite the model by anchoring on the j 'th latent variable z_j as follows:

$$\tilde{\mathbf{z}} := (\overbrace{z_1 - z_j}^{\tilde{z}_1}, \dots, \overbrace{z_{j-1} - z_j}^{\tilde{z}_{j-1}}, \overbrace{z_{j+1} - z_j}^{\tilde{z}_{j+1}}, \dots, \overbrace{z_m - z_j}^{\tilde{z}_m})^\top \in \mathbb{R}^{m-1}.$$

Let $\boldsymbol{\nu}_{(j)}$ and $\boldsymbol{\Omega}_{(j)}$ be the appropriately transformed mean vector and covariance matrix for $\tilde{\mathbf{z}}$. These are indexed by ' (j) ' because the transformation is dependent on which latent variable the \mathbf{z} 's are anchored on. Since this transformation is linear, $\tilde{\mathbf{z}} \sim \text{N}_{m-1}(\boldsymbol{\nu}_{(j)}, \boldsymbol{\Omega}_{(j)})$. For the symmetric and positive definite matrix $\boldsymbol{\Psi}^{-1}$, obtain its Cholesky decomposition as $\boldsymbol{\Omega}_{(j)} = \mathbf{L}\mathbf{L}^\top$, where \mathbf{L} is a lower triangular matrix. Then, $\tilde{\mathbf{z}} = \boldsymbol{\nu}_{(j)} + \mathbf{L}\boldsymbol{\zeta}$, where $\boldsymbol{\zeta} \sim \text{N}_{m-1}(\mathbf{0}, \mathbf{I}_{m-1})$. That is,

$$\begin{pmatrix} \tilde{z}_1 \\ \tilde{z}_2 \\ \vdots \\ \tilde{z}_m \end{pmatrix} = \begin{pmatrix} \nu_{(j)1} \\ \nu_{(j)2} \\ \vdots \\ \nu_{(j)m} \end{pmatrix} + \begin{pmatrix} L_{11} & & & \\ L_{21} & L_{22} & & \\ \vdots & \vdots & \ddots & \\ L_{m1} & L_{m2} & \cdots & L_{mm} \end{pmatrix} \begin{pmatrix} \zeta_1 \\ \zeta_2 \\ \vdots \\ \zeta_m \end{pmatrix} = \begin{pmatrix} \nu_{(j)1} + L_{11}\zeta_1 \\ \nu_{(j)2} + \sum_{k=1}^2 L_{k2}\zeta_k \\ \vdots \\ \nu_{(j)m} + \sum_{k=1}^m L_{km}\zeta_k \end{pmatrix}.$$

With this setup, we can calculate p_j , the probability of class j , which is equivalent to the probability that each $\tilde{z}_k = z_k - z_j < 0$, as follows

$$\begin{aligned} p_j &= \text{P}(\tilde{z}_1 < 0, \dots, \tilde{z}_{j-1} < 0, \tilde{z}_{j+1} < 0, \dots, \tilde{z}_m < 0) \\ &= \text{P}(\zeta_1 < u_1, \dots, \zeta_{j-1} < u_{j-1}, \zeta_{j+1} < u_{j+1}, \dots, \zeta_m < u_m) \\ &= \text{P}(\zeta_1 < u_1) \text{P}(\zeta_2 < u_2 | \zeta_1 < u_1) \cdots \\ &\quad \cdots \text{P}(\zeta_m < u_m | \zeta_1 < u_1, \dots, \zeta_{j-1} < u_{j-1}, \zeta_{j+1} < u_{j+1}, \dots, \zeta_{m-1} < u_{m-1}), \end{aligned}$$

where $u_i = u_i(\zeta_1, \dots, \zeta_{i-1}) = -(\nu_{(j)i} + \sum_{k=1}^{i-1} L_{ki}\zeta_k)/L_{ii}$. Thus, the integral involving a $(m-1)$ -variate normal density (5.16) is turned into a product of $m-1$ univariate normal cdfs, which can be computed fairly efficiently in modern computer systems.

As an aside, the GHK probability simulator, can be used to sample from a truncated multivariate normal distribution:

- Draw $\tilde{\zeta}_1 \sim {}^t\text{N}(0, 1, -\infty, u_1)$.
- Draw $\tilde{\zeta}_2 \sim {}^t\text{N}(0, 1, -\infty, \tilde{u}_2)$, where $\tilde{u}_2 = u_2(\tilde{\zeta}_1)$.
- ...
- Draw $\tilde{\zeta}_{j-1} \sim {}^t\text{N}(0, 1, -\infty, \tilde{u}_{j-1})$, where $\tilde{u}_{j-1} = u_{j-1}(\tilde{\zeta}_1, \dots, \tilde{\zeta}_{j-2})$.

- Draw $\tilde{\zeta}_{j+1} \sim {}^t\text{N}(0, 1, -\infty, \tilde{u}_{j+1})$, where $\tilde{u}_{j+1} = u_{j+1}(\tilde{\zeta}_1, \dots, \tilde{\zeta}_{j-1})$.
- ...
- Draw $\tilde{\zeta}_m \sim {}^t\text{N}(0, 1, -\infty, \tilde{u}_m)$, where $\tilde{u}_m = u_m(\tilde{\zeta}_1, \dots, \tilde{\zeta}_{j-1}, \tilde{\zeta}_{j+1}, \dots, \tilde{\zeta}_{m-1})$.

Then, $\tilde{z} = \boldsymbol{\nu}_{(j)} \mathbf{L} \tilde{\boldsymbol{\zeta}}$ will be distributed according to $\text{N}_{m-1}(\boldsymbol{\nu}_{(j)}, \boldsymbol{\Omega}_{(j)})$. Any quantity of interest, e.g. $\text{Er}(\tilde{z})$, can then be estimated by the sample mean. In the variational algorithm, we require quantities such as first and second moments and also the entropy of a truncated multivariate normal distribution. Alternative methods are also discussed in the appendix.

Finally, a point on independent probit models. As we alluded to earlier in the chapter, the class probabilities condense to a unidimensional integral involving products of normal cdfs (see (5.10)) if $\boldsymbol{\Psi}$ is diagonal. While this represents a massive simplification, care should be taken when dealing with the formula in (5.10). When at least one of the normal cdfs in the product is extremely small, this can cause loss of significance due to floating-point errors. In the **iprobbit** package, the product of normal cdfs is handled as a sum on the log scale to avoid this issue.

5.7.2 Computational complexity of the CAVI algorithm

As with the normal I-prior model, the time complexity of the variational inference algorithm for I-probit models is dominated by the step involving the posterior evaluation of the I-prior random effects \mathbf{w} , which essentially is the inversion of an $nm \times nm$ matrix. The matrix in question is

$$\mathbf{V}_w = [(\boldsymbol{\Psi} \otimes \mathbf{H}_\eta^2) + (\boldsymbol{\Psi}^{-1} \otimes \mathbf{I}_n)]^{-1}. \quad (\text{from 5.14})$$

We can actually exploit the Kronecker product structure to compute the inverse efficiently. Perform an orthogonal eigendecomposition of \mathbf{H}_η to obtain $\mathbf{H}_\eta = \mathbf{V}\mathbf{U}\mathbf{V}^\top$ and of $\boldsymbol{\Psi}$ to obtain $\boldsymbol{\Psi} = \mathbf{Q}\mathbf{P}\mathbf{Q}^\top$. This process takes $O(n^3 + m^3) \approx O(n^3)$ time if $m \ll n$ or if done in parallel, and needs to be performed once per CAVI iteration. Then, manipulate

sec:complxi
probit

\mathbf{V}_w^{-1} as follows:

$$\begin{aligned}
\mathbf{V}_w^{-1} &= (\mathbf{\Psi} \otimes \mathbf{H}_\eta^2) + (\mathbf{\Psi}^{-1} \otimes \mathbf{I}_n) \\
&= (\mathbf{Q}\mathbf{P}\mathbf{Q}^\top \otimes \mathbf{V}\mathbf{U}^2\mathbf{V}^\top) + (\mathbf{Q}\mathbf{P}^{-1}\mathbf{Q}^\top \otimes \mathbf{V}\mathbf{V}^\top) \\
&= (\mathbf{Q} \otimes \mathbf{V})(\mathbf{P} \otimes \mathbf{U}^2)(\mathbf{Q}^\top \otimes \mathbf{V}^\top) + (\mathbf{Q} \otimes \mathbf{V})(\mathbf{P}^{-1} \otimes \mathbf{I}_n)(\mathbf{Q}^\top \otimes \mathbf{V}^\top) \\
&= (\mathbf{Q} \otimes \mathbf{V})(\mathbf{P} \otimes \mathbf{U}^2 + \mathbf{P}^{-1} \otimes \mathbf{I}_n)(\mathbf{Q}^\top \otimes \mathbf{V}^\top)
\end{aligned}$$

Its inverse is

$$\begin{aligned}
\mathbf{V}_w &= (\mathbf{Q}^\top \otimes \mathbf{V}^\top)^{-1}(\mathbf{P} \otimes \mathbf{U}^2 + \mathbf{P}^{-1} \otimes \mathbf{I}_n)^{-1}(\mathbf{Q} \otimes \mathbf{V})^{-1} \\
&= (\mathbf{Q} \otimes \mathbf{V})(\mathbf{P} \otimes \mathbf{U}^2 + \mathbf{P}^{-1} \otimes \mathbf{I}_n)^{-1}(\mathbf{Q}^\top \otimes \mathbf{V}^\top)
\end{aligned}$$

which is easy to compute since the middle term is an inverse of diagonal matrices. This brings time complexity of the CAVI down to a similar requirement as if $\mathbf{\Psi}$ was diagonal.

Storage requirements are still $O(n^2)$, and methods described in the previous chapter are applicable, particularly the discussion surrounding exponential family EM algorithm. Prediction of a new data point is $O(n^2m)$, because there are essentially m ‘separate’ normal I-prior regressions, and each take $O(n^2)$ to evaluate.

5.7.3 Difficulties faced with estimating $\mathbf{\Psi}$

sec:difficu
ltPsi

Suppose that, alongside the \mathbf{y}^* , \mathbf{w} , η and $\boldsymbol{\alpha}$ in the CAVI algorithm described in [Section 5.5](#), $\mathbf{\Psi}$ is a free parameter to be estimated. If so, we find that the variational density q for $\mathbf{\Psi}$ satisfies

$$q(\mathbf{\Psi}) \propto \exp \left[-\frac{1}{2} \text{tr} \left(\overbrace{(\mathbf{E}[(\mathbf{y}^* - \boldsymbol{\mu})^\top (\mathbf{y}^* - \boldsymbol{\mu})])}^{\mathbf{G}_1} \mathbf{\Psi} + \overbrace{\mathbf{E}[\mathbf{w}^\top \mathbf{w}]}^{\mathbf{G}_2} \mathbf{\Psi}^{-1} \right) \right] \times p(\mathbf{\Psi})$$

where $p(\mathbf{\Psi})$ is a prior density chosen for $\mathbf{\Psi}$. Unfortunately, this does not resemble any known distribution, regardless of the prior choice for $\mathbf{\Psi}$. One can resort to sampling techniques to obtain quantities such as the mean or entropy, which are needed, but this has not been studied for this project due to time limitations. Even if this was possible, this requires, among other things, second moments of a truncated multivariate normal density \mathbf{y}^* , and also of $\mathbf{H}_\eta \mathbf{w} \in \mathbb{R}^{n \times m}$ —of which both are a bit awkward to obtain.

What we realise, however, is that the *posterior mode* is relatively easy to obtain, especially with an improper prior $p(\Psi) \propto \text{const.}$ To see this, we look specifically at the case where Ψ is diagonal. On the log scale,

$$\log q(\psi_j) = \text{const.} - \frac{1}{2} \sum_{j=1}^m \psi_j \mathbb{E} \|\mathbf{y}_{\cdot j}^* - \boldsymbol{\mu}_{\cdot j}\|^2 - \frac{1}{2} \sum_{j=1}^m \psi_j^{-1} \mathbb{E} \|\mathbf{w}_{\cdot j}\|^2$$

is maximised, for $j = 1, \dots, m$, at

$$\hat{\psi}_j = \sqrt{\frac{\mathbb{E} \|\mathbf{y}_{\cdot j}^* - \boldsymbol{\mu}_{\cdot j}\|^2}{\mathbb{E} \|\mathbf{w}_{\cdot j}\|^2}}.$$

Perhaps, if the posterior mean is close to the mode, and not withstanding the involved calculations of the require second moments, then this quantity can be used instead in the CAVI algorithm. This ties with the idea of *variational Bayes EM algorithm*, which is an alternative to a fully Bayesian treatment of variational inference. This is discussed in [Sections 5.10.2](#) and [5.10.3](#), but unfortunately, time constraints had made it impossible for us to examine this within the scope of this thesis.

5.8 Examples

sec:iprobit
eg

We present analyses of real-data examples using the I-probit model for a variety of applications, namely binary and multiclass classification, meta-analysis, and spatio-temporal modelling of point processes. Examples in this section have been analysed using the R package **iprobit** developed by us. All of these examples had assumed a fixed error precision $\Psi = \mathbf{I}_m$.

5.8.1 Predicting cardiac arrhythmia

Statistical learning tools are being used in the field of medicine as a means to aid medical diagnosis of diseases. In this example, factors determining the presence or absence of heart diseases are studied. Traditionally, cardiologists inspect patients' cardiac activity (ECG data) in order to reach a diagnosis, which remains the “gold standard” method of obtaining diagnoses. The study by [Guvenir et al. \(1997\)](#) aimed to predict cardiac

abnormalities by way of machine learning, and minimise the difference between the gold standard and computer-based classifications.

The data set³ at hand contains a myriad of ECG readings and other patient attributes such as age, height, and weight. Altogether, there are $n = 451$ observations and $p = 279$ predictors. In order for a valid comparison to be made to other studies, we excluded nominal covariates, leaving us with $p = 194$ continuous predictors, which we then standardised. In the original data set, there are 13 distinct classes of cardiac arrhythmia—again, following the lead of other studies, we had combined all forms of cardiac diseases to form a single class, thus reducing the problem to a binary classification task (normal vs. arrhythmia).

The relationship between patient i 's probability of having a form of cardiac arrhythmia p_i and the predictors $x_i \in \mathcal{X} \equiv \mathbb{R}^{194}$ is modelled as

$$\Phi(p_i) = \alpha + f(x_i).$$

Further, assuming $f \in \mathcal{F}$ a suitable RKHS with kernel h_λ , we may assign an I-prior on the (latent) regression function f . We consider three RKHSs: the canonical (linear) RKHS, the fBm-0.5 RKHS and the SE RKHS. The first of these three assumes an underlying linear relationship of the covariates and the probabilities, while the other two assumes a smooth relationship. As all covariates had been standardised, it is sufficient to assign a single scale parameter λ for the I-probit model.

For reference, fitting an I-probit model on the full data set takes about 4 seconds only, with convergence reached in at most 15 iterations. Figure 5.5 plots the variational lower bound value over time and iterations for the cardiac arrhythmia data set. As expected, the lower bound value increases over time until a convergence criterion is reached.

To measure predictive ability, we fit the I-probit models on a random subset of the data and obtain the out-of-sample test error rates from the remaining held-out observations. We then compare the results against popular machine learning classifiers, namely: 1) linear and quadratic discriminant analysis (LDA/QDA); 2) k -nearest neighbours; 3) support vector machines (SVM) (Steinwart and Christmann, 2008); 4) Gaussian process classification (Rasmussen and Williams, 2006); 5) random forests (Breiman, 2001); 6) nearest shrunken centroids (NSC) (Tibshirani et al., 2002); and 7) L-1 penalised logistic regression. The experiment is set up as follows:

³Data is made publicly available at <https://archive.ics.uci.edu/ml/datasets/arrhythmia>.

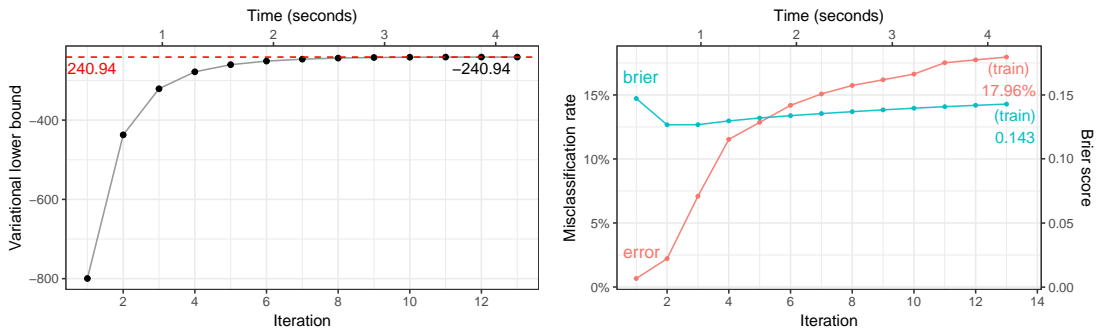


Figure 5.5: Plot of variational lower bound over time (left), and plot of training error rate and Brier scores over time (right).

fig:cardiac
.mod.full.p
lot

1. Form a training set by sub-sampling $s \in \{50, 100, 200\}$ observations.
2. The remaining unsampled data is used as the test set.
3. Fit model on training set, and obtain test error rates defined as

$$\text{test error rate} = \frac{1}{s} \sum_{i=1}^n [y_i^{\text{pred}} \neq y_i^{\text{test}}] \times 100\%.$$

4. Repeat steps 1-3 100 times to obtain the *average* test error rates and standard errors.

Results for the methods listed above were extracted from the in-depth study by [Cannings and Samworth \(2017\)](#), who also conducted an identical experiment using their random projection ensemble classification method (RP). The results are tabulated in [Table 5.3](#).

Of the three I-probit models, the fBm model performed the best. That it performed better than the canonical linear I-probit model is unsurprising, since an underlying smooth function to model the latent variables is expected to generalise better than a rigid straight line function. The poor performance of the SE I-probit model may be due to the fact that the lengthscale parameter was not estimated (fixed at $l = 1$), but then again, we notice reliable performance of the fBm even with fixed Hurst index ($\gamma = 0.5$). It can be seen that the fBm I-probit model also outperform the more popular machine learning algorithms out there including k -nearest neighbours, support vector machines and Gaussian process classification. It came second only to random forests, an ensemble learning method, which depending on the number of random decisions trees generated simultaneously, might be slow. The time complexity of a random forest algorithm is

Table 5.3: Mean out-of-sample misclassification rates and standard errors in parantheses for 100 runs of various training (s) and test ($451 - s$) sizes for the cardiac arrhythmia binary classification task.

tab:cardiac

| Method | Misclassification rate (%) | | |
|------------------|----------------------------|--------------|--------------|
| | $s = 50$ | $s = 100$ | $s = 200$ |
| <i>I-probit</i> | | | |
| Linear | 35.52 (0.44) | 31.35 (0.33) | 29.45 (0.38) |
| Smooth (fBm-0.5) | 33.64 (0.66) | 28.12 (0.34) | 24.33 (0.24) |
| Smooth (SE-1.0) | 48.26 (0.40) | 48.32 (0.43) | 47.11 (0.37) |
| <i>Others</i> | | | |
| RP-LDA | 33.24 (0.42) | 30.19 (0.35) | 27.49 (0.30) |
| RP-QDA | 30.47 (0.33) | 28.28 (0.26) | 26.31 (0.28) |
| RP- k -NN | 33.49 (0.40) | 30.18 (0.33) | 27.09 (0.31) |
| Random forests | 31.65 (0.39) | 26.72 (0.29) | 22.40 (0.31) |
| SVM (linear) | 36.16 (0.47) | 35.61 (0.39) | 35.20 (0.35) |
| SVM (Gaussian) | 48.39 (0.49) | 47.24 (0.46) | 46.85 (0.43) |
| GP (Gaussian) | 37.28 (0.42) | 33.80 (0.40) | 29.31 (0.35) |
| NSC | 34.98 (0.46) | 33.00 (0.40) | 31.08 (0.41) |
| L-1 logistic | 34.92 (0.42) | 30.48 (0.34) | 26.12 (0.27) |

$O(pqn \log(n))$, where p is the number of variables used for training, q is the number of random decision trees, and n is the number of observations.

5.8.2 Meta-analysis of smoking cessation

Consider the smoking cessation data set, as described in [Skrondal and Rabe-Hesketh \(2004\)](#). It contains observations from 27 separate smoking cessation studies in which participants are subjected to either a nicotine gum treatment or a placebo. The interest is to estimate the treatment effect size, and whether it is statistically significant, i.e. whether or not nicotine gum is an effective treatment to quit smoking. The studies are conducted at different times and due to various reasons such as funding and cultural effects, the results from all of the studies may not be in agreement. The number of effective participants plays a major role in determining the power of the statistical tests performed in individual studies. The question then becomes how do we meaningfully aggregate all the data to come up with one summary measure?

Several methods exist to analyse such data sets. One may consider a fixed-effects model, similar to a classical one-way ANOVA model to establish whether or not the effect size is significant. Because of the study-specific characteristics, it is natural to consider multilevel or random-effects models as a means to estimate the effect size. Regardless of method, the approach of analysing study-level treatment effects instead of patient-level data only is the paradigm for meta-analysis, and our I-prior model takes this approach as well.

A summary of the data is displayed by the box-plot in Figure 5.6. On the whole, there are a total of 5908 patients, and they are distributed roughly equally among the control and treatment groups (46.33% and 53.67% respectively, on average). From the box-plots, it is evident that there are more patients who quit smoking in the treatment group as compared to the placebo control group. There are various measures of treatment effect size, such as risk ratio or risk differences, but we shall concentrate on *odds ratios* as defined by

$$\text{odds ratio} = \frac{\text{odds of quitting smoking in } \textit{treatment} \text{ group}}{\text{odds of quitting smoking in } \textit{control} \text{ group}}.$$

The odds of quitting smoking in either group is defined as

$$\text{odds} = \frac{P[\text{quit smoking}]}{1 - P[\text{quit smoking}]},$$

and these probabilities, odds and ultimately the odds ratio can be estimated from sample proportions. This raw odds ratio for all study groups is calculated as $1.66 = e^{0.50}$. It is

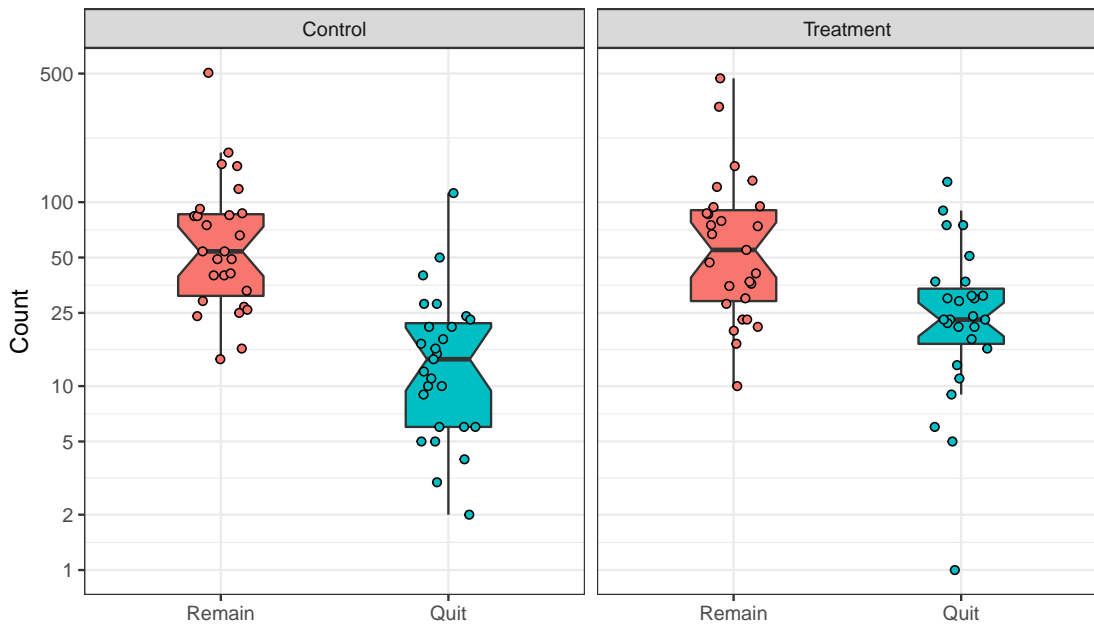


Figure 5.6: Comparative box-plots of the distribution of patients who successfully quit smoking and those who remained smokers, in the two treatment groups.

fig:plot.da
ta.smoke

also common for the odds ratio to be reported on the log scale (usually as a remnant of logistic models). A value greater than one for the odds ratio (or equivalently, greater than zero for the log-odds ratio) indicates a significant treatment effect.

A random-effects analysis using a multilevel logistic model has been considered by [Agresti and Hartzel \(2000\)](#). Let $i = 1, \dots, n_j$ index the patients in study group $j \in \{1, \dots, 27\}$. For patient i in study j , p_{ij} denotes the probability that the patient has successfully quit smoking. Additionally, x_{ij} is the centred dummy variable indicating patient i 's treatment group in study j . These take on two values: 0.5 for treated patients and -0.5 for control patients. The logistic random-effects model is

$$\log \left(\frac{p_{ij}}{1 - p_{ij}} \right) = \beta_{0j} + \beta_{1j}x_{ij}$$

with

$$\begin{pmatrix} \beta_{0j} \\ \beta_{1j} \end{pmatrix} \sim N \left(\begin{pmatrix} \beta_0 \\ \beta_1 \end{pmatrix}, \begin{pmatrix} \sigma_0^2 & \sigma_{01} \\ \sigma_{01} & \sigma_1^2 \end{pmatrix} \right)$$

[Agresti and Hartzel \(2000\)](#) also made the additional assumption $\sigma_{01} = 0$, so that, coupled with the contrast coding used for x_{ij} , the total variance $\text{Var}(\beta_{0j} + \beta_{1j}x_{ij})$ would be

constant in both treatment groups. The overall log odds ratio is represented by β_1 , and this is estimated as $0.57 = \log 1.76$.

In an I-prior model, the Bernoulli probabilities p_{ij} are regressed against the treatment group indicators x_{ij} and also the patients' study group j via the regression function f and a probit link:

$$\begin{aligned}\Phi^{-1}(p_{ij}) &= f(x_{ij}, j) \\ &= f_1(x_{ij}) + f_2(j) + f_{12}(x_{ij}, j).\end{aligned}$$

We have decomposed our function f into three parts: f_1 represents the treatment effect, f_2 represents the effect of the study groups, and f_{12} represents the interaction effect between the treatment and study group on the modelled probabilities. As both x_{ij} and j are nominal variables, the functions f_1 and f_2 both lie in the Pearson RKHS of functions \mathcal{F}_1 and \mathcal{F}_2 , each with RKHS scale parameters λ_1 and λ_2 . As such, it does not matter how the x_{ij} variables are coded (dummy coding 0, 1 vs. centred coding -0.5, 0.5) as the scaling of the function is determined by the RKHS scale parameters. The interaction effect f_{12} lies in the RKHS tensor product $\mathcal{F}_1 \otimes \mathcal{F}_2$. In I-prior modelling, there are only two parameters to estimate, while in the standard logistic random-effects model, there are six. The results of the I-prior fit are summarised in the table below.

Table 5.4: Results of the I-prior model fit for three models.

| Model | Log-likelihood | Error rate (%) | Brier score | No. of parameters |
|----------------------|----------------|----------------|-------------|-------------------|
| f_1 | -3210.76 | 23.65 | 0.179 | 1 |
| $f_1 + f_2$ | -3142.24 | 29.30 | 0.206 | 2 |
| $f_1 + f_2 + f_{12}$ | -3091.20 | 23.48 | 0.168 | 2 |

The approximated marginal log-likelihood value for the I-prior model (i.e. variational lower bound), the Brier score for each model and the number of RKHS scale parameters estimated in the model are reported in Table 5.4. Three models were fitted: 1) A model with only the treatment effect; 2) A model with a treatment effect and a study group effect; and 3) Model 2 with the additional assumption that treatment effect varies across study groups. Model 1 disregards the study group effects, while Model 2 assumes that the effectiveness of the nicotine gum treatment does not vary across study groups (akin to a varying-intercept model). A model comparison using the evidence lower bound indicates that Model 3 has the highest value, and the difference is significant

tab:mod.com
pare.smoke

from a Bayes factor standpoint ($\text{BF}(M_3, M_1)$ and $\text{BF}(M_3, M_2)$ are both greater than 150). The misclassification rate and Brier score indicates good predictive performance of the models, and there is not much to distinguish between the three although Model 3 is the best out of the three models.

Unlike in the logistic random-effects model, where the log odds ratio can be read off directly from the coefficients, with an I-prior probit model the log odds ratio needs to be calculated manually from the fitted probabilities. The probabilities of interest are the probabilities of quitting smoking under each treatment group for each study group j - call these $p_j(\text{treatment})$ and $p_j(\text{control})$. That is,

$$\begin{aligned} p_j(\text{treatment}) &= \Phi(\tilde{\mu}(\text{treatment}, j)) \\ p_j(\text{control}) &= \Phi(\tilde{\mu}(\text{control}, j)), \end{aligned}$$

where $\tilde{\mu}$ represents the posterior mean estimate for the regression function given in [Which section?](#). These log odds ratio for each study group can then be calculated as usual. For the overall log odds ratio, the probabilities that are used are the averaged probabilities weighted according to the sample sizes in each group. This has been calculated as $0.55 = \log 1.73$, slightly lower than both the raw log odds ratio and the log odds ratio estimated by the logistic random-effects model. This can perhaps be attributed to some shrinkage of the estimated probabilities due to placing a prior with zero mean on the regression functions. The credibility intervals in [Figure 5.7](#) for the log odds ratios under an I-prior are also noticeably narrower compared to the multilevel model fitted.

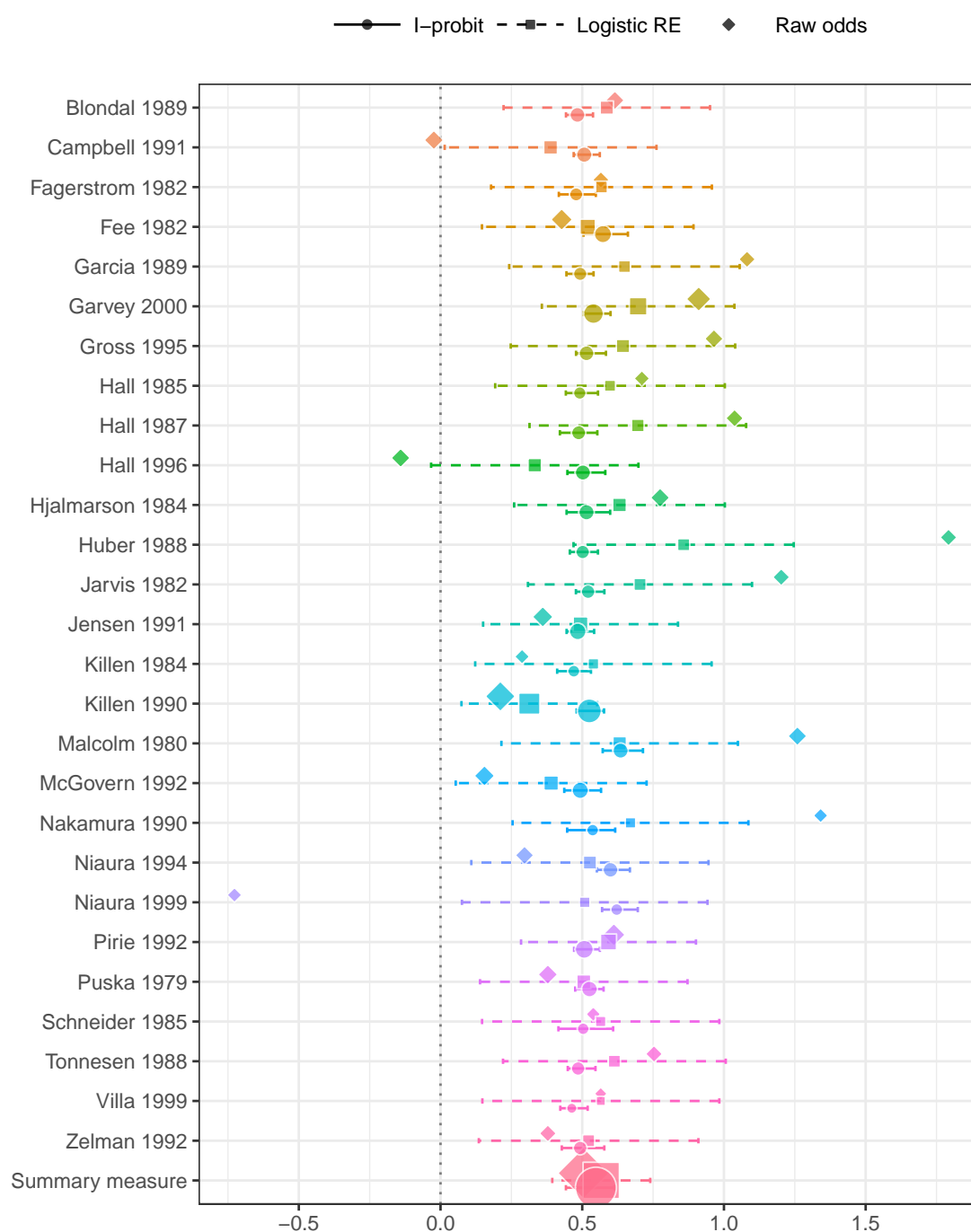


Figure 5.7: Forest plot of effect sizes (log odds ratios) in each group as well as the overall effect size together with their 95% confidence bands. The plot compares the raw log odds ratios, the logistic random-effect estimates, and the I-prior estimates. Sizes of the points indicate the relative sample sizes per study group.

fig:smoke.f
orest.plot

5.8.3 Multiclass classification: Vowel recognition data set

We illustrate multiclass classification using I-priors on a speech recognition data set⁴ with $m = 11$ classes to be predicted from digitized low pass filtered signals generated from voice recordings. Each class corresponds to a vowel sound made when pronouncing a specific word. The words that make up the vowel sounds are shown in Table 5.5. Each word was uttered once by multiple speakers, and the data are split into a training and a test set. Four males and four female speakers contributed to the training set, while four male and three female speakers contributed to the test set. The recordings were manipulated using speech processing techniques, such that each speaker yielded six frames of speech from the eleven vowels, each with a corresponding 10-dimensional numerical input vector (the predictors). This means that the size of the training set is 528, while 462 data points are available for testing the predictive performance of the models. This data set is also known as Deterding’s vowel recognition data (after the original collector, [Deterding, 1989](#)). Machine learning methods such as neural networks and nearest neighbour methods were analysed by [Robinson \(1989\)](#).

Table 5.5: The eleven words that make up the classes of vowels.

| Class | Label | Vowel | Word | Class | Label | Vowel | Word |
|-------|-------|-------|------|-------|-------|-------|-------|
| 1 | hId | i: | heed | 7 | hOd | ɒ | hod |
| 2 | hId | ɪ | hid | 8 | hOd | ɔ: | hoard |
| 3 | hEd | ɛ | head | 9 | hUd | ʊ | hood |
| 4 | hAd | a | had | 10 | hud | u: | who’d |
| 5 | hYd | ʌ | hud | 11 | hed | ə: | heard |
| 6 | had | ɑ: | hard | | | | |

We will fit the data using an I-probit model with the canonical linear kernel, fBm-0.5 kernel, and the SE kernel with lengthscale $l = 1$. Each model took roughly 13 seconds per iteration in fitting the training data set ($n = 528$). In particular, the canonical kernel model took a long time to converge, with each variational inference iteration improving the lower bound only slightly each time. In contrast, both the fBm-0.5 and SE model were quicker to converge. Multiple restarts from different random seeds were conducted, and we found that they all converged to a similar lower bound value. This alleviates any concerns that the model might have converged to different multiple local optima.

⁴Data is publically available from the UCI Machine Learning Repository, URL: [https://archive.ics.uci.edu/ml/datasets/Connectionist+Bench+\(Vowel+Recognition+--+Deterding+Data\)](https://archive.ics.uci.edu/ml/datasets/Connectionist+Bench+(Vowel+Recognition+--+Deterding+Data)).

tab:vowel

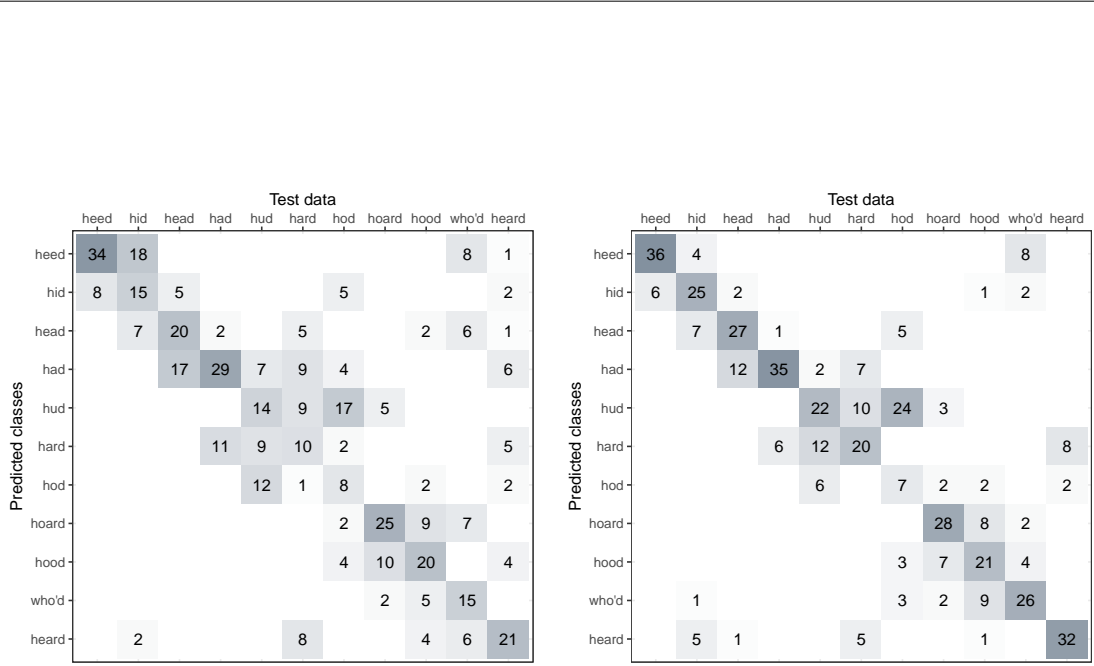
tab:vowel.t
ab

Table 5.6: Results of various classification methods for the vowel data set.

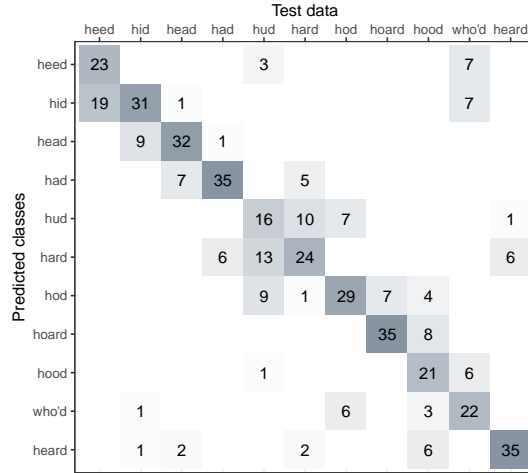
| Model | Error rate (%) | |
|---------------------------------|----------------|------|
| | Train | Test |
| <i>I-probit</i> | | |
| Linear | 29 | 54 |
| Smooth (fBm-0.5) | 22 | 40 |
| Smooth (SE-1.0) | 7 | 34 |
| <i>Others</i> | | |
| Linear regression | 48 | 67 |
| Logistic regression | 22 | 51 |
| Linear discriminant analysis | 32 | 56 |
| Quadratic discriminant analysis | 1 | 53 |
| Decision trees | 5 | 54 |
| Neural networks | | 45 |
| k -nearest neighbours | | 44 |
| FDA/BRUTO | 6 | 44 |
| FDA/MARS | 13 | 39 |

A good way to visualise the performance of model predictions is through a confusion matrix, as shown in Figure 5.8. The numbers in each row indicate the instances of a predicted class, while the numbers in the column indicate instances of the actual classes, while nil values are indicated by blank cells.

Comparisons to other methods that had been used to analyse this data set is given in Table 5.6. In particular, the I-probit model is compared against 1) linear regression; 2) logistic linear regression; 3) linear and quadratic discriminant analysis; 4) decision trees; 5) neural networks; 6) k -nearest neighbours; and 7) flexible discriminant analysis. All of these methods are described in further detail in [Friedman et al. \(2001, Ch.4 & 12, Table 12.3\)](#). The I-probit model using both the fBm-0.5 and SE kernel offers one of the best out-of-sample classification error rates (34.4%) of all the methods compared. The linear I-probit model is seen to be comparable to logistic regression, linear and quadratic discriminant analysis, and also decision trees. It also provides significant improvement over multiple linear regression.



(a) Canonical kernel (b) fBm-0.5 kernel



(c) SE kernel

Figure 5.8.3 Confusion matrices for the vowel classification problem in which predicted values were obtained from the I-probit models. The maximum value for any one cell is 42. Blank cells indicate nil values.

5.8.4 Spatio-temporal modelling of bovine tuberculosis in Cornwall

Data containing the number of breakdowns of bovine tuberculosis (BTB) in Cornwall, the locations of the infected animals, and the year of occurrence is analysed. The interest, as motivated by veterinary epidemiology, is to understand whether or not there is spatial segregation between the herds, and whether there is a time-element to presence or absence of this spatial segregation. There have been previous work done to analyse this data set: [P. Diggle et al., 2005](#) developed a non-parametric method to estimate spatial segregation using a multivariate point process. The occurrences are modelled as Poisson point processes, and spatial segregation is said to have occurred if the model-estimated type-specific breakdown probabilities at any given location are not significantly different from the sample proportions. The authors estimated the probabilities via kernel regression, and the test statistic of interest had to be estimated via Monte Carlo methods. Other work includes [P. J. Diggle et al. \(2013\)](#), who used a fully Bayes scheme for spatio-temporal multivariate log-Gaussian Cox processes, and implemented in the R package `lgcp` ([Taylor et al., 2013](#)).

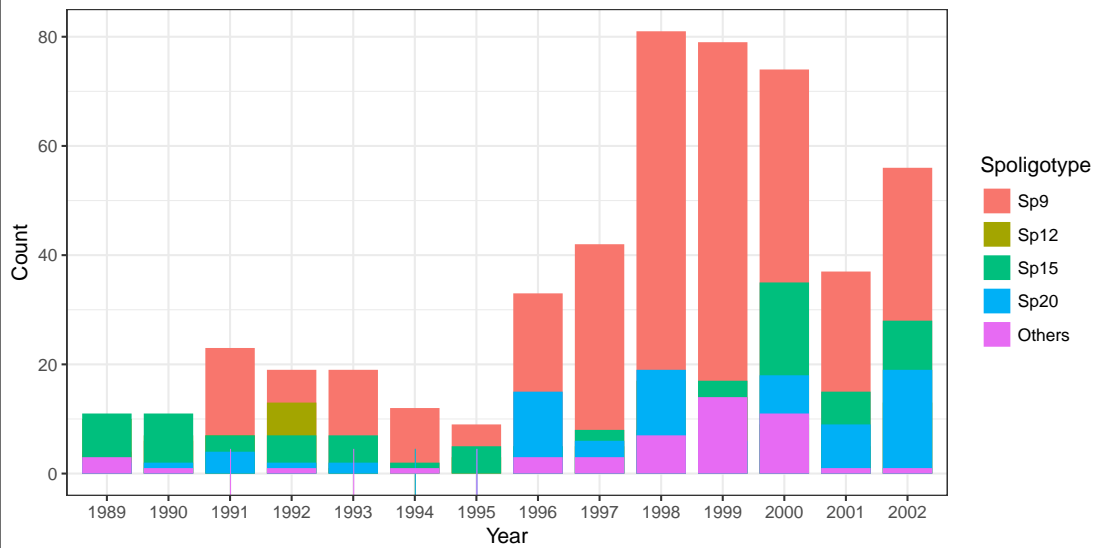


Figure 5.9: Distribution of the different types (Spoligotypes) of bovine tuberculosis affecting herds in Cornwall over the period 1989 to 2002.

fig:plot.co
w

The data set contains $n = 919$ recorded cases over a span of 14 years. For each of the cases, spatial data pertaining to the location of the farm (Northings and Eastings, measured in kilometres) are available. Originally, 11 unique spoligotypes were recorded

in the data, with the four most common spoligotypes being Sp9 ($m = 1$), Sp12 ($m = 2$), Sp15 ($m = 3$) and Sp20 ($m = 4$), as shown by the histogram in Figure 5.9. We had grouped the remaining seven spoligotypes into an ‘Others’ category ($m = 5$), so that the problem becomes a multinomial regression with five distinct outcomes.

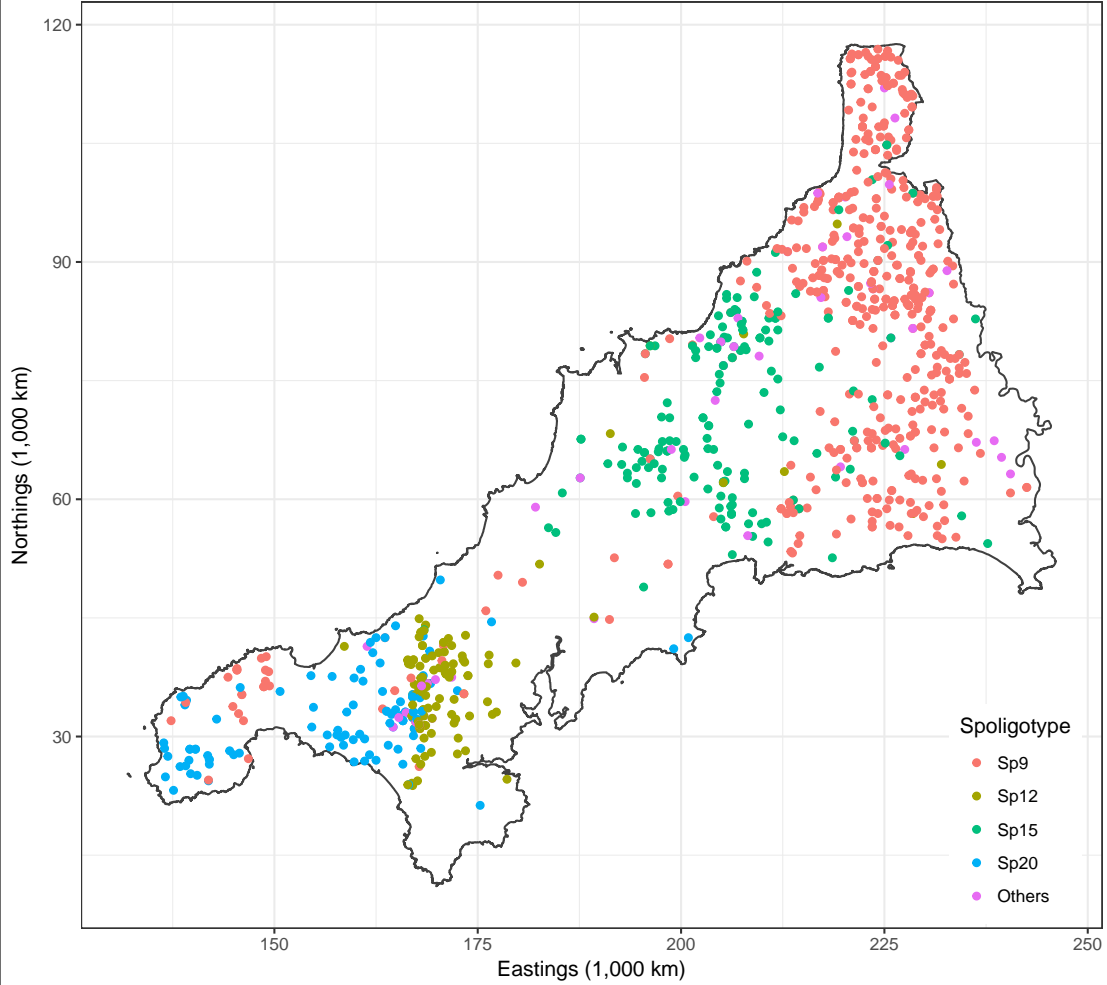


Figure 5.10: Spatial distribution of all cases over the 14 years.

We are able to investigate any spatio-temporal patterns of infection using I-priors rather simply. Let p_{ij} denote the probability that a particular farm i is infected with a BTB disease with spoligotype $j \in \{1, \dots, 5\}$. We model the transformed probabilities $g(p_{ij})$ (as described in the categorical response chapter) as following a smooth function f which takes two covariates: the spatial data $x_1 \in \mathbb{R}^2$, and the temporal data x_2 (year

fig:plot.co
rnwall

of infection):

$$\begin{aligned} g(p_{ij}) &= f_j(x_1, x_2) \\ &= f_{1j}(x_1) + f_{2j}(x_2) + f_{12j}(x_1, x_2) \end{aligned}$$

We assume a smooth effect of space and time on the probabilities, and appropriate RKHSs for the functions $f_1 \in \mathcal{F}_1$ and $f_2 \in \mathcal{F}_2$ are the fBm-0.5 RKHS. Alternatively, as per [P. Diggle et al. \(2005\)](#), divide the data into four distinct time periods: 1) 1996 and earlier; 2) 1997 to 1998; 3) 1999 to 2000; and finally 4) 2001 to 2002. In this case, x_2 would indicate which period the infection took place in, and thus would have a nominal effect on the probabilities. An appropriate RKHS for f_2 in such a case would be the Pearson RKHS. In either case, the function $f_{12} \in \mathcal{F}_1 \otimes \mathcal{F}_2$ would be the “interaction effect”, meaning that with such an effect present, the spatial distribution of the diseases are assumed to vary across the years.

We fitted four different models:

- **M_0 : Intercept only.**

$$p_{ij} = g_j^{-1}(\alpha_k)_{k=1}^m$$

- **M_1 : Spatial segregation.**

$$p_{ij} = g_j^{-1}(\alpha_k + f_{1k}(x_i))_{k=1}^m$$

$f_{1k} \in \mathcal{F}_1$ Pearson RKHS.

- **M_2 : Spatio-temporal.**

$$p_{ij} = g_j^{-1}(\alpha_k + f_{1k}(x_i) + f_{2k}(t_i) + f_{12k}(x_i, t_i))_{k=1}^m$$

$f_{1k} \in \mathcal{F}_1$ Pearson RKHS, $f_{2k} \in \mathcal{F}_2$ fBm-0.5 RKHS, and $f_{12k} \in \mathcal{F}_1 \otimes \mathcal{F}_2$

- **M_3 : Spatio-period.**

$$p_{ij} = g_j^{-1}(\alpha_k + f_{1k}(x_i) + f_{2k}(t_i) + f_{12k}(x_i, t_i))_{k=1}^m$$

$f_{1k} \in \mathcal{F}_1$ Pearson RKHS, $f_{2k} \in \mathcal{F}_2$ Pearson RKHS, and $f_{12k} \in \mathcal{F}_1 \otimes \mathcal{F}_2$

where g^{-1} is the link function described earlier. Model M_0 corresponds to a model which ignores any spatial or temporal effects (the baseline intercept only model). Model M_1

Table 5.7: Results of the fitted I-probit models.

| | M_0 : Intercepts only | | M_1 : Spatial only | | M_2 : Spatio-temporal | | M_3 : Spatio-period | |
|--------------------|-------------------------|-------|----------------------|-------|-------------------------|-------|-----------------------|-------|
| | Mean | S.D. | Mean | S.D. | Mean | S.D. | Mean | S.D. |
| Intercept (Sp9) | 0.948 | 0.033 | 1.364 | 0.033 | 1.401 | 0.033 | 1.395 | 0.033 |
| Intercept (Sp12) | -0.173 | 0.033 | -0.435 | 0.033 | -0.506 | 0.033 | -0.463 | 0.033 |
| Intercept (Sp15) | 0.103 | 0.033 | -0.020 | 0.033 | -0.008 | 0.033 | -0.010 | 0.033 |
| Intercept (Sp20) | -0.202 | 0.033 | -0.775 | 0.033 | -0.795 | 0.033 | -0.783 | 0.033 |
| Intercept (Others) | -0.676 | 0.033 | -0.134 | 0.033 | -0.091 | 0.033 | -0.139 | 0.033 |
| Scale (spatial) | | | 0.194 | 0.003 | -0.176 | 0.003 | 0.172 | 0.003 |
| Scale (temporal) | | | | | -0.006 | 0.000 | -0.004 | 0.000 |
| Log-likelihood | -1187.47 | | -564.33 | | -537.23 | | -543.94 | |
| Error rate (%) | 46.25 | | 19.26 | | 18.06 | | 18.50 | |
| Brier score | 0.249 | | 0.143 | | 0.136 | | 0.138 | |

takes into account only spatial effects. Both models M_2 and M_3 account for spatio-temporal effects, but M_2 assumes a smooth effect of time, while M_3 segregates the points into four distinct time periods for analysis. Model comparison is easily done, and Table 5.7 indicates that model M_2 has the highest log-likelihood of the four models, making it the preferable model.

Alternatively, spatio-temporal effects of the BTB breakdowns can easily be inferred through the RKHS scale parameters. Let h_k , $k \in \{1, 2\}$ denote the reproducing kernel of the spatial and temporal RKHSs respectively. Then, an I-prior on $f_j = f_{1j} + f_{2j} + f_{12j}$, $j = 1, \dots, 5$, takes the form

$$f_j(x_1, x_2) = \sum_{i=1}^n (\lambda_1 h_1(x_1, x_{i1}) + \lambda_2 h_2(x_2, x_{i2}) + \lambda_1 \lambda_2 h_1(x_1, x_{i1}) h_2(x_2, x_{i2})) w_{ij}$$

where it is assumed $(w_{i1}, \dots, w_{i5})^\top \stackrel{\text{iid}}{\sim} N(\mathbf{0}, \mathbf{I}_5)$. The hypothesis of temporal significance is the same as testing the significance of the λ_2 parameter, while the test of both spatial and temporal effects are conducted on λ_1 and λ_2 simultaneously. From Chapter X, we know that these scale parameters follow a normal posterior distribution, so we can calculate the Z -scores by dividing the mean by its corresponding standard deviation. Absolute values greater than three would satisfy a Bayesian hypothesis test of significance at the 0.01 level. The conclusion from Table 5.7 is that the data supports a hypothesis for a spatio-temporal or spatio-period model.

For a more visual approach, we can look at the plots of the surface probabilities. To obtain these probabilities, we first determined the spatial points (Northings and Eastings) which fall inside the polygon which makes up Cornwall. We then obtained predicted probabilities for each class of disease at each location. Figure 5.11 was obtained using the model with spatial covariates only, thus ignoring any temporal effects. In the case of the spatio-temporal model, we used the model which had the period formulation for time (Model 3). This way, we can display the surface probabilities of the time periods in four plots only, which is more economical to exhibit within the margins of this thesis. Note that there is no issue with using the continuous time model—we have produced an animated gif image at <http://phd.haziqj.ml/examples/>, showing the evolution of the surface probabilities over time.

As the model suggests, there is indeed spatial segregation for the four most common spoligotypes, and this is also very prominently seen from Figure 5.11. In comparing the distribution of the spoligotypes over the years, we may refer to Figure 5.12. For

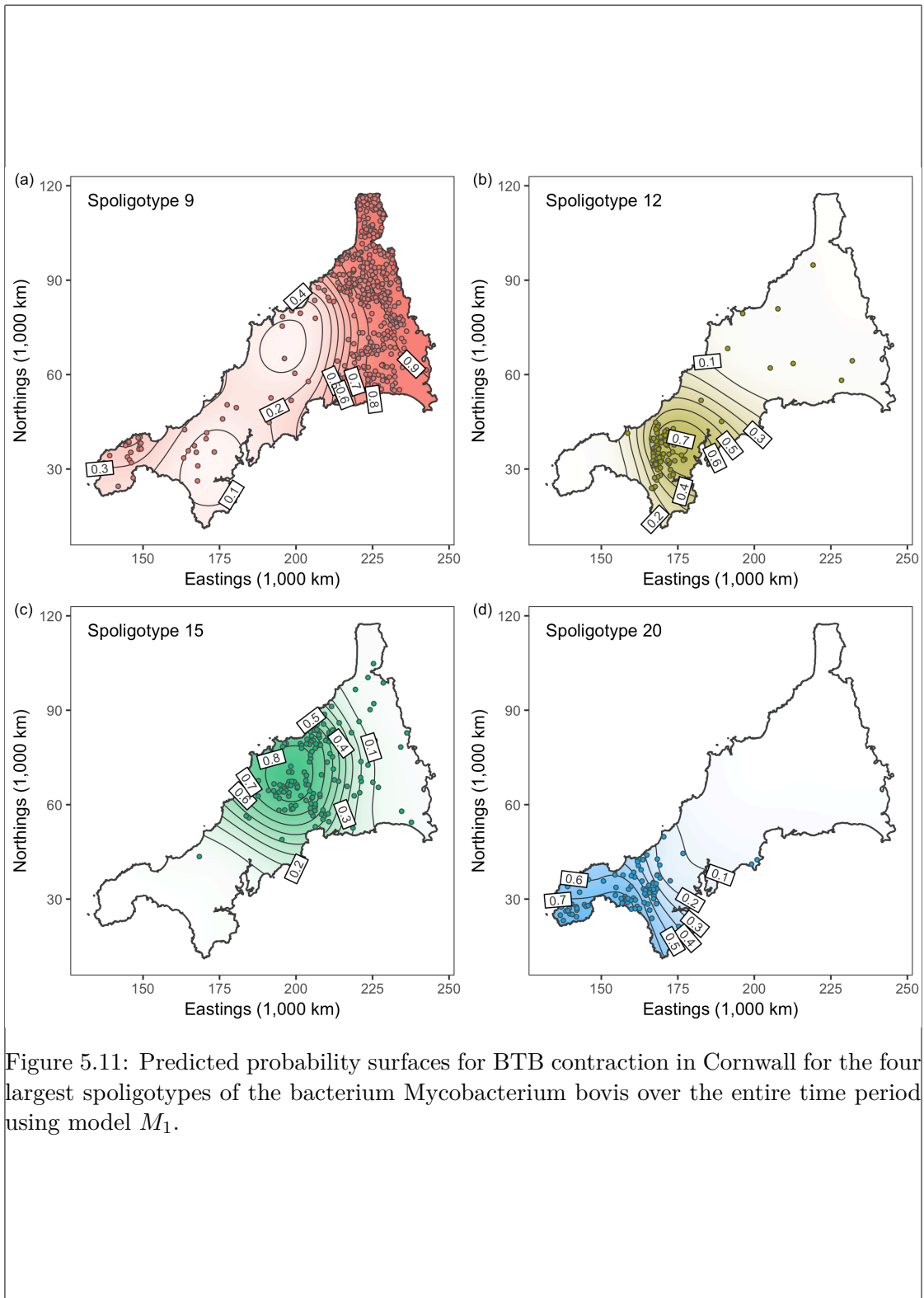


Figure 5.11: Predicted probability surfaces for BTB contraction in Cornwall for the four largest spoligotypes of the bacterium *Mycobacterium bovis* over the entire time period using model M_1 .

fig:plot.bt
b

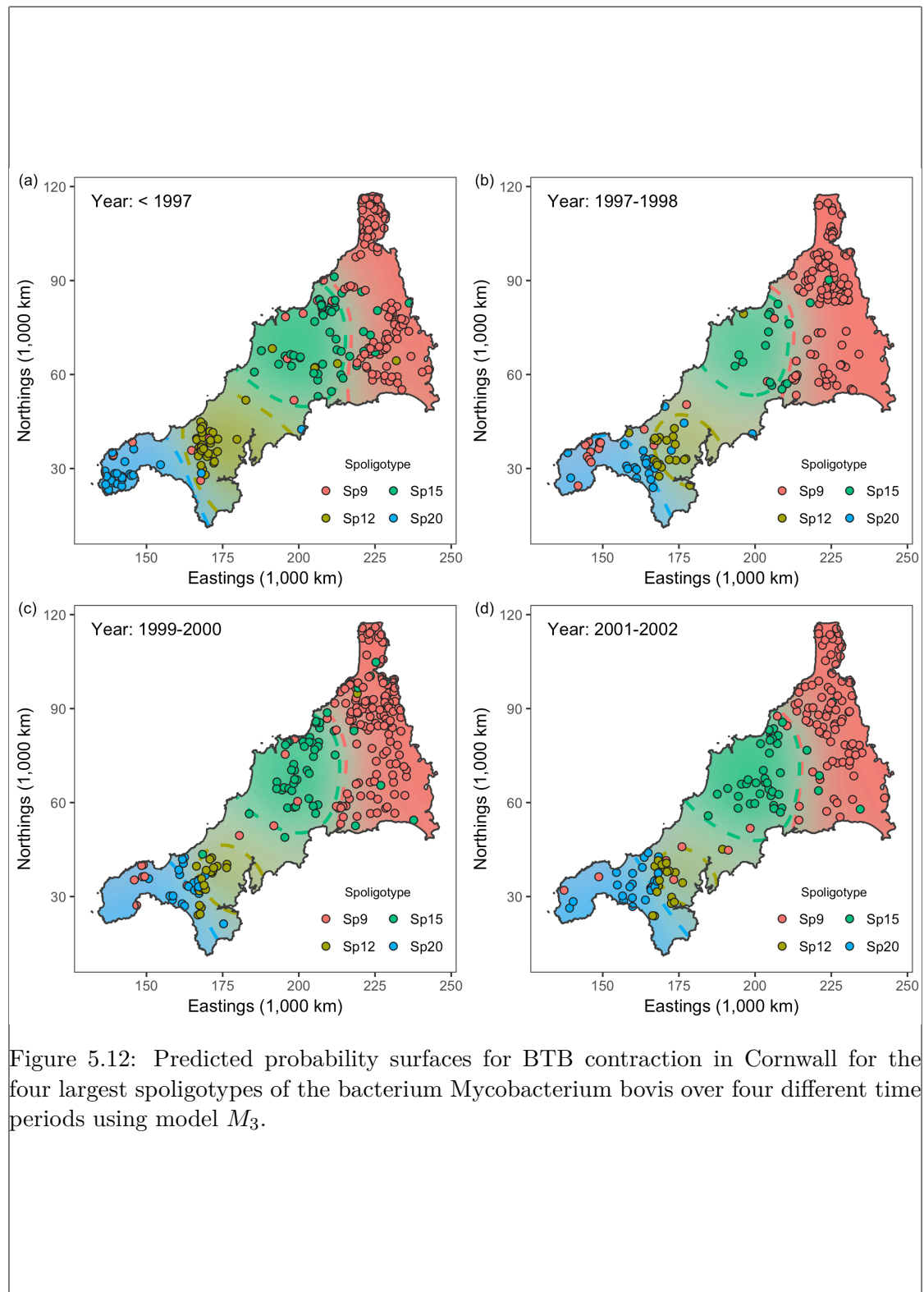


Figure 5.12: Predicted probability surfaces for BTB contraction in Cornwall for the four largest spoligotypes of the bacterium *Mycobacterium bovis* over four different time periods using model M_3 .

fig:plot.te
mporal.btb

each time period, we superimpose the actual observations onto the predicted surface probabilities. In addition, coloured dotted lines are displayed to indicate the “decision boundaries” for each of the four spoligotypes. The most evident change is seen to the spatial distribution of spoligotype 12, with the decision boundary giving it a large area in years 1996 and earlier, but this steadily shrunk over the years. Spoligotype 9, which is most commonly seen in the east of Cornwall, seems to have made its way down to the south-west over the years. The other two spoligotypes seem to be rather constant over the years. This is supported also by the spatio-period model results in [Table 5.7](#), where the test of nullity for the scale parameters of these two spoligotypes are not rejected.

5.9 Conclusion

This work presents an extension of the normal I-prior methodology to fit categorical response models using probit link functions—a methodology we call the I-probit. The main motivation behind this work is to overcome the drawbacks of modelling probabilities using the normal I-prior model. We assumed latent variables that represent ‘class propensities’ exist, modelled these using a normal I-prior, and simply transformed them via a probit link function. In this way, all of the advantages of the I-prior methodology seen for the normal model are preserved for binary and multinomial regression as well.

The core of this work explores ways in which to overcome the intractable integral presented by the I-probit model in [\(5.11\)](#). Techniques such as quadrature methods, Laplace approximation and MCMC tend to fail, or are unsatisfactorily slow to accomplish. The main reason for this is the dimension of this integral, which is nm , and thus for large sample sizes and/or number of classes, is unfeasible with such methods. We turned to variational inference in the face of an intractable posterior density that hampers an EM algorithm, and the result is a sequential updating scheme, similar in time and storage requirements to the EM algorithm.

In terms of similarity to other works, the generalised additive models (GAMs) of [Hastie and Tibshirani \(1986\)](#) comes close. The setup of GAMs is near identical to the I-probit model, although estimation is done differently. GAMs do not assume smooth functions from any RKHS, but instead estimates the f ’s using a local scoring method or a local likelihood method. Kernel methods for classification are extremely popular in computer science and machine learning; examples include support vector machines ([Schölkopf and Smola, 2002](#)) and Gaussian process classification ([Rasmussen and](#)

Williams, 2006), with the latter being more closely related to the I-probit method. However, Gaussian process classification typically uses the logistic sigmoid function, and estimation most commonly performed using Laplace approximation, but other methods such as expectation propagation (Minka, 2001) and MCMC (Neal, 1999) have been explored as well. Variational inference for Gaussian process probit models have been studied by Girolami and Rogers (2006), with their work providing a close reference to the variational algorithm employed by us.

Suggestions for future work include:

1. **Estimation of Ψ .** A limitation we had to face in this work was to treat Ψ as fixed. This limitation was in part due to the non-conjugate nature of the variational density for Ψ . We believe the variational Bayes EM algorithm, which estimates maximum a posteriori values for the parameters, could alleviate this issue. This would bring the estimation procedure on par with the frequentist objective of maximum likelihood via the EM algorithm, albeit with the use of approximate posterior densities (see Sections 5.10.2 and 5.10.3 for further discussions).
2. **Inclusion of class-specific covariates.** Throughout the chapter, we assumed that covariates were unit-specific, rather than class-specific. One such example is modelling the choice of travel mode between two destinations (car, coach, train or aeroplane) as a function of travel time. Clearly, travel time depends on the mode of transport. This would require a careful rethink of the appropriate RKHS/RKKS to which the regression function belongs: the regression on the latent propensities could be extended as such:

$$y_{ij}^* = \alpha_j + f_j(x_i) + e(z_{ij})$$

and $f_j \in \mathcal{F}_{\mathcal{X}}$, the RKHS with kernel $h : (\mathcal{X} \times \mathcal{M})^2 \rightarrow \mathbb{R}$ defined by $\delta_{jj'}h(x, x')$, and $e \in \mathcal{F}_{\mathcal{Z}}$, the RKHS of functions of the form $e : \{z_{ij} | i = 1, \dots, n, j = 1, \dots, m\} \rightarrow \mathbb{R}$. An I-prior would then be applied as usual, but the implications on the estimation would need to be considered as well.

3. **Improving computational efficiency.** The $O(n^3m)$ time requirement for estimating I-probit models hinder its use towards large-data applications. In a limited study, we did not obtain reliable improvements using low-rank approximations of the kernel matrix such as the Nyström method. The key to improving compu-

tational efficiency could lie in sparse variational methods, a suggestion that was made to improve normal I-prior models as well.

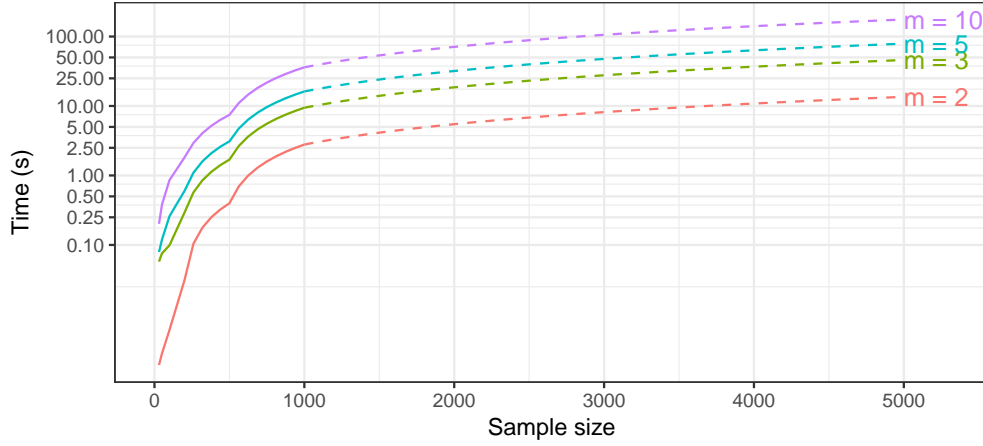


Figure 5.13: Time taken to complete a single variational inference iteration for varying sample sizes and number of classes m . The solid line represents actual timings, while the dotted lines are linear extrapolations.

5.10 Miscellanea

5.10.1 A brief introduction to variational inference

Consider a statistical model for which we have observations $\mathbf{y} := \{y_1, \dots, y_n\}$, but also some latent variables $\mathbf{z} := \{z_1, \dots, z_n\}$. Typically, in such models, there is a want to to evaluate the integral

$$\mathcal{I} = \int p(\mathbf{y}|\mathbf{z})p(\mathbf{z}) d\mathbf{z}. \quad (5.17)$$

Models that include latent variables are plenty, for example: Gaussian mixture models, latent class analysis, factor models, random coefficient models, and so on. Marginalising out the latent variables in (5.17) is usually a precursor to obtaining a log-likelihood function to be maximised, in a frequentist setting. In Bayesian analysis, the \mathbf{z} 's are parameters which are treated as random, and the integral corresponds to the marginal density for \mathbf{y} , on which the posterior depends.

In many instances, for one reason or another, evaluation of \mathcal{I} is difficult, in which case inference is halted unless a way of overcoming the intractable integral (5.17) is

found. Here, we discuss *variational inference* (VI), a fully Bayesian treatment of the statistical model with a deterministic algorithm, i.e. does not involve sampling from posteriors. The crux of variational inference is this: find a suitably close distribution function $q(z)$ that approximates the true posterior $p(\mathbf{z}|\mathbf{y})$, where closeness here is defined in the Kullback-Leibler divergence sense,

$$\text{KL}(q\|p) = \int \log \frac{q(\mathbf{z})}{p(\mathbf{z}|\mathbf{y})} q(\mathbf{z}) \, d\mathbf{z}.$$

Posterior inference is then conducted using $q(\mathbf{z})$ in lieu of $p(\mathbf{z}|\mathbf{y})$. Advantages of this method are that 1) it is fast to implement computationally (compared to MCMC); 2) convergence is assessed simply by monitoring a single convergence criterion; and 3) it works well in practice, as attested to by the many studies implementing VI.

Briefly, we present the motivation behind variational inference and the minimisation of the KL divergence. Denote by $q(\cdot)$ some density function of \mathbf{z} . One may show that log marginal density (the log of the intractable integral (5.17)) holds the following bound:

$$\begin{aligned} \log p(y) &= \log p(\mathbf{y}, \mathbf{z}) - \log p(\mathbf{z}|\mathbf{y}) \quad (\text{Bayes' theorem}) \\ &= \int \left\{ \log \frac{p(\mathbf{y}, \mathbf{z})}{q(\mathbf{z})} - \log \frac{p(\mathbf{z}|\mathbf{y})}{q(\mathbf{z})} \right\} q(\mathbf{z}) \, d\mathbf{z} \quad (\text{expectations both sides}) \\ &= \mathcal{L}(q) + \text{KL}(q\|p) \\ &\geq \mathcal{L}(q) \end{aligned} \tag{5.18}$$

{eq:varbound}

since the KL divergence is a non-negative quantity. The functional $\mathcal{L}(q)$ given by

$$\begin{aligned} \mathcal{L}(q) &= \int \log \frac{p(\mathbf{y}, \mathbf{z})}{q(\mathbf{z})} q(\mathbf{z}) \, d\mathbf{z} \\ &= \mathbb{E}_{\mathbf{z} \sim q} \log p(\mathbf{y}, \mathbf{z}) + H(q), \end{aligned} \tag{5.19}$$

{eq:elbo1}

where H is the entropy functional, is known as the *evidence lower bound* (ELBO). Evidently, the closer q is to the true p , the better, and this is achieved by maximising \mathcal{L} , or equivalently, minimising the KL divergence from p to q . Note that the bound (5.18) achieves equality if and only if $q(\mathbf{z}) \equiv p(\mathbf{z}|\mathbf{y})$, but of course the true form of the posterior is unknown to us—see Section 5.10.2 for a discussion. Maximising $\mathcal{L}(q)$ or minimising $\text{KL}(q\|p)$ with respect to the density q is a problem of calculus of variations, which incidentally, is where variational inference takes its name. The astute reader will realise

that $\text{KL}(q||p)$ is impossible to compute, since one does not know the true distribution $p(\mathbf{z}|\mathbf{y})$. Efforts are concentrated on maximising the ELBO instead.

Maximising \mathcal{L} over all possible density functions q is not possible without considering certain constraints. Two such constraints are described. The first, is to make a distributional assumption regarding q , for which it is parameterised by ν . For instance, we might choose the closest normal distribution to the posterior $p(\mathbf{z}|\mathbf{y})$ in terms of KL divergence. In this case, the task is to find optimal mean and variance parameters of a normal distribution.

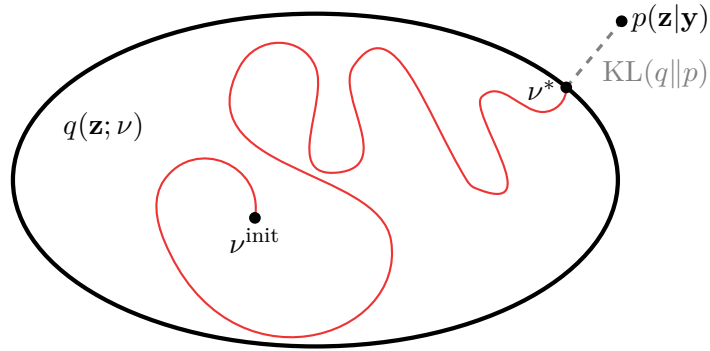


Figure 5.14: Schematic view of variational inference⁵. The aim is to find the closest distribution q (parameterised by a variational parameter ν) to p in terms of KL divergence within the set of variational distributions, represented by the ellipse.

The second type of constraint, and the one considered in this thesis, is simply an assumption that the approximate posterior q factorises into M disjoint factors. Partition \mathbf{z} into M disjoint groups $\mathbf{z} = (z_{[1]}, \dots, z_{[M]})$. Note that each factor $z_{[k]}$ may be multidimensional. Then, the structure

$$q(\mathbf{z}) = \prod_{k=1}^M q_k(z_{[k]})$$

for q is considered. This factorised form of variational inference is known in the statistical physics literature as the *mean-field theory* (Itzykson and Drouffe, 1991).

Let us denote the distributions which minimise the Kullback-Leibler divergence (maximise the variational lower bound) by the use of tildes. By appealing to Bishop (2006,

⁵Reproduced from the talk by David Blei entitled ‘Variational Inference: Foundations and Innovations’, 2017. URL: <https://simons.berkeley.edu/talks/david-blei-2017-5-1>.

equation 10.9, p. 466), we find that for each $z_{[k]}$, $k = 1, \dots, M$, \tilde{q}_k satisfies

$$\log \tilde{q}_k(z_{[k]}) = E_{-k} \log p(\mathbf{y}, \mathbf{z}) + \text{const.} \quad (5.20)$$

{eq:qtilde}

where expectation of the joint log density of \mathbf{y} and \mathbf{z} is taken with respect to all of the unknowns \mathbf{z} , except the one currently in consideration $z_{[k]}$, under their respective \tilde{q}_k densities.

In practice, rather than an explicit calculation of the normalising constant, one simply needs to inspect (5.20) to recognise it as a known log-density function, which is the case when exponential family distributions are considered. That is, suppose that each complete conditional $p(z_{[k]}|\mathbf{z}_{-k}, \mathbf{y})$, where $\mathbf{z}_{-k} = \{z_{[i]}|i \neq k\}$, follows an exponential family distribution

$$p(z_{[k]}|\mathbf{z}_{-k}, \mathbf{y}) = B(z_{[k]}) \exp(\langle \zeta_k(\mathbf{z}_{-k}, \mathbf{y}), z_{[k]} \rangle - A(\zeta_k)).$$

Then, from (5.20),

$$\begin{aligned} \tilde{q}(z_{[k]}) &\propto \exp(E_{-k} \log p(z_{[k]}|\mathbf{z}_{-k}, \mathbf{y})) \\ &= \exp(\log B(z_{[k]}) + E\langle \zeta_k(\mathbf{z}_{-k}, \mathbf{y}), z_{[k]} \rangle - E[A(\zeta_k)]) \\ &\propto B(z_{[k]}) \exp E\langle \zeta_k(\mathbf{z}_{-k}, \mathbf{y}), z_{[k]} \rangle \end{aligned}$$

is also in the same exponential family. In situations where there is no closed form expression for \tilde{q} , then one resorts to sampling methods such as a Metropolis random walk to estimate quantities of interest. This stochastic step within a deterministic algorithm has been explored before in the context of a Monte Carlo EM algorithm—see [Meng and Van Dyk \(1997, §4, pp. 537–538\)](#) and references therein.

One notices that the optimal mean-field variational densities for each component are coupled with one another, in the sense that the distribution \tilde{q}_k depends on the moments of the rest of the components \mathbf{z}_{-k} . For very simple problems, an exact solution for each \tilde{q}_k can be found, but usually, the way around this is to employ an iterative procedure. The *coordinate ascent mean-field variational inference* (CAVI) algorithm cycles through each of the distributions in turn, updating them in sequence starting with arbitrary distributions as initial values.

alg:cavi

Algorithm 2 The CAVI algorithm

```

1: initialise Variational factors  $q_k(z_{[k]})$ 
2: while ELBO  $\mathcal{L}(q)$  not converged do
3:   for  $k = 1, \dots, M$  do
4:      $\tilde{q}_k(z_{[k]}) \leftarrow \text{const.} \times \exp E_{-k} \log p(\mathbf{y}, \mathbf{z})$  ▷ from (5.20)
5:   end for
6:    $\mathcal{L}(q) \leftarrow E_{\mathbf{z} \sim \prod_k \tilde{q}_k} \log p(\mathbf{y}, \mathbf{z}) + \sum_{k=1}^m H[q_k(z_{[k]})]$  ▷ Update ELBO
7: end while
8: return  $\tilde{q}(\mathbf{z}) = \prod_{k=1}^M \tilde{q}_k(z_{[k]})$ 

```

Each iteration of the CAVI brings about an improvement in the ELBO (hence the name coordinate ascent). The algorithm terminates when there is no more significant improvement in the ELBO, indicating a convergence of the CAVI. Blei et al. (2017) notes that the ELBO is typically a non-convex function, in which case convergence may be to (one of possibly many) local optima. A simple solution would be to restart the CAVI at multiple initial values, and the solution giving the highest ELBO is the distribution that is closest to the true posterior.

5.10.2 Variational methods and the EM algorithm

sec:varEM

Consider again the latent variable setup described in Section 5.10.1, but suppose the goal now is to maximise the (marginal) log-likelihood of the parameters θ of the model. We will see how the EM algorithm relates to minimising the KL divergence between a density $q(\mathbf{z})$ and the posterior of \mathbf{z} , and connect this idea to variational methods.

As we did in deriving (5.18), we decompose the marginal log-likelihood as

$$\log p(y|\theta) = E \left[\log \frac{p(\mathbf{y}, \mathbf{z}|\theta)}{q(\mathbf{z})} \right] - E \left[\log \frac{p(\mathbf{z}|\mathbf{y}, \theta)}{q(\mathbf{z})} \right] = \mathcal{L}(q) + \text{KL}(q||p).$$

This decomposition is shown in Figure 5.15. We realise that the KL divergence non-negative, and is zero exactly when $q(\mathbf{z}) \equiv p(\mathbf{z}|\mathbf{y}, \theta)$. Substituting this into the above equation yields the relationship

$$\begin{aligned} \log p(y|\theta) &= E \left[\log \frac{p(\mathbf{y}, \mathbf{z}|\theta)}{p(\mathbf{z}|\mathbf{y}, \theta)} \right] - E \left[\log \frac{p(\mathbf{z}|\mathbf{y}, \theta)}{p(\mathbf{z}|\mathbf{y}, \theta)} \right] \\ &= E \log p(\mathbf{y}, \mathbf{z}|\theta) - E p(\mathbf{z}|\mathbf{y}, \theta). \end{aligned}$$

⁶Reproduced from Bishop (2006, Figure 9.11).

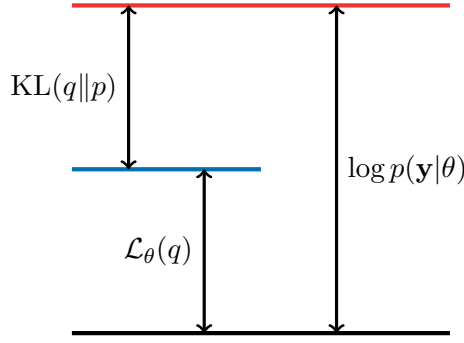


Figure 5.15: Illustration⁶ of the decomposition of the log-likelihood into $\mathcal{L}_\theta(q)$ and $\text{KL}[q(\mathbf{z})||p(\mathbf{z}|\mathbf{y})]$. The quantity $\mathcal{L}_\theta(q)$ is a lower bound for the log-likelihood.

fig:loglikd
ecom

By taking expectations under the posterior distribution with known parameter values $\theta^{(t)}$, the term on the left becomes the Q function of the E-step

$$Q(\theta) = Q(\theta|\theta^{(t)}) = \mathbb{E}_{\mathbf{z}} \left[\log p(\mathbf{y}, \mathbf{z}|\theta) \mid \mathbf{y}, \theta^{(t)} \right],$$

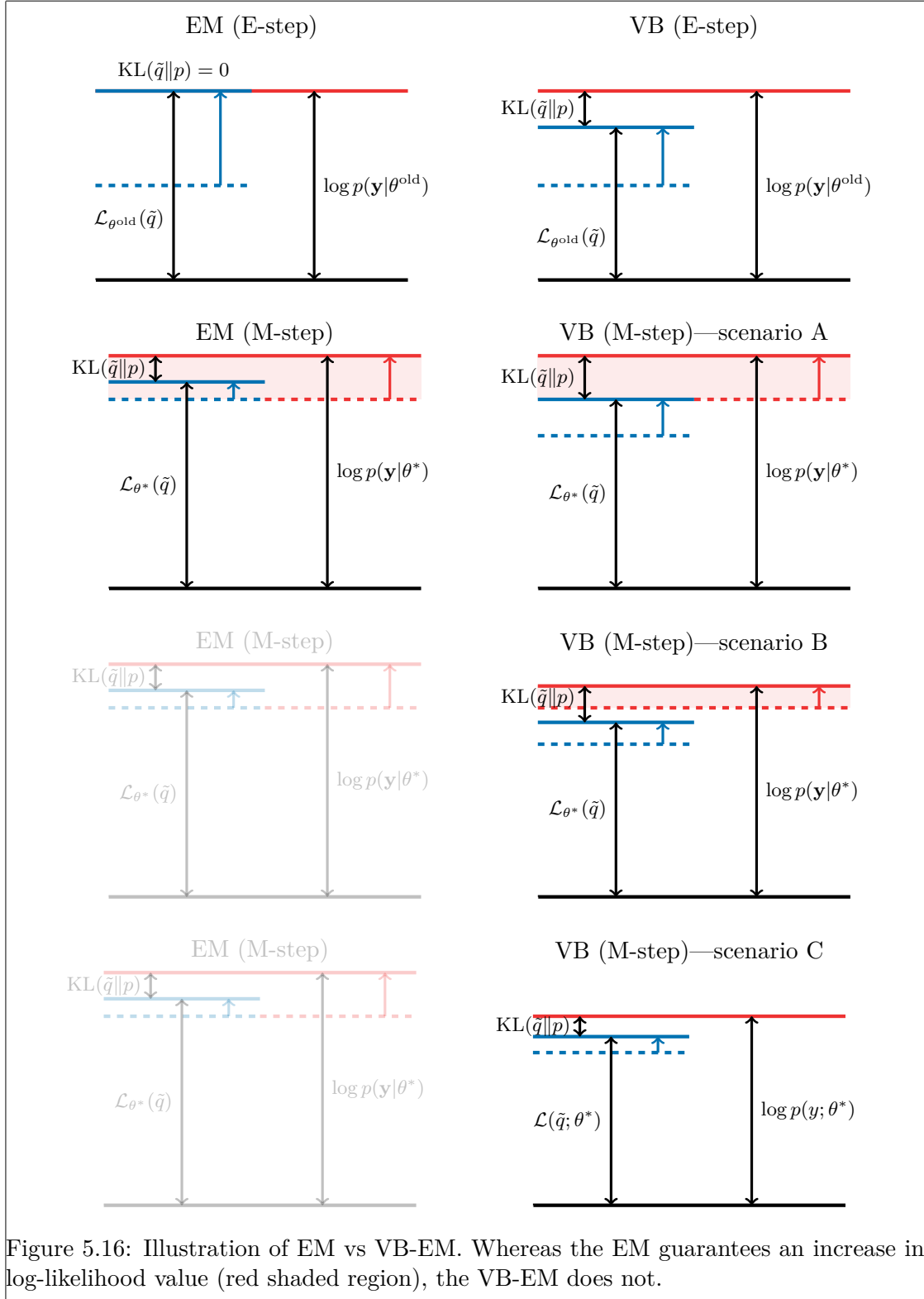
while the term on the left is an entropy term. Thus, minimising the KL divergence corresponds to the E-step in the EM algorithm. As a side fact, for any θ , we find that

$$\begin{aligned} \log p(\mathbf{y}|\theta) - \log p(\mathbf{y}|\theta^{(t)}) &= Q(\theta|\theta^{(t)}) - Q(\theta^{(t)}|\theta^{(t)}) + \Delta \text{ entropy} \\ &\geq Q(\theta|\theta^{(t)}) - Q(\theta^{(t)}|\theta^{(t)}). \end{aligned}$$

because entropy differences are positive by Gibbs' inequality. We see that maximising Q with respect to θ (the M-step) brings about an improvement to the log-likelihood value. To summarise, the EM algorithm is seen as

- **E-step.** Maximise $\mathcal{L}_\theta[q(\mathbf{z})]$ with respect to q , keeping θ fixed. This is equivalent to minimising $\text{KL}(q||p)$.
- **M-step.** Maximise $\mathcal{L}[q(\mathbf{z}|\theta)]$ with respect to θ , keeping q fixed.

When the true posterior distribution $p(\mathbf{z}|\mathbf{y})$ is not tractable, then the E-step becomes intractable as well. By constraining the maximisation in the E-step to consider q belonging to a family of tractable densities, the E-step yields a variational approximation \tilde{q} to the true posterior. In [Section 5.10.1](#), we saw that constraining q to be of a factorised form, then \tilde{q} is a mean-field density. This form of the EM is known as *variational Bayes EM algorithm* (VB-EM) ([Beal and Ghahramani, 2003](#)).



In variational inference, a fully Bayesian treatment of the parameters is considered, with the aim of obtaining approximation to their posterior distributions. In VB-EM, the variational approximation is only performed on the latent, or ‘missing’ variables, to use the EM nomenclature. After a variational E-step, the M-step proceeds as usual, and as such, all of the material relating to the EM in the previous chapter is applicable. The VB-EM can also be seen as obtaining (approximate) maximum a posteriori estimates with diffuse priors on the parameters.

5.10.3 The EM algorithm for I-probit models is intractable—variational Bayes EM?

Consider employing an EM algorithm, similar to the one seen in the previous chapter, to estimate I-probit models. This time, treat both the latent propensities \mathbf{y}^* and the I-prior random effects \mathbf{w} as ‘missing’, so the complete data is $\{\mathbf{y}, \mathbf{y}^*, \mathbf{w}\}$. Now, due to the independence of the observations $i = 1, \dots, n$, the complete data log-likelihood is

$$\begin{aligned} \log p(\mathbf{y}, \mathbf{y}^*, \mathbf{w}) &= \sum_{i=1}^n \left\{ \log p(y_i | \mathbf{y}_{i\cdot}^*) + \log p(\mathbf{y}_{i\cdot}^* | \mathbf{w}_{i\cdot}) + \log p(\mathbf{w}_{i\cdot}) \right\} \\ &= -\frac{1}{2} \sum_{i=1}^n \mathbb{1}[y_{ij}^* = \max_k y_{ik}^*] \left[(\mathbf{y}_{i\cdot}^* - \boldsymbol{\alpha} - \mathbf{w}_{i\cdot}^\top \mathbf{h}_\eta(x_i))^\top \boldsymbol{\Psi} (\mathbf{y}_{i\cdot}^* - \boldsymbol{\alpha} - \mathbf{w}_{i\cdot}^\top \mathbf{h}_\eta(x_i)) \right. \\ &\quad \left. + \mathbf{w}_{i\cdot}^\top \boldsymbol{\Psi}^{-1} \mathbf{w}_{i\cdot} \right] + \text{const.} \end{aligned}$$

which looks like the complete data log-likelihood seen previously in (4.9), except that here, together with the $\mathbf{w}_{i\cdot}$ ’s, the $\mathbf{y}_{i\cdot}^*$ ’s are never observed.

For the E-step, it is of interest to determine the posterior density $p(\mathbf{y}^*, \mathbf{w} | \mathbf{y}) = p(\mathbf{y}^* | \mathbf{w}, \mathbf{y}) p(\mathbf{w} | \mathbf{y})$, which apparently is hard to obtain. We can go as far as determining that the full conditional of the latent propensities is multivariate subject to a conical truncation $\mathcal{C}_j = \{y_{ij}^* > y_{ik}^* | \forall k \neq j\}$, i.e. $\mathbf{y}_{i\cdot}^* | \mathbf{w}_{i\cdot}, \{y_i = j\} \stackrel{\text{iid}}{\sim} \text{tN}_m(\boldsymbol{\alpha} + \mathbf{w}_{i\cdot}^\top \mathbf{h}_\eta(x_i), \boldsymbol{\Psi}^{-1}, \mathcal{C}_j)$, for each $i = 1, \dots, n$, and that $\text{vec } \mathbf{w} | \mathbf{y}^* \sim \text{N}(\tilde{\mathbf{w}}, \tilde{\mathbf{V}}_w)$ is found to be similar to the distribution in (5.14). To obtain the first and second posterior moments for the I-prior

sec:vbemipr
obit

random effects, we can use the law of total expectations:

$$\begin{aligned} E[\text{vec } \mathbf{w} | \mathbf{y}] &= E_{\mathbf{y}^*} [E[\text{vec } \mathbf{w} | \mathbf{y}^*] | \mathbf{y}] =: \hat{\mathbf{w}} \\ &\text{and} \\ E[\text{vec } \mathbf{w} (\text{vec } \mathbf{w})^\top | \mathbf{y}] &= E_{\mathbf{y}^*} [E[\text{vec } \mathbf{w} (\text{vec } \mathbf{w})^\top | \mathbf{y}^*] | \mathbf{y}] =: \hat{\mathbf{W}}, \end{aligned}$$

but this requires $p(\mathbf{y}^* | \mathbf{y})$ which does not come by easily. A similar problem has been faced by [Chan and Kuk \(1997\)](#), who analysed binary linear probit models with random effects. The authors ultimately resort to Monte Carlo sampling within an EM framework to overcome the difficult distributions of interest.

Suppose that, instead of the true posterior distribution $p(\mathbf{y}^*, \mathbf{w} | \mathbf{y})$ being used, a mean-field variational approximation $q(\mathbf{y}^*, \mathbf{w}) = q(\mathbf{y}^*)q(\mathbf{w})$ is used instead. As we know from [Section 5.5](#), $q(\mathbf{y}^*)$ is a truncated multivariate normal distribution, and $q(\mathbf{w})$ is multivariate normal, whose means and second moments can be computed with some effort. Let $\bar{\mathbf{y}}^* = \mathbf{y}^* - \mathbf{1}_n \boldsymbol{\alpha}^\top$. The (approximate) E-step then entails computing

$$\begin{aligned} Q(\theta) &= E_{\mathbf{y}^*, \mathbf{w} \sim q} \log p(\mathbf{y}, \mathbf{y}^*, \mathbf{w} | \theta) \\ &= \text{const.} - \frac{1}{2} \text{tr} E_{\mathbf{y}^*, \mathbf{w} \sim q} \left[\boldsymbol{\Psi} (\bar{\mathbf{y}}^{*\top} \bar{\mathbf{y}}^* + \mathbf{w}^\top \mathbf{H}_\eta^2 \mathbf{w} - 2\bar{\mathbf{y}}^* \boldsymbol{\Psi} \mathbf{w}^\top \mathbf{H}_\eta) + \boldsymbol{\Psi}^{-1} \mathbf{w}^\top \mathbf{w} \right]. \end{aligned}$$

In the M-step, this is maximised with respect to θ . This is the VB-EM algorithm described in [Section 5.10.2](#). As per the discussion in [Section 5.7.3](#), this alleviates the problem of non-conjugacy of the complete conditional for $\boldsymbol{\Psi}$. One downside to VB-EM is that it is not entirely certain how one could obtain standard errors for the parameters, other than by bootstrapping, which for the I-probit model, is likely to be computationally intensive.

Appendix

5.11 Some distributions and their properties

This is a reference relating to the multivariate normal, matrix normal, truncated univariate and multivariate normal, Wishart, and gamma distributions which are collated from various sources for convenience. Of interest are probability density functions, first and second moments, and entropy ([Definition 3.5](#), page 18).

5.11.1 Multivariate normal distribution

Let $X \in \mathbb{R}^d$ be distributed according to a multivariate normal (Gaussian) distribution with mean $\mu \in \mathbb{R}^d$ and covariance matrix $\Sigma \in \mathbb{R}^d$ (a square, symmetric, positive-definite matrix). We say that $X \sim N_d(\mu, \Sigma)$. Then,

- **Pdf.** $p(X|\mu, \Sigma) = (2\pi)^{-d/2} |\Sigma|^{-1/2} \exp\left(-\frac{1}{2}(X - \mu)^\top \Sigma^{-1}(X - \mu)\right)$.
- **Moments.** $E X = \mu$, $E[XX^\top] = \Sigma + \mu\mu^\top$.
- **Entropy.** $H(p) = \frac{1}{2} \log|2\pi e \Sigma| = \frac{d}{2}(1 + \log 2\pi) + \frac{1}{2} \log|\Sigma|$.

Lemma 5.1 (Properties of multivariate normal). *Assume that $X \sim N_d(\mu, \Sigma)$ and $Y \sim N_d(\nu, \Psi)$, where*

$$X = \begin{pmatrix} X_a \\ X_b \end{pmatrix}, \quad \mu = \begin{pmatrix} \mu_a \\ \mu_b \end{pmatrix}, \quad \text{and} \quad \Sigma = \begin{pmatrix} \Sigma_a & \Sigma_{ab} \\ \Sigma_{ab}^\top & \Sigma_b \end{pmatrix}.$$

Then,

- **Marginal distributions.**

$$X_a \sim N_{\dim X_a}(\mu_a, \Sigma_a) \quad \text{and} \quad X_b \sim N_{\dim X_b}(\mu_b, \Sigma_b).$$

- **Conditional distributions.**

$$X_a|X_b \sim N_{\dim X_a}(\tilde{\mu}_a, \tilde{\Sigma}_a) \quad \text{and} \quad X_b \sim N_{\dim X_b}(\tilde{\mu}_b, \tilde{\Sigma}_b),$$

where

$$\begin{aligned} \tilde{\mu}_a &= \mu_a + \Sigma_{ab} \Sigma_b^{-1} (X_b - \mu_b) & \tilde{\mu}_b &= \mu_b + \Sigma_{ab}^\top \Sigma_a^{-1} (X_a - \mu_a) \\ \tilde{\Sigma}_a &= \Sigma_a - \Sigma_{ab} \Sigma_b^{-1} \Sigma_{ab}^\top & \tilde{\Sigma}_b &= \Sigma_b - \Sigma_{ab}^\top \Sigma_a^{-1} \Sigma_{ab} \end{aligned}$$

- **Linear combinations.**

$$AX + BY + C \sim N_d(A\mu + B\nu + C, A\Sigma A^\top + B\Psi B^\top)$$

where A and B are appropriately sized matrices, and $C \in \mathbb{R}^d$.

- **Product of Gaussian densities.**

$$p(X|\mu, \Sigma)p(Y|\nu, \Psi) \propto p(Z|m, S)$$

where $p(Z)$ is a Gaussian density, $m = S(\Sigma^{-1}\mu + \Psi^{-1}\nu)$ and $S = (\Sigma^{-1} + \Psi^{-1})^{-1}$.
The normalising constant is equal to the density of $\mu \sim N(\nu, \Sigma + \Psi)$.

Proof. Omitted—see [Petersen and Pedersen \(2008, §8\)](#). □

Frequently, in Bayesian statistics especially, the following identities will be useful in deriving posterior distributions involving multivariate normals.

Lemma 5.2. Let $x, b \in \mathbb{R}^d$ be a vector, $X, B \in \mathbb{R}^{n \times d}$ a matrix, and $A \in \mathbb{R}^{d \times d}$ a symmetric, invertible matrix. Then,

$$\begin{aligned} -\frac{1}{2}x^\top Ax + b^\top x &= -\frac{1}{2}(x - A^{-1}b)^\top A(x - A^{-1}b) + \frac{1}{2}b^\top A^{-1}b \\ -\frac{1}{2}\text{tr}(X^\top AX) + \text{tr}(B^\top X) &= -\frac{1}{2}\text{tr}((X - A^{-1}B)^\top A(X - A^{-1}B)) + \frac{1}{2}\text{tr}(B^\top A^{-1}B). \end{aligned}$$

Proof. Omitted—see [Petersen and Pedersen \(2008, §8.1.6\)](#). □

5.11.2 Matrix normal distribution

The matrix normal distribution is an extension of the Gaussian distribution to matrices. Let $X \in \mathbb{R}^{n \times m}$ matrix, and let X follow a matrix normal distribution with mean $\mu \in \mathbb{R}^{n \times m}$ and row and column variances $\Sigma \in \mathbb{R}^{n \times n}$ and $\Psi \in \mathbb{R}^{m \times m}$ respectively, which we denote by $X \sim \text{MN}_{n,m}(\mu, \Sigma, \Psi)$. Then,

- **Pdf.** $p(X|\mu, \Sigma, \Psi) = (2\pi)^{-nm/2} |\Sigma|^{-m/2} |\Psi|^{-n/2} e^{-\frac{1}{2}\text{tr}(\Psi^{-1}(X-\mu)^\top \Sigma^{-1}(X-\mu))}$.
- **Moments.** $\mathbb{E} X = \mu$, $\text{Var}(X_{i\cdot}) = \Psi$ for $i = 1, \dots, n$, and $\text{Var}(X_{\cdot j}) = \Sigma$ for $j = 1, \dots, m$.
- **Entropy.** $H(p) = \frac{1}{2} \log |2\pi e(\Psi \otimes \Sigma)| = \frac{nm}{2}(1 + \log 2\pi) + \frac{1}{2} \log |\Sigma|^m |\Psi|^n$.

In the above, ‘ \otimes ’ denotes the Kronecker matrix product defined by

$$\Psi \otimes \Sigma = \begin{pmatrix} \Psi_{11}\Sigma & \Psi_{12}\Sigma & \cdots & \Psi_{1m}\Sigma \\ \Psi_{21}\Sigma & \Psi_{22}\Sigma & \cdots & \Psi_{2m}\Sigma \\ \vdots & \vdots & \ddots & \vdots \\ \Psi_{m1}\Sigma & \Psi_{m2}\Sigma & \cdots & \Psi_{mm}\Sigma \end{pmatrix} \in \mathbb{R}^{nm \times nm}.$$

Of use will be these properties of the Kronecker product (Zhang and Ding, 2013).

- **Bilinearity and associativity.** For appropriately sized matrices A , B and C , and a scalar λ ,

$$\begin{aligned} A \otimes (B + C) &= A \otimes B + A \otimes C \\ (A + B) \otimes C &= A \otimes C + B \otimes C \\ \lambda A \otimes B &= A \otimes \lambda B = \lambda(A \otimes B) \\ (A \otimes B) \otimes C &= A \otimes (B \otimes C) \end{aligned}$$

- **Non-commutative.** In general, $A \otimes B \neq B \otimes A$, but they are *permutation equivalent*, i.e. $A \otimes B \neq P(B \otimes A)Q$ for some permutation matrices P and Q .
- **The mixed product property.** $(A \otimes B)(C \otimes D) = AC \otimes BD$.
- **Inverse.** $A \otimes B$ is invertible if and only if A and B are both invertible, and $(A \otimes B)^{-1} = A^{-1} \otimes B^{-1}$.
- **Transpose.** $(A \otimes B)^\top = A^\top \otimes B^\top$.
- **Determinant.** If A is $n \times n$ and B is $m \times m$, then $|A \otimes B| = |A|^m |B|^n$. Note that the exponent of $|A|$ is the order of B and vice versa.
- **Trace.** Suppose A and B are square matrices. Then $\text{tr}(A \otimes B) = \text{tr } A \text{tr } B$.
- **Rank.** $\text{rank}(A \otimes B) = \text{rank } A \text{rank } B$.
- **Matrix equations.** $AXB = C \Leftrightarrow (B^\top \otimes A) \text{vec } X = \text{vec}(AXB) = \text{vec } C$.

The vectorisation operation ‘ vec ’ stacks the columns of the matrices into one long vector, for instance,

$$\text{vec } \Psi = (\Psi_{11}, \dots, \Psi_{m1}, \Psi_{12}, \dots, \Psi_{m2}, \dots, \Psi_{1m}, \dots, \Psi_{mm})^\top \in \mathbb{R}^{m \times m}.$$

Lemma 5.3 (Equivalence between matrix and multivariate normal). $X \sim \text{MN}_{n,m}(\mu, \Sigma, \Psi)$ if and only if $\text{vec } X \sim \text{N}_{nm}(\text{vec } \mu, \Psi \otimes \Sigma)$.

Proof. In the exponent of the matrix normal pdf, we have

$$\begin{aligned} -\frac{1}{2} \text{tr}(\Psi^{-1}(X - \mu)^\top \Sigma^{-1}(X - \mu)) \\ &= -\frac{1}{2} \text{vec}(X - \mu)^\top \text{vec}(\Sigma^{-1}(X - \mu)\Psi^{-1}) \\ &= -\frac{1}{2} \text{vec}(X - \mu)^\top (\Psi^{-1} \otimes \Sigma^{-1}) \text{vec}(X - \mu) \\ &= -\frac{1}{2} (\text{vec } X - \text{vec } \mu)^\top (\Psi \otimes \Sigma)^{-1} (\text{vec } X - \text{vec } \mu). \end{aligned}$$

Also, $|\Sigma|^{-m/2} |\Psi|^{-n/2} = |\Psi \otimes \Sigma|^{-1/2}$. This converts the matrix normal pdf to that of a multivariate normal pdf. \square

Some useful properties of the matrix normal distribution are listed:

- **Expected values.**

$$\begin{aligned} \mathbb{E}(X - \mu)(X - \mu)^\top &= \text{tr}(\Psi)\Sigma \in \mathbb{R}^{n \times n} \\ \mathbb{E}(X - \mu)^\top (X - \mu) &= \text{tr}(\Sigma)\Psi \in \mathbb{R}^{m \times m} \\ \mathbb{E} X A X^\top &= \text{tr}(A^\top \Psi)\Sigma + \mu A \mu^\top \\ \mathbb{E} X^\top B X &= \text{tr}(\Sigma B^\top)\Psi + \mu^\top B \mu \\ \mathbb{E} X C X &= \Sigma C^\top \Psi + \mu C \mu \end{aligned}$$

- **Transpose.** $X^\top \sim \text{MN}_{m,n}(\mu^\top, \Psi, \Sigma)$.
- **Linear transformation.** Let $A \in \mathbb{R}^{a \times n}$ be of full-rank $a \leq n$ and $B \in \mathbb{R}^{m \times b}$ be of full-rank $b \leq m$. Then $A X B \sim \text{MN}_{a,b}(\mu^\top, A \Sigma A^\top, B^\top \Psi B)$.
- **Iid.** If $X_i \stackrel{\text{iid}}{\sim} \text{N}_m(\mu, \Psi)$ for $i = 1, \dots, n$, and we arranged these vectors row-wise into the matrix $X = (X_1^\top, \dots, X_n^\top)^\top \in \mathbb{R}^{n \times m}$, then $X \sim \text{MN}(1_n \mu^\top, I_n, \Psi)$.

5.11.3 Truncated univariate normal distribution

Let $X \sim N(\mu, \sigma^2)$ with X lying in the interval (a, b) . Then we say that X follows a truncated normal distribution, and we denote this by $X \sim {}^tN(\mu, \sigma^2, a, b)$. Let $\alpha = (a - \mu)/\sigma$, $\beta = (b - \mu)/\sigma$, and $C = \Phi(\beta) - \Phi(\alpha)$. Then,

- **Pdf.** $p(X|\mu, \sigma, a, b) = C^{-1}(2\pi\sigma^2)^{-1/2}e^{-\frac{1}{2\sigma^2}(X-\mu)^2} = \sigma C^{-1}\phi(\frac{x-\mu}{\sigma})$.

- **Moments.**

$$\begin{aligned} E X &= \mu + \sigma \frac{\phi(\alpha) - \phi(\beta)}{C} \\ E X^2 &= \sigma^2 + \mu^2 + \sigma^2 \frac{\alpha\phi(\alpha) - \beta\phi(\beta)}{C} + 2\mu\sigma \frac{\phi(\alpha) - \phi(\beta)}{C} \\ \text{Var } X &= \sigma^2 \left[1 + \frac{\alpha\phi(\alpha) - \beta\phi(\beta)}{C} - \left(\frac{\phi(\alpha) - \phi(\beta)}{C} \right)^2 \right] \end{aligned}$$

- **Entropy.**

$$\begin{aligned} H(p) &= \frac{1}{2} \log 2\pi e \sigma^2 + \log C + \frac{\alpha\phi(\alpha) - \beta\phi(\beta)}{2C} \\ &= \frac{1}{2} \log 2\pi e \sigma^2 + \log C + \frac{1}{2\sigma^2} \cdot \overbrace{\sigma^2 \frac{\alpha\phi(\alpha) - \beta\phi(\beta)}{C}}^{\text{Var } X - \sigma^2 + (E X - \mu)^2} \\ &= \frac{1}{2} \log 2\pi \sigma^2 + \log C + \frac{1}{2\sigma^2} E[X - \mu]^2 \end{aligned}$$

$$\text{because } \text{Var } X + (E X - \mu)^2 = E X^2 - (E X)^2 + (E X)^2 + \mu^2 - 2\mu E X.$$

For binary probit models, the distributions that come up are one-sided truncations at zero, i.e. ${}^tN(\mu, \sigma^2, 0, +\infty)$ (upper tail/positive part) and ${}^tN(\mu, \sigma^2, -\infty, 0)$ (lower tail/negative part), for which their moments are of interest. As an aside, if $\mu = 0$ then the truncation ${}^tN(0, \sigma^2, 0, +\infty)$ is called the *half-normal* distribution. For the positive one-sided truncation at zero, $C = \Phi(+\infty) - \Phi(-\mu/\sigma) = 1 - \Phi(-\mu/\sigma) = \Phi(\mu/\sigma)$, and for the negative one-sided truncation at zero, $C = \Phi(-\mu/\sigma) - \Phi(-\infty) = 1 - \Phi(\mu/\sigma)$.

One may simulate random draws from a truncated normal distribution by drawing from $N(\mu, \sigma^2)$ and discarding samples that fall outside (a, b) . Alternatively, the inverse-transform method using

$$X = \mu + \sigma \Phi^{-1}(\Phi(\alpha) + UC)$$

with $U \sim \text{Unif}(0, 1)$ will work too. Either of these methods will work reasonably well as long as the truncation region is not too far away from μ , but neither is particularly fast.

Efficient algorithms have been explored which are along the lines of either accept/reject algorithms (Robert, 1995), Gibbs sampling (Damien and Walker, 2001), or pseudo-random number generation algorithms (Chopin, 2011). The latter algorithm is inspired by the Ziggurat algorithm (Marsaglia and Tsang, 2000) which is considered to be the fastest Gaussian random number generator.

5.11.4 Truncated multivariate normal distribution

Consider the restriction of $X \sim N_d(\mu, \Sigma)$ to a convex subset⁷ $\mathcal{A} \subset \mathbb{R}^d$. Call this distribution the truncated multivariate normal distribution, and denote it $X \sim {}^tN_d(\mu, \Sigma, \mathcal{A})$. The pdf is $p(X|\mu, \Sigma, \mathcal{A}) = C^{-1}\phi(X|\mu, \Sigma)\mathbb{1}[X \in \mathcal{A}]$, where

$$C = \int_{\mathcal{A}} \phi(x|\mu, \Sigma) dx = P(X \in \mathcal{A}).$$

Generally speaking, there are no closed-form expressions for $Eg(X)$ for any well-defined functions g on X . One strategy to obtain values such as EX (mean), EX^2 (second moment) and $E \log p(X)$ (entropy) would be Monte Carlo integration. If $X^{(1)}, \dots, X^{(T)}$ are samples from $X \sim {}^tN_d(\mu, \Sigma, \mathcal{A})$, then $\widehat{Eg(X)} = \frac{1}{T} \sum_{i=1}^T g(X^{(i)})$.

Sampling from a truncated multivariate normal distribution is described by Robert (1995) and Damien and Walker (2001). In the latter, the authors explore a simple Gibbs-based approach that is easy to implement in practice. Assume that the one-dimensional slices of \mathcal{A}

$$\mathcal{A}_k(X_{-j}) = \{X_j | (X_1, \dots, X_{j-1}, X_j, X_{j+1}, \dots, X_d) \in \mathcal{A}\}$$

are readily available so that the bounds or anti-truncation region of X_j given the rest of the components X_{-j} are known to be (x_j^-, x_j^+) . Using properties of the normal distribution, the full conditionals of X_j given X_{-j} is

$$\begin{aligned} X_j &\sim {}^tN(\tilde{\mu}_j, \tilde{\sigma}_j^2, x_j^-, x_j^+) \\ \tilde{\mu}_j &= \mu_j + \Sigma_{j,-j}^\top \Sigma_{-j,-j} (x_{-j} - \mu_{-j}) \\ \tilde{\sigma}_j^2 &= \Sigma_{11} - \Sigma_{j,-j}^\top \Sigma_{-j,-j} \Sigma_{j,-j}. \end{aligned}$$

⁷A convex subset is a subset of a space that is closed under convex combinations. In Euclidean space, for every pair of points in a convex set, all the points that lie on the straight line segment which joins the pair of points are also in the set.

According to [Robert \(1995\)](#), if $\Psi = \Sigma^{-1}$, then

$$\Sigma_{-j,-j}^{-1} = \Psi_{-j,-j} - \Psi_{j,-j} \Psi_{-j,-j}^{\top} / \Psi_{jj}$$

which means that we need only compute one global inverse Σ^{-1} . Introduce a latent variable $Y \in \mathbb{R}$ such that the joint pdf of X and Y is

$$p(X_1, \dots, X_d, Y) \propto \exp(-Y/2) \mathbb{1}[y > (x - \mu)^{\top} \Sigma^{-1}(x - \mu)] \mathbb{1}[X \in \mathcal{A}].$$

Now, the Gibbs conditional densities for the X_k 's are given by

$$p(X_j | X_{-j}, Y) \propto \mathbb{1}[X_j \in \mathcal{B}_j]$$

where

$$\mathcal{B}_j \in (x_j^-, x_j^+) \cap \{X_j | (X - \mu)^{\top} \Sigma^{-1}(X - \mu) < Y\}.$$

Thus, given values for X_{-j} and Y , the bounds for X_j involves solving a quadratic equation in X_j . The Gibbs conditional density for $Y|X$ is a shifted exponential distribution, which can be sampled using the inverse-transform method. Thus, both X and Y can be sampled directly from uniform variates.

For probit models, we are interested in the conical truncations $\mathcal{C}_j = \{X_j > X_k | k \neq j, \text{ and } k = 1, \dots, m\}$ for which the j 'th component of X is largest. These truncations form cones in d -dimensional space such that $\mathcal{C}_1 \cup \dots \cup \mathcal{C}_d = \mathbb{R}^d$, and hence the name.

In the case where Σ is a diagonal matrix, the conically truncated multivariate normal distributions are easier to deal with due to the independence structure in the covariance matrix. In particular, most calculations of interest involve only a one dimensional integral of products of normal cdfs. We present some results that we have not previously seen before elsewhere.

Lemma 5.4. *Let $X \sim \text{N}_d(\mu, \Sigma, \mathcal{C}_j)$, with $\mu = (\mu_1, \dots, \mu_d)^{\top}$ and $\Sigma = \text{diag}(\sigma_1^2, \dots, \sigma_d^2)$, and $\mathcal{C}_j = \{X_j > X_k | k \neq j, \text{ and } k = 1, \dots, m\}$ a conical truncation of \mathbb{R}^d such that the j 'th component is largest. Then,*

(i) **Pdf.** *The pdf of X has the following functional form:*

$$p(X) = \frac{C^{-1}}{\sigma_1 \dots \sigma_d (2\pi)^{d/2}} \exp \left[-\frac{1}{2} \sum_{i=1}^d \left(\frac{x_i - \mu_i}{\sigma_i} \right)^2 \right]$$

thm:contrun
cn

where ϕ is the pdf of a standard normal distribution and

$$C = \mathbb{E}_Z \left[\prod_{\substack{i=1 \\ i \neq j}}^d \Phi \left(\frac{\sigma_j}{\sigma_i} Z + \frac{\mu_j - \mu_i}{\sigma_i} \right) \right]$$

where $Z \sim \mathcal{N}(0, 1)$.

(ii) **Moments.** The expectation $\mathbb{E} X = (\mathbb{E} X_1, \dots, \mathbb{E} X_d)^\top$ is given by

$$\mathbb{E} X_i = \begin{cases} \mu_i - \sigma_i C^{-1} \mathbb{E}_Z \left[\phi_i \prod_{k \neq i, j} \Phi_k \right] & \text{if } i \neq j \\ \mu_j - \sigma_j \sum_{i \neq j} (\mathbb{E} X_i - \mu_i) & \text{if } i = j \end{cases}$$

and the second moments $\mathbb{E}[X - \mu]^2$ are given by

$$\mathbb{E}[X_i - \mu_i]^2 = \begin{cases} \sigma_i^2 + (\mu_j - \mu_i)(\mathbb{E} X_i - \mu_i) + \sigma_i \sigma_j C^{-1} \mathbb{E}_Z \left[Z \phi_i \prod_{k \neq i, j} \Phi_k \right] & \text{if } i \neq j \\ C^{-1} \sigma_j^2 \mathbb{E}_Z \left[Z^2 \prod_{k \neq j} \Phi_k \right] & \text{if } i = j \end{cases}$$

where we had defined

$$\begin{aligned} \phi_i &= \phi_i(Z) = \phi \left(\frac{\sigma_j Z + \mu_j - \mu_i}{\sigma_i} \right), \text{ and} \\ \Phi_i &= \Phi_i(Z) = \Phi \left(\frac{\sigma_j Z + \mu_j - \mu_i}{\sigma_i} \right). \end{aligned}$$

(iii) **Entropy.** The entropy is given by

$$H(p) = \log C + \frac{d}{2} \log 2\pi + \frac{1}{2} \sum_{i=1}^d \log \sigma_i^2 + \frac{1}{2} \sum_{i=1}^d \frac{1}{\sigma_i^2} \mathbb{E}[x_i - \mu_i]^2.$$

Proof. See [Section 5.12](#) for the proof. □

apx:contrun
proof

5.12 Proofs related to conically truncated multivariate normal distribution

5.12.1 Proof of Lemma 5.4: Pdf

Using the fact that $\int p(x) dx = 1$, and that

$$\begin{aligned}
 & \int \cdots \int \mathbb{1}[x_i < x_j, \forall i \neq j] \prod_{i=1}^d \phi(x_i | \mu_i, \sigma_i^2) dx_1 \cdots dx_d \\
 &= \int \cdots \int \mathbb{1}[x_i < x_j, \forall i \neq j] \prod_{i=1}^d \left[\frac{1}{\sigma_i} \phi\left(\frac{x_i - \mu_i}{\sigma_i}\right) \right] dx_1 \cdots dx_d \\
 &= \int \cdots \int \mathbb{1}[x_i < x_j, \forall i \neq j] \frac{1}{\sigma_j} \phi\left(\frac{x_j - \mu_j}{\sigma_j}\right) \prod_{\substack{i=1 \\ i \neq j}}^d \left[\frac{1}{\sigma_i} \phi\left(\frac{x_i - \mu_i}{\sigma_i}\right) \right] dx_1 \cdots dx_d \\
 &= \int \prod_{\substack{i=1 \\ i \neq j}}^d \Phi\left(\frac{x_j - \mu_i}{\sigma_i}\right) \frac{1}{\sigma_j} \phi\left(\frac{x_j - \mu_j}{\sigma_j}\right) dx_j \\
 &= \int \prod_{\substack{i=1 \\ i \neq j}}^d \Phi\left(\frac{\sigma_j z + \mu_j - \mu_i}{\sigma_i}\right) \phi(z) dz \\
 &\quad \text{(by using the standardisation } z = (x_j - \mu_j)/\sigma_j) \\
 &= \mathbb{E}_Z \left[\prod_{\substack{i=1 \\ i \neq j}}^d \Phi\left(\frac{\sigma_j}{\sigma_i} Z + \frac{\mu_j - \mu_i}{\sigma_i}\right) \right]
 \end{aligned}$$

the proof follows directly.

5.12.2 Proof of Lemma 5.4: Moments

Recall that for $Y \sim {}^t\text{N}(\mu, \sigma^2, -\infty, b)$, for some function g of Y , we have that

$$\mathbb{E} g(Y) = \Phi(\beta)^{-1} \int g(y) \mathbb{1}[y < b] \phi(y | \mu, \sigma^2) dy,$$

and in particular, we have

$$\mathbb{E}[Y - \mu] = -\sigma \frac{\phi(\beta)}{\Phi(\beta)} \quad (5.21)$$

$$\mathbb{E}[Y - \mu]^2 - \sigma^2 = -\sigma^2 \frac{\beta \phi(\beta)}{\Phi(\beta)} \quad (5.22)$$

where $\beta = (b - \mu)/\sigma$. For the conically truncated multivariate normal distribution $X \sim {}^t\text{N}_d(\mu, \Sigma, \mathcal{A}_j)$, where $\Sigma = \text{diag}(\sigma_1^2, \dots, \sigma_d^2)$, the independence structure of Σ makes it possible to consider the expectations of each of the components separately by marginalising out the rest of the components. For simplicity, denote $p(x_k) = \phi(x_k|\mu_k, \sigma_k) = \sigma_k^{-1} \phi(\frac{x_k - \mu_k}{\sigma_k})$. For $i \neq j$, we have

$$\begin{aligned} \mathbb{E} g(X_i) &= C^{-1} \int \cdots \int g(x_i) \mathbb{1}[x_k < x_j, \forall k \neq j] \prod_{k=1}^d p(x_k) dx_1 \cdots dx_d \\ &= C^{-1} \frac{\Phi((x_j - \mu_j)/\sigma_j)}{\Phi((x_j - \mu_j)/\sigma_j)} \iint g(x_i) \mathbb{1}[x_i < x_j] p(x_i) p(x_j) \prod_{\substack{k=1 \\ k \neq i, j}}^d \Phi\left(\frac{x_j - \mu_k}{\sigma_k}\right) dx_i dx_j \\ &= C^{-1} \int \mathbb{E}_{X_i \sim {}^t\text{N}(\mu_i, \sigma_i^2, -\infty, x_j)} g(X_i) \prod_{\substack{k=1 \\ k \neq j}}^d \Phi\left(\frac{x_j - \mu_k}{\sigma_k}\right) p(x_j) dx_j \end{aligned} \quad (5.23)$$

where C is the normalising constant for X , while for the j 'th component we have

$$\begin{aligned} \mathbb{E} g(X_j) &= C^{-1} \int \cdots \int g(x_j) \mathbb{1}[x_k < x_j, \forall k \neq j] \prod_{k=1}^d p(x_k) dx_1 \cdots dx_d \\ &= C^{-1} \int g(x_j) \prod_{\substack{k=1 \\ k \neq j}}^d \Phi\left(\frac{x_j - \mu_k}{\sigma_k}\right) p(x_j) dx_j. \end{aligned} \quad (5.24)$$

Plugging in (5.21) for $g(X_i) = X_i - \mu_i$ in (5.23) we get

$$\begin{aligned}
 \mathbb{E} X_i - \mu_i &= -C^{-1} \int \left(\sigma_i \phi \left(\frac{x_j - \mu_i}{\sigma_i} \right) / \Phi \left(\frac{x_j - \mu_i}{\sigma_i} \right) \right) \prod_{\substack{k=1 \\ k \neq j}}^d \Phi \left(\frac{x_j - \mu_k}{\sigma_k} \right) p(x_j) dx_j \\
 &= -\sigma_i C^{-1} \int \phi \left(\frac{x_j - \mu_i}{\sigma_i} \right) \prod_{\substack{k=1 \\ k \neq i, j}}^d \Phi \left(\frac{x_j - \mu_k}{\sigma_k} \right) p(x_j) dx_j \\
 &= -\sigma_i C^{-1} \int \phi \left(\frac{\sigma_j z + \mu_j - \mu_i}{\sigma_i} \right) \prod_{\substack{k=1 \\ k \neq j}}^d \Phi \left(\frac{\sigma_j z + \mu_j - \mu_k}{\sigma_k} \right) \phi(z) dz \\
 &= -\sigma_i C^{-1} \mathbb{E}_Z \left[\phi \left(\frac{\sigma_j Z + \mu_j - \mu_i}{\sigma_i} \right) \prod_{\substack{k=1 \\ k \neq j}}^d \Phi \left(\frac{\sigma_j Z + \mu_j - \mu_k}{\sigma_k} \right) \right]
 \end{aligned}$$

where Z is the distribution of $N(0, 1)$, and we had used a change of variable $x_j = \sigma_j z + \mu_j$, so that $p(x_j) = \sigma_j^{-1} \phi(z)$ and $dx_j = \sigma_j dz$. For the j 'th component, substitute $g(x_j) = x_j - \mu_j$ in (5.24) to get

$$\begin{aligned}
 \mathbb{E} X_j - \mu_j &= C^{-1} \int (x_j - \mu_j) \prod_{\substack{k=1 \\ k \neq j}}^d \Phi \left(\frac{x_j - \mu_k}{\sigma_k} \right) p(x_j) dx_j \\
 &= C^{-1} \sigma_j \int z \prod_{\substack{k=1 \\ k \neq j}}^d \Phi \left(\frac{\sigma_j z + \mu_j - \mu_k}{\sigma_k} \right) \phi(z) dz \\
 &= \sigma_j \sum_{\substack{i=1 \\ i \neq j}}^d \sigma_i C^{-1} \mathbb{E} \left[\phi \left(\frac{\sigma_j Z + \mu_j - \mu_i}{\sigma_i} \right) \prod_{\substack{k=1 \\ k \neq i, j}}^d \Phi \left(\frac{\sigma_j Z + \mu_j - \mu_k}{\sigma_k} \right) \right] \\
 &= -\sigma_j \sum_{\substack{i=1 \\ i \neq j}}^d (\mathbb{E} X_i - \mu_i),
 \end{aligned}$$

where we have made use of Lemma 5.5 in the second last step.

For the second moments, plug in (5.22) for $g(X_i) = (X_i - \mu_i)^2 - \sigma_i^2$ in (5.23) to get

$$\begin{aligned}
 \mathbb{E}[X_i - \mu_i]^2 - \sigma_i^2 &= -\sigma_i^2 C^{-1} \int \frac{x_j - \mu_i}{\sigma_i} \cdot \frac{\phi((x_j - \mu_i)/\sigma_i)}{\Phi((x_j - \mu_i)/\sigma_i)} \prod_{\substack{k=1 \\ k \neq j}}^d \Phi\left(\frac{x_j - \mu_k}{\sigma_k}\right) p(x_j) dx_j \\
 &= -\sigma_i C^{-1} \int (x_j - \mu_j) \phi\left(\frac{x_j - \mu_i}{\sigma_i}\right) \prod_{\substack{k=1 \\ k \neq i, j}}^d \Phi\left(\frac{x_j - \mu_k}{\sigma_k}\right) p(x_j) dx_j \\
 &\quad + \overbrace{(\mu_j - \mu_i) \cdot -\sigma_i C^{-1} \int \phi\left(\frac{x_j - \mu_i}{\sigma_i}\right) \prod_{\substack{k=1 \\ k \neq i, j}}^d \Phi\left(\frac{x_j - \mu_k}{\sigma_k}\right) p(x_j) dx_j}^{\mathbb{E} X_i - \mu_i} \\
 &= (\mu_j - \mu_i)(\mathbb{E} X_i - \mu_i) \\
 &\quad + \sigma_i C^{-1} \int \sigma_j z \phi\left(\frac{x_j - \mu_i}{\sigma_i}\right) \prod_{\substack{k=1 \\ k \neq i, j}}^d \Phi\left(\frac{\sigma_j z + \mu_j - \mu_k}{\sigma_k}\right) \phi(z) dz \\
 &= (\mu_j - \mu_i)(\mathbb{E} X_i - \mu_i) \\
 &\quad + \sigma_i \sigma_j C^{-1} \mathbb{E} \left[Z \phi\left(\frac{\sigma_j Z + \mu_j - \mu_i}{\sigma_i}\right) \prod_{\substack{k=1 \\ k \neq i, j}}^d \Phi\left(\frac{\sigma_j Z + \mu_j - \mu_k}{\sigma_k}\right) \right]
 \end{aligned}$$

And similarly, for the j 'th component

$$\begin{aligned}
 \mathbb{E}[X_j - \mu_j]^2 &= C^{-1} \int (x_j - \mu_j)^2 \prod_{\substack{k=1 \\ k \neq j}}^d \Phi\left(\frac{x_j - \mu_k}{\sigma_k}\right) p(x_j) dx_j \\
 &= C^{-1} \sigma_j^2 \int z^2 \prod_{\substack{k=1 \\ k \neq j}}^d \Phi\left(\frac{z \sigma_j + \mu_j - \mu_k}{\sigma_k}\right) p(x_j) dz \\
 &= C^{-1} \sigma_j^2 \mathbb{E}_Z \left[Z^2 \prod_{\substack{k=1 \\ k \neq j}}^d \Phi\left(\frac{Z \sigma_j + \mu_j - \mu_k}{\sigma_k}\right) \right].
 \end{aligned}$$

Lastly, we use the following result in the derivation above.

lem:EZgZ

Lemma 5.5. *Let $Z \sim N(0, 1)$. Then for all $m \in \{\mathbb{N} \mid m > 1\}$ and $(\mu, \sigma) \in \mathbb{R} \times \mathbb{R}^+$,*

$$\mathbb{E} \left[Z \prod_{\substack{k=1 \\ k \neq j}}^m \Phi(\sigma_k Z + \mu_k) \right] = \sum_{\substack{i=1 \\ i \neq j}}^m \mathbb{E} \left[\sigma_i \phi(\sigma_i Z + \mu_i) \prod_{\substack{k=1 \\ k \neq i, j}}^m \Phi(\sigma_k Z + \mu_k) \right]$$

for some $j \in \{1, \dots, m\}$.

Proof. Use the fact that for any differentiable function g , $\mathbb{E}[Zg(Z)] = \mathbb{E}[g'(Z)]$, and apply the result with the function $g_m : z \mapsto \prod_{k \neq j} \Phi(\sigma_k z + \mu_k)$. All that is left is to derive the derivative of g , and we use an inductive proof to do this. Introduce the following notation for convenience:

$$\begin{aligned} \phi_i &= \phi(\sigma_i z + \mu_i) \\ \Phi_i &= \Phi(\sigma_i z + \mu_i) \end{aligned}$$

The simplest case is when $m = 2$, which can be trivially shown to be true. Without loss of generality, let $j = 1$. Then

$$\begin{aligned} g_2(z) &= \Phi_2 \\ \Rightarrow \dot{g}_2(z) &= \sigma_2 \phi_2 = \sum_{\substack{i=1 \\ i \neq 1}}^2 \left[\sigma_i \phi_i \sum_{\substack{k=1 \\ k \neq 1, 2}}^2 \Phi_k \right]. \end{aligned}$$

Now assume that the inductive hypothesis holds for some $m \in \{\mathbb{N} \mid m > 1\}$. That is, the derivative of $g_m(z) = \prod_{k \neq j} \Phi_k$,

$$\dot{g}_m(z) = \sum_{\substack{i=1 \\ i \neq j}}^m \left[\sigma_i \phi_i \prod_{\substack{k=1 \\ k \neq i, j}}^m \Phi_k \right],$$

is assumed to be true. Also assume that, without loss of generality, $j \neq m + 1$. Then, the derivative of

$$g_{m+1}(z) = \prod_{\substack{k=1 \\ k \neq j}}^{m+1} \Phi_k = g_m(z) \Phi_{m+1}$$

is found to be

$$\begin{aligned}
 \dot{g}_{m+1}(z) &= \sigma_{m+1} \phi_{m+1} g_m(z) + \dot{g}_m(z) \Phi_{m+1} \\
 &= \sigma_{m+1} \phi_{m+1} \prod_{\substack{k=1 \\ k \neq j}}^m \Phi_k + \sum_{\substack{i=1 \\ i \neq j}}^m \left[\sigma_i \phi_i \prod_{\substack{k=1 \\ k \neq i, j}}^m \Phi_k \right] \Phi_{m+1} \\
 &= \sigma_{m+1} \phi_{m+1} \prod_{\substack{k=1 \\ k \neq j, m+1}}^{m+1} \Phi_k + \sum_{\substack{i=1 \\ i \neq j}}^m \left[\sigma_i \phi_i \prod_{\substack{k=1 \\ k \neq i, j}}^{m+1} \Phi_k \right] \\
 &= \sum_{\substack{i=1 \\ i \neq j}}^{m+1} \left[\sigma_i \phi_i \prod_{\substack{k=1 \\ k \neq i, j}}^{m+1} \Phi_k \right],
 \end{aligned}$$

as required for the inductive proof. Using linearity of expectations, the proof is complete. \square

5.12.3 Proof of [Lemma 5.4](#): Entropy

As a direct consequence of the definition of entropy,

$$\begin{aligned}
 H(p) &= -\mathbb{E} \log p(X) \\
 &= -\mathbb{E} \left[-\log C - \frac{d}{2} \log 2\pi - \frac{1}{2} \sum_{i=1}^d \log \sigma_i^2 - \frac{1}{2} \sum_{i=1}^d \left(\frac{x_i - \mu_i}{\sigma_i} \right)^2 \right] \\
 &= \log C + \frac{d}{2} \log 2\pi + \frac{1}{2} \sum_{i=1}^d \log \sigma_i^2 + \frac{1}{2} \sum_{i=1}^d \frac{1}{\sigma_i^2} \mathbb{E}[x_i - \mu_i]^2.
 \end{aligned}$$

5.13 Derivation of the CAVI algorithm

Let $\mathcal{Z} = \{\mathbf{y}^*, \mathbf{w}, \alpha, \eta, \Psi\}$. Approximate the posterior for \mathcal{Z} by a mean-field variational distribution

$$\begin{aligned}
 p(\mathbf{y}^*, \mathbf{w}, \alpha, \eta, \Psi | \mathbf{y}) &\approx q(\mathbf{y}^*) q(\mathbf{w}) q(\alpha) q(\eta) q(\Psi) \\
 &= \prod_{i=1}^n q(\mathbf{y}_i^*) q(\mathbf{w}) q(\alpha) q(\eta) q(\Psi).
 \end{aligned}$$

The first line is by assumption, while the second line follows from an induced factorisation on the latent propensities, as we will see later. If needed, we also assume that $q(\eta)$ factorises into its constituents components. Recall that, for each $\xi \in \mathcal{Z}$, the optimal mean-field variational density \tilde{q} for ξ satisfies

$$\log \tilde{q}(\xi) = \mathbb{E}_{-\xi}[\log p(\mathbf{y}, \mathcal{Z})] + \text{const.} \quad (5.20)$$

Write $\mathbf{f} = \mathbf{H}_\eta \mathbf{w} \in \mathbb{R}^{n \times m}$. The joint likelihood $p(\mathbf{y}, \mathcal{Z})$ is given by

$$\begin{aligned} p(\mathbf{y}, \mathcal{Z}) &= p(\mathbf{y}|\mathcal{Z})p(\mathcal{Z}) \\ &= p(\mathbf{y}|\mathbf{y}^*)p(\mathbf{y}^*|\boldsymbol{\alpha}, \mathbf{w}, \eta, \boldsymbol{\Psi})p(\mathbf{w}|\boldsymbol{\Psi})p(\eta)p(\boldsymbol{\Psi})p(\boldsymbol{\alpha}). \end{aligned}$$

For reference, the relevant distributions are listed below.

- $p(\mathbf{y}|\mathbf{y}^*)$. For each observation $i \in \{1, \dots, n\}$, given the corresponding latent propensities $\mathbf{y}_i^* = (y_{i1}^*, \dots, y_{im}^*)$, the distribution for y_i is a degenerate distribution which depends on the j 'th component of \mathbf{y}_i^* being largest, where the value observed for y_i was j . Since each of the y_i 's are independent, everything is multiplicative.

$$p(\mathbf{y}|\mathbf{y}^*) = \prod_{i=1}^n \prod_{j=1}^m p_{ij}^{[y_i=j]} = \prod_{i=1}^n \prod_{j=1}^m \mathbb{1}[y_{ij}^* = \max_k y_{ik}^*] \mathbb{1}[y_i=j].$$

- $p(\mathbf{y}^*|\boldsymbol{\alpha}, \mathbf{w}, \eta, \boldsymbol{\Psi})$. Given values for the parameters and I-prior random effects, the distribution of the latent propensities is matrix normal

$$\mathbf{y}^*|\boldsymbol{\alpha}, \mathbf{w}, \eta, \boldsymbol{\Psi} \sim \text{MN}_{n,m}(\mathbf{1}_n \boldsymbol{\alpha}^\top + \mathbf{H}_\eta \mathbf{w}, \mathbf{I}_n, \boldsymbol{\Psi}^{-1}).$$

Write $\boldsymbol{\mu} = \mathbf{1}_n \boldsymbol{\alpha}^\top + \mathbf{H}_\eta \mathbf{w}$. Its pdf is

$$\begin{aligned} p(\mathbf{y}^*|\boldsymbol{\alpha}, \mathbf{w}, \eta, \boldsymbol{\Psi}) &= \exp \left[-\frac{nm}{2} \log 2\pi + \frac{n}{2} \log |\boldsymbol{\Psi}| - \frac{1}{2} \text{tr}((\mathbf{y}^* - \boldsymbol{\mu}) \boldsymbol{\Psi} (\mathbf{y}^* - \boldsymbol{\mu})^\top) \right] \\ &= \exp \left[-\frac{nm}{2} \log 2\pi + \frac{n}{2} \log |\boldsymbol{\Psi}| - \frac{1}{2} \sum_{i=1}^n (\mathbf{y}_{i\cdot}^* - \boldsymbol{\mu}_{i\cdot})^\top \boldsymbol{\Psi} (\mathbf{y}_{i\cdot}^* - \boldsymbol{\mu}_{i\cdot}) \right], \end{aligned}$$

where $\mathbf{y}_i^* \in \mathbb{R}^m$ and $\boldsymbol{\mu}_i \in \mathbb{R}^m$ are the rows of \mathbf{y}^* and $\boldsymbol{\mu}$ respectively. The second line follows directly from the definition of the trace, but also emanates from the fact that \mathbf{y}_i^* are independent multivariate normal with mean $\boldsymbol{\mu}_i$ and variance $\boldsymbol{\Psi}^{-1}$.

- $p(\mathbf{w}|\Psi)$. The \mathbf{w} 's are normal random matrices $\mathbf{w} \sim \text{MN}_{n,m}(\mathbf{0}, \mathbf{I}_n, \Psi)$ with pdf

$$\begin{aligned} p(\mathbf{w}|\Psi) &= \exp \left[-\frac{nm}{2} \log 2\pi - \frac{n}{2} \log |\Psi| - \frac{1}{2} \text{tr}(\mathbf{w}\Psi^{-1}\mathbf{w}^\top) \right] \\ &= \exp \left[-\frac{nm}{2} \log 2\pi - \frac{n}{2} \log |\Psi| - \frac{1}{2} \sum_{i=1}^n \mathbf{w}_{i\cdot}^\top \Psi^{-1} \mathbf{w}_{i\cdot} \right]. \end{aligned}$$

- $p(\eta)$. The most common scenario would be $\eta = \{\lambda_1, \dots, \lambda_p\}$ only. In this case, choose independent normal priors for each $\lambda_k \sim \text{N}(m_k, v_k)$, $k = 1, \dots, p$, whose pdf is

$$p(\eta) = \prod_{k=1}^p \exp \left[-\frac{1}{2} \log 2\pi - \frac{1}{2} \log v_k - \frac{1}{2v_k} (\lambda_k - m_k)^2 \right].$$

An improper prior $p(\eta) \propto \text{const.}$ can be used as well, and this is the same as letting $m_k \rightarrow 0$ and $v_k \rightarrow 0$. The resulting posterior will be proper. If η contains other parameters as well, such as the Hurst coefficient $\gamma \in (0, 1)$, SE lengthscale $l > 0$ or polynomial offset $c > 0$, then appropriate priors should be used to match the support of the parameter. Choices include $p(\gamma) = \mathbf{1}(\gamma \in (0, 1))$ and $l, c \sim \Gamma(a, b)$.

- $p(\Psi)$. Our analysis shows that regardless of prior choice of Ψ , be it in the full or independent I-probit model, the posterior for Ψ will not be of a recognisable form. Without giving too much thought, assume an improper prior on Ψ , i.e. $p(\Psi) \propto \text{const.}$
- $p(\alpha)$. Choose independent normal priors for the intercept, $\alpha_j \sim \text{N}(a_j, A_j)$ for $j = 1, \dots, m$. The pdf is

$$p(\alpha) = \prod_{j=1}^m \exp \left[-\frac{1}{2} \log 2\pi - \frac{1}{2} \log A_j - \frac{1}{2A_j} (\alpha_j - a_j)^2 \right].$$

Remark 5.1. The priors on the parameters $\{\alpha, \eta\}$ can be set to very vague or even improper priors, and the resulting posterior will still yield a proper distribution. Using improper priors eases the algebra slightly. For the precision matrix Ψ , it is best to stick with the Wishart prior to avoid positive-definite issues, unless the independent I-probit model is used, in which case Jeffreys' prior for the precisions $p(\sigma_j^{-2}) \propto \sigma_j^2$ is a convenient choice.

5.13.1 Derivation of $\tilde{q}(\mathbf{y}^*)$

The rows of \mathbf{y}^* are independent, and thus we can consider the variational density for each \mathbf{y}_i^* separately. Consider the case where y_i takes one particular value $j \in \{1, \dots, m\}$. The mean-field density $q(\mathbf{y}_i^*)$ for each $i = 1, \dots, n$ is found to be

$$\begin{aligned} \log \tilde{q}(\mathbf{y}_i^*) &= \mathbb{1}[y_{ij}^* = \max_k y_{ik}^*] \mathbb{E}_{\mathcal{Z} \setminus \{\mathbf{y}^*\} \sim q} \left[-\frac{1}{2} (\mathbf{y}_i^* - \boldsymbol{\mu}_i)^\top \boldsymbol{\Psi} (\mathbf{y}_i^* - \boldsymbol{\mu}_i) \right] + \text{const.} \\ &= \mathbb{1}[y_{ij}^* = \max_k y_{ik}^*] \left[-\frac{1}{2} (\mathbf{y}_i^* - \tilde{\boldsymbol{\mu}}_i)^\top \tilde{\boldsymbol{\Psi}} (\mathbf{y}_i^* - \tilde{\boldsymbol{\mu}}_i) \right] + \text{const.} \quad (\star) \\ &\equiv \begin{cases} \phi(\mathbf{y}_i^* | \tilde{\boldsymbol{\mu}}_i, \tilde{\boldsymbol{\Psi}}) & \text{if } y_{ij}^* > y_{ik}^*, \forall k \neq j \\ 0 & \text{otherwise} \end{cases} \end{aligned}$$

where $\tilde{\boldsymbol{\mu}}_i = \mathbb{E} \boldsymbol{\alpha} + (\mathbb{E} \mathbf{H}_\eta \mathbb{E} \mathbf{w})_i$, and expectations are taken under the optimal mean-field distribution \tilde{q} . The distribution $q(\mathbf{y}_i^*)$ is a truncated m -variate normal distribution such that the j 'th component is always largest. Unfortunately, the expectation of this distribution cannot be found in closed-form, and must be approximated by techniques such as Monte Carlo integration. If, however, the independent I-probit model is used and $\tilde{\boldsymbol{\Psi}}$ is diagonal, then [Lemma 5.4](#) provides a simplification.

Remark 5.2. In (\star) above, we needn't consider the second order terms in the expectations because they do not involve \mathbf{y}^* and can be absorbed into the constant. To see this,

$$\begin{aligned} \mathbb{E}[(\mathbf{y}_i^* - \boldsymbol{\mu}_i)^\top \boldsymbol{\Psi} (\mathbf{y}_i^* - \boldsymbol{\mu}_i)] &= \mathbb{E}[\mathbf{y}_i^{*\top} \boldsymbol{\Psi} \mathbf{y}_i^* + \boldsymbol{\mu}_i^\top \boldsymbol{\Psi} \boldsymbol{\mu}_i - 2\boldsymbol{\mu}_i^\top \boldsymbol{\Psi} \mathbf{y}_i^*] \\ &= \mathbf{y}_i^{*\top} \boldsymbol{\Psi} \mathbf{y}_i^* - 2 \mathbb{E}[\boldsymbol{\mu}_i^\top] \mathbb{E}[\boldsymbol{\Psi}] \mathbf{y}_i^* + \text{const.} \\ &= \mathbf{y}_i^{*\top} \boldsymbol{\Psi} \mathbf{y}_i^* - 2\tilde{\boldsymbol{\mu}}_i^\top \tilde{\boldsymbol{\Psi}} \mathbf{y}_i^* + \text{const.} \\ &= (\mathbf{y}_i^* - \tilde{\boldsymbol{\mu}}_i)^\top \tilde{\boldsymbol{\Psi}} (\mathbf{y}_i^* - \tilde{\boldsymbol{\mu}}_i) + \text{const.} \end{aligned}$$

We will see this occurring a lot later on and we shall take note of this fact.

5.13.2 Derivation of $\tilde{q}(\mathbf{w})$

The terms involving \mathbf{w} in [\(5.20\)](#) are the $p(\mathbf{y}^* | \boldsymbol{\alpha}, \mathbf{w}, \eta, \boldsymbol{\Psi})$ and $p(\mathbf{w} | \boldsymbol{\Psi})$ terms, and the rest are absorbed into the constant. The easiest way to derive $\tilde{q}(\mathbf{w})$ is to vectorise \mathbf{y}^* and \mathbf{w} .

We know that

$$\begin{aligned} \text{vec } \mathbf{y}^* | \boldsymbol{\alpha}, \mathbf{w}, \eta, \boldsymbol{\Psi} &\sim N_{nm} \left(\text{vec}(\mathbf{1}_n \boldsymbol{\alpha}^\top + \mathbf{H}_\eta \mathbf{w}), \boldsymbol{\Psi}^{-1} \otimes \mathbf{I}_n \right) \\ &\text{and} \\ \text{vec } \mathbf{w} | \boldsymbol{\Psi} &\sim N_{nm}(\mathbf{0}, \boldsymbol{\Psi} \otimes \mathbf{I}_n) \end{aligned}$$

using properties of matrix normal distributions. We also use the fact that $\text{vec}(\mathbf{H}_\eta \mathbf{w}) = (\mathbf{I}_m \otimes \mathbf{H}_\eta) \text{vec } \mathbf{w}$. For simplicity, write $\tilde{\mathbf{y}}^* = \text{vec}(\mathbf{y}^* - \mathbf{1}_n \boldsymbol{\alpha}^\top)$, and $\mathbf{M} = (\mathbf{I}_m \otimes \mathbf{H}_\eta)$. Thus,

$$\begin{aligned} \log \tilde{q}(\mathbf{w}) &= E_{\mathcal{Z} \setminus \{\mathbf{w}\} \sim q} \left[-\frac{1}{2} (\tilde{\mathbf{y}}^* - \mathbf{M} \text{vec } \mathbf{w})^\top (\boldsymbol{\Psi}^{-1} \otimes \mathbf{I}_n)^{-1} (\tilde{\mathbf{y}}^* - \mathbf{M} \text{vec } \mathbf{w}) \right] \\ &\quad + E_{\mathcal{Z} \setminus \{\mathbf{w}\} \sim q} \left[-\frac{1}{2} (\text{vec } \mathbf{w})^\top (\boldsymbol{\Psi} \otimes \mathbf{I}_n)^{-1} \text{vec}(\mathbf{w}) \right] + \text{const.} \\ &= -\frac{1}{2} E_{\mathcal{Z} \setminus \{\mathbf{w}\} \sim q} \left[(\text{vec } \mathbf{w})^\top \left(\overbrace{\mathbf{M}^\top (\boldsymbol{\Psi} \otimes \mathbf{I}_n) \mathbf{M} + (\boldsymbol{\Psi}^{-1} \otimes \mathbf{I}_n)}^{\mathbf{A}} \right) \text{vec}(\mathbf{w}) \right] \\ &\quad + E_{\mathcal{Z} \setminus \{\mathbf{w}\} \sim q} \left[\overbrace{\tilde{\mathbf{y}}^{*\top} (\boldsymbol{\Psi} \otimes \mathbf{I}_n) \mathbf{M} \text{vec}(\mathbf{w})}^{\mathbf{a}^\top} \right] + \text{const.} \\ &= -\frac{1}{2} E_{\mathcal{Z} \setminus \{\mathbf{w}\} \sim q} \left[(\text{vec } \mathbf{w} - \mathbf{A}^{-1} \mathbf{a})^\top \mathbf{A} (\text{vec } \mathbf{w} - \mathbf{A}^{-1} \mathbf{a}) \right] + \text{const.} \end{aligned}$$

This is recognised as a multivariate normal of dimension nm with mean and precision given by $\text{vec } \tilde{\mathbf{w}} = E[\mathbf{A}^{-1} \mathbf{a}]$ and $\tilde{\mathbf{V}}_w^{-1} = E[\mathbf{A}]$ respectively. With a little algebra, we find that

$$\begin{aligned} \mathbf{V}_w^{-1} &= E_{\mathcal{Z} \setminus \{\mathbf{w}\} \sim q} [\mathbf{A}] \\ &= E_{\mathcal{Z} \setminus \{\mathbf{w}\} \sim q} \left[(\mathbf{I}_m \otimes \mathbf{H}_\eta)^\top (\boldsymbol{\Psi} \otimes \mathbf{I}_n) (\mathbf{I}_m \otimes \mathbf{H}_\eta) + (\boldsymbol{\Psi}^{-1} \otimes \mathbf{I}_n) \right] \\ &= E_{\mathcal{Z} \setminus \{\mathbf{w}\} \sim q} \left[(\boldsymbol{\Psi} \otimes \mathbf{H}_\eta^2) + (\boldsymbol{\Psi}^{-1} \otimes \mathbf{I}_n) \right] \\ &= (\tilde{\boldsymbol{\Psi}} \otimes \tilde{\mathbf{H}}_\eta^2) + (\tilde{\boldsymbol{\Psi}}^{-1} \otimes \mathbf{I}_n) \end{aligned}$$

and making a first-order approximation $(E \mathbf{A})^{-1} \approx E[\mathbf{A}^{-1}]^8$,

$$\begin{aligned} \text{vec } \tilde{\mathbf{w}} &= E_{\mathcal{Z} \setminus \{\mathbf{w}\} \sim q} [\mathbf{A}^{-1} \mathbf{a}] \\ &= \tilde{\mathbf{V}}_w E_{\mathcal{Z} \setminus \{\mathbf{w}\} \sim q} \left[(\mathbf{I}_m \otimes \mathbf{H}_\eta) (\boldsymbol{\Psi} \otimes \mathbf{I}_n) \text{vec}(\mathbf{y}^* - \mathbf{1}_n \boldsymbol{\alpha}^\top) \right] \\ &= \tilde{\mathbf{V}}_w E_{\mathcal{Z} \setminus \{\mathbf{w}\} \sim q} \left[(\boldsymbol{\Psi} \otimes \mathbf{H}_\eta) \text{vec}(\mathbf{y}^* - \mathbf{1}_n \boldsymbol{\alpha}^\top) \right] \\ &= \tilde{\mathbf{V}}_w (\tilde{\boldsymbol{\Psi}} \otimes \tilde{\mathbf{H}}_\eta) \text{vec}(\tilde{\mathbf{y}}^* - \mathbf{1}_n \tilde{\boldsymbol{\alpha}}^\top). \end{aligned}$$

Ideally, we do not want to work with the $nm \times nm$ matrix \mathbf{V}_w , since its inverse is expensive to compute. Refer to [Section 5.7.2](#) for details.

In the case of the I-probit model, where $\Psi = \text{diag}(\psi_1, \dots, \psi_m)$, then the covariance matrix takes a simpler form. Specifically, it has the block diagonal structure:

$$\begin{aligned}\tilde{\mathbf{V}}_w &= \text{E} \left[\text{diag}(\psi_1, \dots, \psi_m) \otimes \mathbf{H}_\eta^2 + \text{diag}(\psi_1, \dots, \psi_m) \otimes \mathbf{I}_n \right]^{-1} \\ &= \text{diag} \left(\text{E} (\psi_1 \mathbf{H}_\eta^2 + \psi_1^{-1} \mathbf{I}_n)^{-1}, \dots, \text{E} (\psi_m \mathbf{H}_\eta^2 + \psi_m^{-1} \mathbf{I}_n)^{-1} \right) \\ &\approx \text{diag} \left((\tilde{\psi}_1 \tilde{\mathbf{H}}_\eta^2 + \tilde{\psi}_1^{-1} \mathbf{I}_n)^{-1}, \dots, (\tilde{\psi}_m \tilde{\mathbf{H}}_\eta^2 + \tilde{\psi}_m^{-1} \mathbf{I}_n)^{-1} \right) \\ &=: \text{diag}(\tilde{\mathbf{V}}_{w_1}, \dots, \tilde{\mathbf{V}}_{w_m}).\end{aligned}$$

The mean $\text{vec } \tilde{\mathbf{w}}$ is

$$\begin{aligned}\text{vec } \tilde{\mathbf{w}} &= \tilde{\mathbf{V}}_w (\text{diag}(\tilde{\psi}_1, \dots, \tilde{\psi}_m) \otimes \tilde{\mathbf{H}}_\eta) \text{vec}(\tilde{\mathbf{y}}^* - \mathbf{1}_n \tilde{\boldsymbol{\alpha}}^\top) \\ &= \text{diag}(\tilde{\mathbf{V}}_{w_1}, \dots, \tilde{\mathbf{V}}_{w_m}) \text{diag}(\tilde{\psi}_1 \tilde{\mathbf{H}}_\eta, \dots, \tilde{\psi}_m \tilde{\mathbf{H}}_\eta) \text{vec}(\tilde{\mathbf{y}}^* - \mathbf{1}_n \tilde{\boldsymbol{\alpha}}^\top) \\ &= \text{diag}(\tilde{\psi}_1 \tilde{\mathbf{V}}_{w_1} \tilde{\mathbf{H}}_\eta, \dots, \tilde{\psi}_m \tilde{\mathbf{V}}_{w_m} \tilde{\mathbf{H}}_\eta) (\tilde{\mathbf{y}}^* - \mathbf{1}_n \tilde{\boldsymbol{\alpha}}^\top) \\ &= \begin{pmatrix} \tilde{\mathbf{w}}_{\cdot,1} & \dots & \tilde{\mathbf{w}}_{\cdot,m} \end{pmatrix} \\ &= \begin{pmatrix} \tilde{\psi}_1 \tilde{\mathbf{V}}_{w_1} \tilde{\mathbf{H}}_\eta (\tilde{\mathbf{y}}^*_{\cdot,1} - \tilde{\alpha}_1 \mathbf{1}_n) & \dots & \tilde{\psi}_m \tilde{\mathbf{V}}_{w_m} \tilde{\mathbf{H}}_\eta (\tilde{\mathbf{y}}^*_{\cdot,m} - \tilde{\alpha}_m \mathbf{1}_n) \end{pmatrix}^\top.\end{aligned}$$

Therefore, we can consider the distribution of $\mathbf{w} = (\mathbf{w}_{\cdot,1}, \dots, \mathbf{w}_{\cdot,m})$ columnwise, and each are normally distributed with mean and variance

$$\tilde{\mathbf{w}}_{\cdot,j} = \tilde{\sigma}_j^{-2} \tilde{\mathbf{V}}_{w_j} \tilde{\mathbf{H}}_\eta (\tilde{\mathbf{y}}^*_{\cdot,j} - \tilde{\alpha}_j \mathbf{1}_n) \quad \text{and} \quad \tilde{\mathbf{V}}_{w_j} = (\tilde{\sigma}_j^{-2} \tilde{\mathbf{H}}_\eta^2 + \tilde{\sigma}_j^2 \mathbf{I}_n)^{-1}.$$

A quantity that we will be requiring time and again will be $\text{tr}(\mathbf{C} \text{E}[\mathbf{w}^\top \mathbf{D} \mathbf{w}])$, where $\mathbf{C} \in \mathbb{R}^{m \times m}$ and $\mathbf{D} \in \mathbb{R}^{n \times n}$ are both square and symmetric matrices. Using the definition of the trace directly, we get

$$\begin{aligned}\text{tr}(\mathbf{C} \text{E}[\mathbf{w}^\top \mathbf{D} \mathbf{w}]) &= \sum_{i,j=1}^m \mathbf{C}_{ij} \text{E}[\mathbf{w}^\top \mathbf{D} \mathbf{w}]_{ij} \\ &= \sum_{i,j=1}^m \mathbf{C}_{ij} \text{E}[\mathbf{w}_{\cdot,i}^\top \mathbf{D} \mathbf{w}_{\cdot,j}].\end{aligned} \tag{5.25}$$

⁸[Groves and Rothenberg \(1969\)](#) show that $\text{E}[\mathbf{A}^{-1}] = (\text{E} \mathbf{A})^{-1} + \mathbf{B}$, where \mathbf{B} is a positive-definite matrix. This approximation has been used also by [Girolami and Rogers \(2006\)](#) in their work.

The expectation of the univariate quantity $\mathbf{w}_{\cdot i}^\top \mathbf{D} \mathbf{w}_{\cdot j}$ is inspected below:

$$\begin{aligned} \mathbb{E}[\mathbf{w}_{\cdot i}^\top \mathbf{D} \mathbf{w}_{\cdot j}] &= \text{tr}(\mathbf{D} \mathbb{E}[\mathbf{w}_{\cdot j} \mathbf{w}_{\cdot i}^\top]) \\ &= \text{tr}(\mathbf{D}(\text{Cov}(\mathbf{w}_{\cdot j}, \mathbf{w}_{\cdot i}) + \mathbb{E}[\mathbf{w}_{\cdot j}] \mathbb{E}[\mathbf{w}_{\cdot i}]^\top)) \\ &= \text{tr}(\mathbf{D}(\mathbf{V}_w[i, j] + \tilde{\mathbf{w}}_{\cdot j} \tilde{\mathbf{w}}_{\cdot i}^\top)). \end{aligned}$$

where $\mathbf{V}_w[i, j] \in \mathbb{R}^{n \times n}$ refers to the (i, j) 'th submatrix block of \mathbf{V}_w . Of course, in the independent the I-probit model, this is equal to

$$\mathbf{V}_w[i, j] = \delta_{ij}(\psi_j \mathbf{H}_\eta^2 + \psi_j^{-1} \mathbf{I}_n)^{-1}$$

where δ is the Kronecker delta. Continuing on (5.25) leads us to

$$\text{tr}(\mathbf{C} \mathbb{E}[\mathbf{w}^\top \mathbf{D} \mathbf{w}]) = \sum_{i,j=1}^m \mathbf{C}_{ij} \left(\text{tr}(\mathbf{D}(\delta_{ij} \mathbf{V}_{w_j} + \tilde{\mathbf{w}}_{\cdot j} \tilde{\mathbf{w}}_{\cdot i}^\top)) \right).$$

If $\mathbf{C} = \text{diag}(c_1, \dots, c_m)$, then

$$\begin{aligned} \text{tr}(\mathbf{C} \mathbb{E}[\mathbf{w}^\top \mathbf{D} \mathbf{w}]) &= \sum_{j=1}^m c_j \left(\text{tr}(\mathbf{D} \tilde{\mathbf{V}}_{w_j}) + \tilde{\mathbf{w}}_{\cdot j}^\top \mathbf{D} \tilde{\mathbf{w}}_{\cdot j} \right) \\ &= \sum_{j=1}^m c_j \text{tr}(\mathbf{D}(\tilde{\mathbf{V}}_{w_j} + \tilde{\mathbf{w}}_{\cdot j} \tilde{\mathbf{w}}_{\cdot j}^\top)) \end{aligned}$$

5.13.3 Derivation of $\tilde{q}(\eta)$

By looking at only the terms involving η in (5.20), we deduce that \tilde{q} for η satisfies

$$\begin{aligned} \log \tilde{q}(\eta) &= -\frac{1}{2} \text{tr} \mathbb{E}_{\mathcal{Z} \setminus \{\eta\} \sim q} \left[(\mathbf{y}^* - \mathbf{1}_n \boldsymbol{\alpha}^\top - \mathbf{H}_\eta \mathbf{w}) \boldsymbol{\Psi} (\mathbf{y}^* - \mathbf{1}_n \boldsymbol{\alpha}^\top - \mathbf{H}_\eta \mathbf{w})^\top \right] + \log p(\eta) \\ &\quad + \text{const.} \\ &= -\frac{1}{2} \text{tr} \mathbb{E}_{\mathcal{Z} \setminus \{\eta\} \sim q} \left(\boldsymbol{\Psi} \mathbf{w}^\top \mathbf{H}_\eta^2 \mathbf{w} - 2 \boldsymbol{\Psi} \mathbf{w}^\top \mathbf{H}_\eta (\mathbf{y}^* - \boldsymbol{\alpha}) \right) + \log p(\eta) + \text{const.} \\ &= -\frac{1}{2} \text{tr} \left(\tilde{\boldsymbol{\Psi}} \mathbb{E}[\mathbf{w}^\top \mathbf{H}_\eta^2 \mathbf{w}] - 2 \tilde{\boldsymbol{\Psi}} \tilde{\mathbf{w}}^\top \mathbf{H}_\eta (\tilde{\mathbf{y}}^* - \tilde{\boldsymbol{\alpha}}) \right) + \log p(\eta) + \text{const.} \end{aligned}$$

with some appropriate prior $p(\eta)$. In general, this does not have a recognisable form in η , especially when it is not linearly dependent on the kernel matrix. This happens when considering parameters other than the scales of the RKHSs. Our interest would

be to obtain $\tilde{\mathbf{H}}_\eta := \mathbb{E}_{\eta \sim q} \mathbf{H}_\eta$ and $\tilde{\mathbf{H}}_\eta^2 := \mathbb{E}_{\eta \sim q} \mathbf{H}_\eta^2$. We use a Metropolis random-walk algorithm to obtain these quantities, as detailed in the algorithm below.

Algorithm 3 Metropolis random-walk to sample η

- 1: **inputs** $\tilde{\alpha}$, $\tilde{\mathbf{w}}$, $\tilde{\Psi}$, and s Metropolis sampling s.d.
- 2: **initialise** $\eta^{(0)} \in \mathbb{R}^q$ and $t \leftarrow 0$
- 3: **for** $t = 1, \dots, T$ **do**
- 4: Draw $\eta^* \sim N_q(\eta^{(t)}, s^2)$
- 5: Accept/reject proposal state, i.e.

$$\eta^{(t+1)} \leftarrow \begin{cases} \eta^* & \text{if } u \sim \text{Unif}(0, 1) < \pi_{\text{acc}} \\ \eta^{(t)} & \text{otherwise} \end{cases}$$

where

$$\pi_{\text{acc}} = \min \left(1, \exp \left(\log \tilde{q}(\eta^*) - \log \tilde{q}(\eta^{(t)}) \right) \right).$$

- 6: **end for**
 - 7: $\tilde{\mathbf{H}}_\eta \leftarrow \frac{1}{T} \sum_{i=1}^T \mathbf{H}_{\eta^{(i)}}$ and $\tilde{\mathbf{H}}_\eta^2 \leftarrow \frac{1}{T} \sum_{i=1}^T \mathbf{H}_{\eta^{(i)}}^2$
-

Now consider the case where $\eta = \{\lambda_1, \dots, \lambda_p\}$ (RKHS scale parameters only), and the scenario described in the exponential family EM algorithm of [Section 4.3.3](#) applies. In particular, for $k = 1, \dots, p$, we can decompose the kernel matrix as $\mathbf{H}_\eta = \lambda_k \mathbf{R}_k + \mathbf{S}_k$ and its square as $\mathbf{H}_\eta^2 = \lambda_k^2 \mathbf{R}_k^2 + \lambda_k \mathbf{U}_k + \mathbf{S}_k^2$. Then, for $j = 1, \dots, m$, assuming each of

the $q(\lambda_k)$ densities are independent of each other, we find that

$$\begin{aligned}
 \log \tilde{q}(\lambda_k) &= \mathbb{E}_{\mathcal{Z} \setminus \{\eta\} \sim q} \left[-\frac{1}{2} \text{tr} \left((\mathbf{y}^* - \boldsymbol{\mu}) \boldsymbol{\Psi} (\mathbf{y}^* - \boldsymbol{\mu})^\top \right) \right] - \frac{1}{2v_k^2} (\lambda_k - m_k)^2 + \text{const.} \\
 &= -\frac{1}{2} \text{tr} \mathbb{E}_{\mathcal{Z} \setminus \{\eta\} \sim q} \left[\boldsymbol{\Psi} \mathbf{w}^\top \mathbf{H}_\eta^2 \mathbf{w} - 2\boldsymbol{\Psi} (\mathbf{y}^* - \mathbf{1} \boldsymbol{\alpha}^\top)^\top \mathbf{H}_\eta \mathbf{w} \right] \\
 &\quad - \frac{1}{2v_k^2} (\lambda_k - m_k)^2 + \text{const.} \\
 &= -\frac{1}{2} \text{tr} \mathbb{E}_{\mathcal{Z} \setminus \{\eta\} \sim q} \left[\boldsymbol{\Psi} \mathbf{w}^\top (\lambda_k^2 \mathbf{R}_k^2 + \lambda_k \mathbf{U}_k) \mathbf{w} - 2\boldsymbol{\Psi} (\mathbf{y}^* - \mathbf{1} \boldsymbol{\alpha}^\top)^\top (\lambda_k \mathbf{R}_k) \mathbf{w} \right] \\
 &\quad - \frac{1}{2v_k^2} (\lambda_k^2 - 2m_k \lambda_k) + \text{const.} \\
 &= -\frac{1}{2} \text{tr} \mathbb{E}_{\mathcal{Z} \setminus \{\eta\} \sim q} \left[\lambda_k^2 \boldsymbol{\Psi} \mathbf{w}^\top \mathbf{R}_k^2 \mathbf{w} - 2\lambda_k \left(\boldsymbol{\Psi} (\mathbf{y}^* - \mathbf{1} \boldsymbol{\alpha}^\top)^\top \mathbf{R}_k \mathbf{w} - \frac{1}{2} \boldsymbol{\Psi} \mathbf{w}^\top \mathbf{U}_k \mathbf{w} \right) \right] \\
 &\quad - \frac{1}{2} \left(\frac{1}{v_k^2} \lambda_k^2 - 2 \frac{m_k}{v_k^2} \lambda_k \right) + \text{const.} \\
 &= -\frac{1}{2} \left[\lambda_k^2 \overbrace{(\text{tr}(\tilde{\boldsymbol{\Psi}} \mathbb{E}[\mathbf{w}^\top \mathbf{R}_k^2 \mathbf{w}]) + v_k^{-2})}^{c_k} \right. \\
 &\quad \left. - 2\lambda_k \overbrace{\left(\text{tr} \left(\tilde{\boldsymbol{\Psi}} (\tilde{\mathbf{y}}^* - \mathbf{1}_n \tilde{\boldsymbol{\alpha}}^\top)^\top \mathbf{R}_k \tilde{\mathbf{w}} - \frac{1}{2} \tilde{\boldsymbol{\Psi}} \mathbb{E}[\mathbf{w}^\top \mathbf{U}_k \mathbf{w}] \right) + m_k v_k^{-2} \right)}^{d_k} \right]
 \end{aligned}$$

By completing the squares, we recognise this is as the kernel of a univariate normal density. Specifically, $\lambda_k \sim \mathcal{N}(d_k/c_k, 1/c_k)$. The quantity $\tilde{\mathbf{H}}_\eta$ can be obtained by substituting $\lambda_k \mapsto \mathbb{E}_{\lambda_k \sim q}[\lambda_k]$ in the expression $\mathbf{H}_\eta = \lambda_k \mathbf{R}_k + \mathbf{S}_k$. However, in the calculation of $\tilde{\mathbf{H}}_\eta^2$ using $\lambda_k^2 \mathbf{R}_k^2 + \lambda_k \mathbf{U}_k + \mathbf{S}_k^2$, we must replace occurrences of λ_k^2 with $\mathbb{E}_{\lambda_k \sim q}[\lambda_k]^2 + \text{Var}_{\lambda_k \sim q}[\lambda_k]$. This can be cumbersome, so if felt necessary, use the approximation $\lambda_k^2 \mapsto \mathbb{E}_{\lambda_k \sim q}[\lambda_k]^2$ instead.

Example 5.1. Suppose $k = 1$, and we only have λ to estimate. Then, $\mathbf{H}_\eta = \lambda \mathbf{H}$, $\mathbf{R}_k = \mathbf{H}$, $\mathbf{R}_k^2 = \mathbf{H}^2$, and $\mathbf{U}_k = \mathbf{0}$. Suppose also we use an improper prior $\lambda_k \propto \text{const.}$, which is the same as having $v_k^2 \rightarrow 0$ and $m_k v_k^{-2} \rightarrow 0$. The mean field distribution for λ is then

$$\lambda \sim \mathcal{N} \left(\frac{\text{tr}(\tilde{\boldsymbol{\Psi}} (\tilde{\mathbf{y}}^* - \mathbf{1} \tilde{\boldsymbol{\alpha}}^\top)^\top \mathbf{H} \tilde{\mathbf{w}})}{\text{tr}(\tilde{\boldsymbol{\Psi}} \mathbb{E}[\mathbf{w}^\top \mathbf{H}^2 \mathbf{w}])}, \frac{1}{\text{tr}(\tilde{\boldsymbol{\Psi}} \mathbb{E}[\mathbf{w}^\top \mathbf{H}^2 \mathbf{w}])} \right)$$

Further, if $\tilde{\boldsymbol{\Psi}} = \tilde{\psi} \mathbf{I}_m$, then

$$\lambda \sim \mathcal{N} \left(\frac{\sum_{j=1}^m (\tilde{\mathbf{y}}_{\cdot j}^* - \tilde{\alpha}_j \mathbf{1})^\top \mathbf{H} \tilde{\mathbf{w}}_{\cdot j}}{\sum_{j=1}^m \text{tr}(\mathbf{H}^2 \mathbb{E}[\mathbf{w}_{\cdot j} \mathbf{w}_{\cdot j}^\top])}, \frac{1}{\sum_{j=1}^m \text{tr}(\mathbf{H}^2 \mathbb{E}[\mathbf{w}_{\cdot j} \mathbf{w}_{\cdot j}^\top])} \right)$$

which bears a resemblance to the exponential family EM algorithm solutions described in Chapter 4. Now, $\tilde{\mathbf{H}}_\eta = \mathbb{E}[\lambda \mathbf{H}] = \tilde{\lambda} \mathbf{H}$, and $\tilde{\mathbf{H}}_\eta^2 = \mathbb{E}[\lambda^2 \mathbf{H}^2] = (\text{Var } \lambda + \tilde{\lambda}^2) \mathbf{H}^2$.

5.13.4 Derivation of $\tilde{q}(\Psi)$

We find that $q(\Psi)$ satisfies

$$\begin{aligned} \log q(\Psi) &= \mathbb{E}_{\mathcal{Z} \setminus \{\Psi\} \sim q} \left[-\frac{1}{2} \text{tr}((\mathbf{y}^* - \boldsymbol{\mu})^\top (\mathbf{y}^* - \boldsymbol{\mu}) \Psi) - \frac{1}{2} \text{tr}(\mathbf{w}^\top \mathbf{w} \Psi^{-1}) \right] \\ &\quad + \log p(\Psi) + \text{const.} \\ &= -\frac{1}{2} \text{tr} \left(\overbrace{(\mathbb{E}[(\mathbf{y}^* - \boldsymbol{\mu})^\top (\mathbf{y}^* - \boldsymbol{\mu})])}^{\mathbf{G}_1} \Psi + \overbrace{\mathbb{E}[\mathbf{w}^\top \mathbf{w}]}^{\mathbf{G}_2} \Psi^{-1} \right) \\ &\quad + \log p(\Psi) + \text{const.} \end{aligned}$$

This seems to be the pdf of $\text{Wis}(\mathbf{G} + \mathbf{G}_1, g)$ plus the pdf of a distribution which almost resembles an inverse Wishart pdf. Unfortunately, the properties such as its moments and entropy are unknown.

The matrix \mathbf{G}_1 is

$$\begin{aligned} \mathbf{G}_1 &= \mathbb{E}[(\mathbf{y}^* - \boldsymbol{\mu})^\top (\mathbf{y}^* - \boldsymbol{\mu})] \\ &= \mathbb{E}[\mathbf{y}^{*\top} \mathbf{y}^* + \boldsymbol{\alpha} \mathbf{1}_n^\top \mathbf{1}_n \boldsymbol{\alpha}^\top + \mathbf{w}^\top \mathbf{H}_\eta^2 \mathbf{w} - 2\mathbf{y}^{*\top} \mathbf{1}_n \boldsymbol{\alpha}^\top - 2\mathbf{y}^{*\top} \mathbf{H}_\eta \mathbf{w} - 2\boldsymbol{\alpha} \mathbf{1}_n^\top \mathbf{H}_\eta \mathbf{w}] \\ &= \mathbb{E}[\mathbf{y}^{*\top} \mathbf{y}^*] + n \mathbb{E}[\boldsymbol{\alpha} \boldsymbol{\alpha}^\top] + \mathbb{E}[\mathbf{w}^\top \mathbf{H}_\eta \mathbf{w}] - 2(\tilde{\mathbf{y}}^{*\top} \mathbf{1}_n \tilde{\boldsymbol{\alpha}}^\top + \tilde{\mathbf{y}}^{*\top} \tilde{\mathbf{H}}_\eta \tilde{\mathbf{w}} + \tilde{\boldsymbol{\alpha}} \mathbf{1}_n^\top \tilde{\mathbf{H}}_\eta \tilde{\mathbf{w}}), \end{aligned}$$

and this involves second order moments of a conically truncated multivariate normal distribution, which needs to be obtained via simulation. Meanwhile,

$$\begin{aligned} \mathbf{G}_{2,ij} &= \mathbb{E}[\mathbf{w}^\top \mathbf{w}]_{ij} \\ &= \mathbb{E}[\mathbf{w}_{\cdot i}^\top \mathbf{w}_{\cdot j}] \\ &= \tilde{\mathbf{V}}_w[i, j] + \tilde{\mathbf{w}}_{\cdot i}^\top \tilde{\mathbf{w}}_{\cdot j}. \end{aligned}$$

In the case of the independent I-probit model, we use a gamma prior on each of the precisions in the diagonal entries of $\Psi = \text{diag}(\psi_1, \dots, \psi_m)$. Then, the variational density

for each ψ_j is found to be

$$\begin{aligned} \log q(\psi_j) &= \mathbb{E}_{\mathcal{Z} \setminus \{\Psi\} \sim q} \left[\frac{n}{2} \log(\psi_1 \cdots \psi_m) - \frac{1}{2} \sum_{j=1}^m \sum_{i=1}^n \psi_j (\mathbf{y}_{ij}^* - \boldsymbol{\mu}_{ij})^2 \right] \\ &\quad + \mathbb{E}_{\mathcal{Z} \setminus \{\Psi\} \sim q} \left[-\frac{n}{2} \log(\psi_1 \cdots \psi_m) - \frac{1}{2} \sum_{j=1}^m \sum_{i=1}^n \psi_j^{-1} \mathbf{w}_{ij}^2 \right] \\ &\quad + \sum_{j=1}^m ((s_j - 1) \log \psi_j - r_j \psi_j) + \text{const.} \\ &= (s_j - 1) \log \psi_j - \psi_j \left(\frac{1}{2} \mathbb{E} \|\mathbf{y}_{\cdot,j}^* - \boldsymbol{\mu}_{\cdot,j}\|^2 + r_j \right) \\ &\quad - \psi_j^{-1} \left(\frac{1}{2} \mathbb{E} \|\mathbf{w}_{\cdot,j}\|^2 \right) + \text{const.} \end{aligned}$$

which again, is a pdf of an unknown distribution. However, its posterior mode can be computed. Write $a = -\left(\frac{1}{2} \mathbb{E} \|\mathbf{y}_{\cdot,j}^* - \boldsymbol{\mu}_{\cdot,j}\|^2 + r_j\right)$, $b = s_j - 1$, and $c = \left(\frac{1}{2} \mathbb{E} \|\mathbf{w}_{\cdot,j}\|^2\right)$. Then,

$$\frac{\partial}{\partial \psi_j} \log q(\psi_j) = \frac{\partial}{\partial \psi_j} (a\psi_j + b \log \psi_j - c\psi_j^{-1}) = a + b\psi_j^{-1} + c\psi_j^{-2}$$

equated to zero means solving a quadratic equation in ψ_j . Suppose that $p(\psi_j) \propto \text{const.}$, then $s_j = 1$ and $r_j = 0$ so $\tilde{\psi}_j$ can be solved directly to be

$$\hat{\psi}_j = \sqrt{\frac{\mathbb{E} \|\mathbf{y}_{\cdot,j}^* - \boldsymbol{\mu}_{\cdot,j}\|^2}{\mathbb{E} \|\mathbf{w}_{\cdot,j}\|^2}}.$$

If the posterior mean is close to its mode, then $\hat{\psi}_j$ is a good approximation for $\tilde{\psi}_j$.

To calculate $\mathbb{E} \|\mathbf{y}_{\cdot,j}^* - \boldsymbol{\mu}_{\cdot,j}\|^2 = \mathbb{E} \sum_{i=1}^n (\mathbf{y}_{ij}^* - \mu_{ij})^2$, one first needs $\mathbb{E} (y_{ij}^* - \alpha_j - \mathbf{w}_{\cdot,j}^\top \mathbf{h}_\eta(x_i))^2$. This, in itself, presents a challenge to compute analytically, because it requires, among other things, the second moments $\mathbb{E} y_{ij}^{*2}$ and $\mathbb{E} [\mathbf{w}_{\cdot,j}^\top \mathbf{h}_\eta(x_i) \mathbf{h}_\eta(x_i)^\top \mathbf{w}_{\cdot,j}]$. Although not entirely accurate, it is simpler to use the approximation

$$\mathbb{E} \|\mathbf{y}_{\cdot,j}^* - \boldsymbol{\mu}_{\cdot,j}\|^2 \approx \|\tilde{\mathbf{y}}_{\cdot,j}^* - \tilde{\boldsymbol{\mu}}_{\cdot,j}\|^2.$$

(see note 2 on page 88). Also, we have $\mathbf{w}_{\cdot,j} \sim N_n(\tilde{\mathbf{w}}_{\cdot,j}, \tilde{\mathbf{V}}_{w_j})$, and so $\mathbb{E} \|\mathbf{w}_{\cdot,j}\|^2 = \text{tr}(\tilde{\mathbf{V}}_{w_j} + \tilde{\mathbf{w}}_{\cdot,j} \tilde{\mathbf{w}}_{\cdot,j}^\top)$.

5.13.5 Derivation of $\tilde{q}(\boldsymbol{\alpha})$

Let $\mathbf{A} = \text{diag}(A_1, \dots, A_m)$ and $\mathbf{a} = (a_1, \dots, a_m)^\top$. The terms involving α_j in (5.20) are

$$\begin{aligned} \log q(\boldsymbol{\alpha}) &= \mathbb{E}_{\mathcal{Z} \setminus \{\boldsymbol{\alpha}\} \sim q} \left[-\frac{1}{2} \sum_{i=1}^n (\mathbf{y}_{i.}^* - \boldsymbol{\alpha} - \mathbf{w}^\top \mathbf{h}_\eta(x_i))^\top \boldsymbol{\Psi} (\mathbf{y}_{i.}^* - \boldsymbol{\alpha} - \mathbf{w}^\top \mathbf{h}_\eta(x_i)) \right] \\ &\quad - \frac{1}{2} (\boldsymbol{\alpha} - \mathbf{a})^\top \mathbf{A}^{-1} (\boldsymbol{\alpha} - \mathbf{a}) + \text{const.} \\ &= -\frac{1}{2} \left[\boldsymbol{\alpha}^\top \overbrace{(n\boldsymbol{\Psi} + \mathbf{A}^{-1})}^{\tilde{\mathbf{A}}} \boldsymbol{\alpha} - 2 \overbrace{\left(\sum_{i=1}^n \boldsymbol{\Psi} (\tilde{\mathbf{y}}_{i.}^* - \tilde{\mathbf{w}}^\top \tilde{\mathbf{h}}_\eta(x_i)) + \mathbf{A}^{-1} \mathbf{a} \right)}^{\tilde{\mathbf{a}}} \boldsymbol{\alpha} \right] \end{aligned}$$

which implies a normal mean-field distribution for $\boldsymbol{\alpha}$ whose mean and variance are $\tilde{\boldsymbol{\alpha}} = \tilde{\mathbf{A}}^{-1} \tilde{\mathbf{a}}$ and $\tilde{\mathbf{A}}^{-1}$ respectively. If $\boldsymbol{\Psi}$ is diagonal, the components of $\boldsymbol{\alpha}$ would be independent.

As a remark, due to identifiability, only $m - 1$ of these intercept are estimable. We can either put a constraint that one of the intercepts is fixed at zero, or the sum of the intercepts equals zero. The latter constraint is implemented in this thesis, and this is realised by estimating all the intercepts and then centring them.

5.14 Deriving the ELBO expression

The evidence lower bound (ELBO) expression involves the following calculation:

$$\begin{aligned} \mathcal{L} &= \int \cdots \int q(\mathbf{y}^*, \mathbf{w}, \theta) \log \frac{p(\mathbf{y}, \mathbf{y}^*, \mathbf{w}, \theta)}{q(\mathbf{y}^*, \mathbf{w}, \theta)} d\mathbf{y}^* d\mathbf{w} d\theta \\ &= \mathbb{E} \overbrace{\log p(\mathbf{y}, \mathbf{y}^*, \mathbf{w}, \theta)}^{\text{joint likelihood}} + \mathbb{E} \overbrace{(-\log q(\mathbf{y}^*, \mathbf{w}, \theta))}^{\text{entropy}} \\ &= \mathbb{E} \left[\sum_{i=1}^n \sum_{j=1}^m \log p(y_i | y_{ij}^*) + \sum_{i=1}^n \log p(\mathbf{y}_{i.}^* | \boldsymbol{\alpha}, \mathbf{w}, \boldsymbol{\Psi}, \eta) + \log p(\mathbf{w} | \boldsymbol{\Psi}) + \log p(\boldsymbol{\Psi}) \right. \\ &\quad \left. + \log p(\eta) + \log p(\boldsymbol{\alpha}) \right] \\ &\quad + \sum_{i=1}^n H[q(\mathbf{y}_{i.}^*)] + H[q(\mathbf{w})] + H[q(\boldsymbol{\Psi})] + H[q(\eta)] + H[q(\boldsymbol{\alpha})]. \end{aligned}$$

As we saw earlier, the distribution of $q(\Psi)$ is not of recognisable form. This makes computation of $E \log |\Psi|$, $E \log p(\Psi)$, and $H[q(\Psi)]$, which are required in the expression of the ELBO, problematic. For simplicity, we present the ELBO calculations for when Ψ is treated to be fixed.

Remark 5.3. As discussed, given the latent propensities \mathbf{y}^* , the pdf of \mathbf{y} is degenerate and hence can be disregarded.

Remark 5.4. When using improper priors for the hyperparameters, i.e. $p(\eta, \alpha) \propto \text{const.}$, then these terms can be disregarded.

5.14.1 Terms involving distributions of \mathbf{y}^*

$$\begin{aligned} & \sum_{i=1}^n \left(E \log p(\mathbf{y}_{i.}^* | \alpha, \mathbf{w}, \Psi, \eta) + H[q(\mathbf{y}_{i.}^*)] \right) \\ &= -\frac{nm}{2} \log 2\pi + \frac{n}{2} \log |\Psi| - \frac{1}{2} E \sum_{i=1}^n (\mathbf{y}_{i.}^* - \boldsymbol{\mu}_{i.})^\top \Psi (\mathbf{y}_{i.}^* - \boldsymbol{\mu}_{i.}) \\ & \quad + \frac{nm}{2} \log 2\pi - \frac{n}{2} \log |\tilde{\Psi}| + \frac{1}{2} E \sum_{i=1}^n (\mathbf{y}_{i.}^* - \tilde{\boldsymbol{\mu}}_{i.})^\top \Psi (\mathbf{y}_{i.}^* - \tilde{\boldsymbol{\mu}}_{i.}) + \log C_i \\ &= \text{const.} + \sum_{i=1}^n \log C_i \end{aligned}$$

where C_i is the normalising constant for the distribution of multivariate truncated normal $\mathbf{y}_{i.}$.

Notes:

1. $p(\mathbf{y}_{i.}^*)$ is the pdf of $N(\boldsymbol{\mu}_{i.}, \Psi^{-1})$, and $q(\mathbf{y}_{i.}^*)$ is the pdf of ${}^tN(\tilde{\boldsymbol{\mu}}_{i.}, \Psi^{-1}, \mathcal{C}_{y_i})$, where $\boldsymbol{\mu}_{i.} = \alpha + \mathbf{w}^\top \mathbf{h}_\eta(x_i) \in \mathbb{R}^m$.
2. It is simpler to use the approximation

$$E(\mathbf{y}_{i.}^* - \boldsymbol{\mu}_{i.})^\top \Psi (\mathbf{y}_{i.}^* - \boldsymbol{\mu}_{i.}) \approx E(\mathbf{y}_{i.}^* - \tilde{\boldsymbol{\mu}}_{i.})^\top \Psi (\mathbf{y}_{i.}^* - \tilde{\boldsymbol{\mu}}_{i.}). \quad (5.26)$$

rather than work out the actual quantity, which is

$$E(\mathbf{y}_{i.}^* - \boldsymbol{\mu}_{i.})^\top \Psi (\mathbf{y}_{i.}^* - \boldsymbol{\mu}_{i.}) = E(\mathbf{y}_{i.}^* - \tilde{\boldsymbol{\mu}}_{i.})^\top \Psi (\mathbf{y}_{i.}^* - \tilde{\boldsymbol{\mu}}_{i.}) + \text{tr}(\Psi \text{Var } \boldsymbol{\mu}_{i.}) \quad (5.27)$$

{eq:elboyap
rx}

{eq:elboyac
t}

note2

where $\text{Var } \boldsymbol{\mu}_i = \text{Var } \boldsymbol{\alpha} + \text{Var } \mathbf{w}^\top \mathbf{h}_\eta(x_i)$, obtained by taking expectations with respect to everything except \mathbf{y}_i^* . The first term is a diagonal matrix of the posterior variances of the intercepts. The second term is where things get complicated. Let $\boldsymbol{\Omega}_i = \text{Var } \mathbf{w}^\top \mathbf{h}_\eta(x_i)$. Then $\boldsymbol{\Omega}_{i,kj} \approx \text{Cov}(\mathbf{w}_{\cdot k}^\top \mathbf{h}_\eta(x_i), \mathbf{w}_{\cdot j}^\top \mathbf{h}_\eta(x_i)) = \mathbf{h}_\eta(x_i)^\top \tilde{\mathbf{V}}_w[k, j] \mathbf{h}_\eta(x_i)$. So

$$\text{tr}(\boldsymbol{\Psi} \boldsymbol{\Omega}_i) \approx \sum_{k,j=1}^m \boldsymbol{\Psi}_{kj} \mathbf{h}_\eta(x_i)^\top \tilde{\mathbf{V}}_w[k, j] \mathbf{h}_\eta(x_i)$$

However, we know that $\text{Var } XY = \text{E } X^2 Y^2 - (\text{E } XY)^2 = \text{Var } X \text{Var } Y + \text{Var } X (\text{E } Y)^2 + \text{Var } Y (\text{E } X)^2$, so there is actually some covariance terms which need to be considered, and these are not so easily computed. In practice, we find that using (5.26) gives satisfactory results as far as determining convergence for the variational algorithm goes.

5.14.2 Terms involving distributions of \mathbf{w}

$$\begin{aligned} \text{E} \log p(\mathbf{w} | \boldsymbol{\Psi}) + H[q(\mathbf{w})] &= -\frac{nm}{2} \log 2\pi - \frac{n}{2} \log |\boldsymbol{\Psi}| - \frac{1}{2} \text{E} \text{tr}(\mathbf{w} \boldsymbol{\Psi}^{-1} \mathbf{w}^\top) \\ &\quad + \frac{nm}{2} (1 + \log 2\pi) + \frac{1}{2} \log |\tilde{\mathbf{V}}_w| \\ &= \text{const.} - \frac{1}{2} \sum_{j=1}^m \text{tr}(\boldsymbol{\Psi}^{-1} (\tilde{\mathbf{V}}_w[j, j] + \tilde{\mathbf{w}}_{\cdot j} \tilde{\mathbf{w}}_{\cdot j}^\top)) \end{aligned}$$

Notes:

1. $p(\mathbf{w})$ is the pdf of $\text{MN}(\mathbf{0}, \mathbf{I}_n, \boldsymbol{\Psi})$, and $q(\mathbf{w})$ is the pdf of $\text{N}(\text{vec } \tilde{\mathbf{w}}, \tilde{\mathbf{V}}_w)$.
2. $\tilde{\mathbf{V}}_w[j, j]$ are the $n \times n$ sub matrices along the diagonal of $\tilde{\mathbf{V}}_w$.

5.14.3 Terms involving distributions of η

If no closed-form expression for $q(\eta)$ is found, then the expression $\text{E}[\log p(\eta) - q(\eta)]$ must be obtained by sampling methods. Otherwise, consider the case where $\eta = \{\lambda_1, \dots, \lambda_p\}$.

Then, the contribution to the ELBO is

$$\begin{aligned}
& \mathbb{E} \log p(\lambda_1, \dots, \lambda_p) + H[q(\lambda_1, \dots, \lambda_p)] \\
&= -\frac{p}{2} \log 2\pi - \frac{1}{2} \log v_1 \cdots v_k - \frac{1}{2} \sum_{k=1}^p \frac{\mathbb{E}(\lambda_k - m_k)^2}{v_k} \\
&\quad + \frac{p}{2} (1 + \log 2\pi) + \frac{1}{2} \log \tilde{v}_1 \cdots \tilde{v}_p \\
&= \text{const.} + \frac{1}{2} \sum_{k=1}^p \log \tilde{v}_k - \frac{1}{2} \sum_{k=1}^p \frac{\tilde{v}_k + \tilde{\lambda}_k^2 - 2\tilde{\lambda}_k m_k}{v_k}
\end{aligned}$$

Notes:

1. The priors on the λ_k 's are $N(m_k, v_k)$, and $q(\lambda_k)$ is the density of $N(\tilde{\lambda}_k, v_{\lambda_k})$.
2. When using improper priors $\lambda_k \propto \text{const.}$, then we need only consider the middle term involving the sums of $\log \tilde{v}_{\lambda_k}$.

5.14.4 Terms involving distribution of α

For the intercepts, consider only

$$\begin{aligned}
\mathbb{E} \log p(\alpha) + H[q(\alpha)] &= \text{const.} - \frac{1}{2} \mathbb{E} \sum_{j=1}^m \frac{(\alpha_j - a_j)^2}{A_j} + \frac{1}{2} \log \tilde{v}_{\alpha_1} \cdots \tilde{v}_{\alpha_m} \\
&= \text{const.} + \frac{1}{2} \sum_{j=1}^m \log \tilde{v}_{\alpha_j} - \frac{1}{2} \sum_{j=1}^m \frac{v_{\alpha_j} + \tilde{\alpha}_j^2 - 2a_j \tilde{\alpha}_j}{A_j}
\end{aligned}$$

Notes:

1. $p(\alpha)$ is $\prod_{j=1}^m \phi(\alpha_j | a_j, A_j)$, and $q(\alpha) \prod_{j=1}^m \phi(\alpha_j | \tilde{\alpha}_j, \tilde{v}_{\alpha_j})$.

5.14.5 ELBO summarised

In the example section of Chapter 5, we considered only 1) the independent I-probit model; 2) fixed $\Sigma = \mathbf{I}_m$; 3) only RKHS scale parameters to estimate; and 4) and improper priors on the hyperparameters. In such situations, the ELBO expression is

simply

$$\mathcal{L} = \text{const.} + \sum_{i=1}^n \log C_i - \frac{1}{2} \sum_{j=1}^m \text{tr}(\tilde{\mathbf{V}}_{w_j} + \tilde{\mathbf{w}}_{\cdot,j} \tilde{\mathbf{w}}_{\cdot,j}^\top) + \frac{1}{2} \sum_{k=1}^p \log \tilde{v}_k.$$

As a final remark, often times the ELBO is treated as a proxy for the (penalised) marginal likelihood of the model, in which case it must be noted that the ELBO as we had derived is correct up to a constant. We find that keeping track of the constants is slightly tedious, and hence decided not to do so. When comparing ELBOs of two or more models, the comparison is still valid as only differences between the ELBOs matter, in which case the constants would cancel out.

Bibliography

- agresti2000
tutorial Agresti, Alan and Jonathan Hartzel (2000). “Tutorial in biostatistics: Strategies comparing treatment on binary response with multi-centre data”. In: *Statistics in medicine* 19, pp. 1115–1139.
- albert1993b
ayesian Albert, James H and Siddhartha Chib (1993). “Bayesian analysis of binary and polychotomous response data”. In: *Journal of the American statistical Association* 88.422, pp. 669–679.
- beal2003 Beal, M. J. and Z. Ghahramani (2003). “The variational Bayesian EM algorithm for incomplete data: With application to scoring graphical model structures”. In: *Bayesian Statistics 7*. Proceedings of the Seventh Valencia International Meeting. Ed. by José M. Bernardo, A. Philip Dawid, James O. Berger, Mike West, David Heckerman, M.J. Bayarri, and Adrian F.M. Smith. Oxford: Oxford University Press, pp. 453–464.
- bishop2006p
attern Bishop, Christopher (2006). *Pattern Recognition and Machine Learning*. Springer-Verlag.
- blei2017var
iational Blei, David M, Alp Kucukelbir, and Jon D McAuliffe (2017). “Variational inference: A review for statisticians”. In: *Journal of the American Statistical Association* just-accepted.
- breiman2001
random Breiman, Leo (2001). “Random forests”. In: *Machine learning* 45.1, pp. 5–32.
- cannings2017
random Cannings, Timothy I and Richard J Samworth (2017). “Random-projection ensemble classification”. In: *Journal of the Royal Statistical Society: Series B (Statistical Methodology) with discussion* 79.4, pp. 959–1035.
- chan1997max
imum Chan, Jennifer SK and Anthony YC Kuk (1997). “Maximum likelihood estimation for probit-linear mixed models with correlated random effects”. In: *Biometrics*, pp. 86–97.

| | |
|-------------------------|---|
| chopin2011fast | Chopin, Nicolas (2011). “Fast simulation of truncated Gaussian distributions”. In: <i>Statistics and Computing</i> 21.2, pp. 275–288. |
| damien2001sampling | Damien, Paul and Stephen G Walker (2001). “Sampling truncated normal, beta, and gamma densities”. In: <i>Journal of Computational and Graphical Statistics</i> 10.2, pp. 206–215. |
| deterding1989speaker | Deterding, David Henry (1989). “Speaker normalization for automatic speech recognition”. PhD thesis. University of Cambridge. |
| diggle2013spatial | Diggle, Peter J, Paula Moraga, Barry Rowlingson, and Benjamin M Taylor (2013). “Spatial and spatio-temporal log-Gaussian Cox processes: extending the geostatistical paradigm”. In: <i>Statistical Science</i> , pp. 542–563. |
| diggle2005nonparametric | Diggle, Peter, Pingping Zheng, and Peter Durr (2005). “Nonparametric estimation of spatial segregation in a multivariate point process: bovine tuberculosis in Cornwall, UK”. In: <i>Journal of the Royal Statistical Society: Series C (Applied Statistics)</i> 54.3, pp. 645–658. |
| friedman2001elements | Friedman, Jerome, Trevor Hastie, and Robert Tibshirani (2001). <i>The elements of statistical learning</i> . Vol. 1. Springer series in statistics New York. |
| geweke1991efficient | Geweke, John (1991). <i>Efficient simulation from the multivariate normal and student-t distributions subject to linear constraints and the evaluation of constraint probabilities</i> . |
| geweke1994alternative | Geweke, John, Michael Keane, and David Runkle (1994). “Alternative computational approaches to inference in the multinomial probit model”. In: <i>The review of economics and statistics</i> , pp. 609–632. |
| girolami2006variational | Girolami, Mark and Simon Rogers (2006). “Variational Bayesian Multinomial Probit Regression with Gaussian Process Priors”. In: <i>Neural Computation</i> 18.8, pp. 1790–1817. |
| groves1969note | Groves, Theodore and Thomas Rothenberg (1969). “A note on the expected value of an inverse matrix”. In: <i>Biometrika</i> 56.3, pp. 690–691. |
| guvenir1997supervised | Guvenir, H Altay, Burak Acar, Gulsen Demiroz, and Ayhan Cekin (1997). “A supervised machine learning algorithm for arrhythmia analysis”. In: <i>Computers in Cardiology 1997</i> . IEEE, pp. 433–436. |

| | |
|-----------------------------|--|
| hajivassiliou1996simulation | Hajivassiliou, Vassilis, Daniel McFadden, and Paul Ruud (1996). “Simulation of multivariate normal rectangle probabilities and their derivatives theoretical and computational results”. In: <i>Journal of econometrics</i> 72.1-2, pp. 85–134. |
| hastie1986 | Hastie, Trevor and Robert Tibshirani (Aug. 1986). “Generalized Additive Models”. In: <i>Statist. Sci.</i> 1.3, pp. 297–310. DOI: 10.1214/ss/1177013604 . URL: https://doi.org/10.1214/ss/1177013604 . |
| itzzykson1991statistical | Itzykson, Claude and Jean Michel Drouffe (1991). <i>Statistical Field Theory: Volume 2, Strong Coupling, Monte Carlo Methods, Conformal Field Theory and Random Systems</i> . Cambridge University Press. |
| kass1995bayes | Kass, Robert E and Adrian E Raftery (1995). “Bayes factors”. In: <i>Journal of the american statistical association</i> 90.430, pp. 773–795. |
| keane1994computationally | Keane, Michael P (1994). “A computationally practical simulation estimator for panel data”. In: <i>Econometrica: Journal of the Econometric Society</i> , pp. 95–116. |
| Keane1992 | Keane, Michael P. (1992). “A Note on Identification in the Multinomial Probit Model”. In: <i>Journal of Business & Economic Statistics</i> 10.2, pp. 193–200. ISSN: 0735-0015. DOI: 10.2307/1391677 . URL: http://www.jstor.org/stable/1391677%5Cnhttp://www.jstor.org/stable/pdfplus/1391677.pdf?acceptTC=true . |
| kuss2005assessing | Kuss, Malte and Carl Edward Rasmussen (2005). “Assessing approximate inference for binary Gaussian process classification”. In: <i>Journal of machine learning research</i> 6.Oct, pp. 1679–1704. |
| marsaglia2000ziggurat | Marsaglia, George and Wai Wan Tsang (2000). “The ziggurat method for generating random variables”. In: <i>Journal of statistical software</i> 5.8, pp. 1–7. |
| mccullagh1989 | McCullagh, P. and John A. Nelder (1989). <i>Generalized Linear Models</i> . 2nd. Chapman & Hall/CRC Press. |
| meng1997algorithm | Meng, Xiao-Li and David Van Dyk (1997). “The EM Algorithm—an Old Folk-song Sung to a Fast New Tune”. In: <i>Journal of the Royal Statistical Society: Series B (Statistical Methodology)</i> 59.3, pp. 511–567. |
| minka2001expectation | Minka, Thomas P (2001). “Expectation propagation for approximate Bayesian inference”. In: <i>Proceedings of the Seventeenth conference on Uncertainty in artificial intelligence</i> . Morgan Kaufmann Publishers Inc., pp. 362–369. |

| | |
|-------------------------|--|
| neal1999 | Neal, Radford M. (1999). “Regression and Classification using Gaussian Process Priors”. In: <i>Bayesian Statistics</i> . Ed. by J M Bernardo, J O Berger, A P Dawid, and A F M Smith. Vol. 6. Oxford University Press. (with discussion), pp. 475–501. |
| petersen2008matrix | Petersen, Kaare Brandt and Michael Syskind Pedersen (2008). “The matrix cookbook”. In: <i>Technical University of Denmark</i> 7.15, p. 510. |
| rasmussen2006gaussian | Rasmussen, Carl Edward and Christopher K I Williams (2006). <i>Gaussian Processes for Machine Learning</i> . The MIT Press. |
| robert1995simulation | Robert, Christian P (1995). “Simulation of truncated normal variables”. In: <i>Statistics and computing</i> 5.2, pp. 121–125. |
| robinson1989dynamic | Robinson, Anthony John (1989). “Dynamic error propagation networks”. PhD thesis. University of Cambridge. |
| scholkopf2002learning | Schölkopf, Bernhard and Alexander J Smola (2002). <i>Learning with Kernels: Support Vector Machines, Regularization, Optimization, and Beyond</i> . MIT Press. |
| skrondal2004generalized | Skrondal, Anders and Sophia Rabe-Hesketh (2004). <i>Generalized latent variable modeling: Multilevel, longitudinal, and structural equation models</i> . Crc Press. |
| steinwart2008support | Steinwart, Ingo and Andreas Christmann (2008). <i>Support vector machines</i> . Springer Science & Business Media. |
| taylor2013lrgcp | Taylor, Benjamin M, Tilman M Davies, Barry S Rowlingson, Peter J Diggle, et al. (2013). “lrgcp: an R package for inference with spatial and spatio-temporal log-Gaussian Cox processes”. In: <i>Journal of Statistical Software</i> 52.4, pp. 1–40. |
| tibshirani2002diagnoses | Tibshirani, Robert, Trevor Hastie, Balasubramanian Narasimhan, and Gilbert Chu (2002). “Diagnosis of multiple cancer types by shrunken centroids of gene expression”. In: <i>Proceedings of the National Academy of Sciences</i> 99.10, pp. 6567–6572. |
| train2009discrete | Train, Kenneth E (2009). <i>Discrete choice methods with simulation</i> . Cambridge university press. |
| zhang2013kronecker | Zhang, Huamin and Feng Ding (2013). “On the Kronecker products and their applications”. In: <i>Journal of Applied Mathematics</i> 2013. |